Supporting Information

Self-Induced Charge Transfer Activation Enables Metal-Free C–H Coupling of Polycyclic Aromatic Hydrocarbons under Visible Light

Kazuma Kurokawa,[a] Aki Kohyama,[a] Yusuke Kuroda,[a] Keisuke Tao-Kakuyama,[b] Hiroshi Takikawa[a] and Kiyosei Takasu*[a]

[a]Graduate School of Pharmaceutical Sciences, Kyoto University, Yoshida, Sakyo-ku, Kyoto 606-8501, Japan

[b]Institute for Chemical Research, Kyoto University, Gokasho Uji-city, Kyoto 611-0011, Japan

E-mail: takasu.kiyosei.6r@ kyoto-u.ac.jp; Fax: +81 75 753 4604; Tel: +81 75 753 4553

Table of Contents

1. General S3
2. Preparation of substrates S4
3. Optimization of reaction conditions
   3-1. General reaction setup S9
   3-2. Dibenzo[*j*,*l*]fluoranthene **1a** as a model substrate S10
   3-3. 2-Naphthol (**3d**) as a model substrate S12
   3-4. Optimization for substrate **3** S14
4. Photo-induced oxidative biaryl coupling of polycyclic aromatic hydrocarbons S17
5. X-ray crystallographic data S23
6. Chiroptical and photophysical properties
   6-1. Optical resolution of **2a** S31
   6-2. CD spectra of **2a** S32
   6-3. Experimental determination of the racemization barrier of **2a** S33
   6-4. UV-vis and fluorescence spectra of **1a**–**1d** and **2a**–**2d** S34
7. Mechanistic studies
   7-1. UV-vis absorption spectra S35
   7-2. Biaryl coupling reaction using TEMPO as a single electron oxidant S36
   7-3. Electron spin resonance (ESR) experiments S36
   7-4. Biaryl coupling reaction using Magic Blue as a single electron oxidant S37
8. Computational results
   8-1. Exploration of possible CT complex geometries of two 2-naphthols and TFA S39
   8-2. Exploration of possible CT complex geometry of two 2-methoxynaphthalenes and TFA S40
   8-3. Predicted UV-vis and ECD spectra S42
   8-4. Racemization process of **2a'** S45
9. References S73
10. ^{1}H and ^{13}C NMR spectra S74

1. General

All non-aqueous reactions were carried out in dried glassware under an atmosphere of dry argon unless otherwise noted. For reactions that require heating, oil bath was used as a heat source. All dehydrated solvents for the reactions were purchased and used without further desiccation. All reagents were purchased and used without further purification. Analytical TLC was performed on pre-coated silica gel plate (Wako Silicagel 70 F_{254}). Preparative TLC was prepared in our laboratory and performed (Merck Silicagel 60 P F_{254}). Column chromatography was performed on Wakogel 60 N unless otherwise stated. ^{1}H, ^{13}C NMR spectra were recorded on a JEOL JNM ECZ600R at 600 and 151 MHz, respectively. Chemical shifts (δ) and coupling constants (*J*) are presented in parts per million and hertz, respectively. Tetramethylsilane (δ 0.0 ppm) was used as internal standard for ^{1}H NMR. Residual $CDCl_3$ (δ 77.0 ppm) and acetone-d_6 (δ 29.8 ppm) were used as internal standard for ^{13}C NMR. Multiplicities are indicated as s (singlet), d (doublet), t (triplet), sep (septet), m (multiplet), and br (broad). High-resolution mass spectra (HRMS) were recorded on a Shimadzu LCMS-IT-TOF fitted with an electrospray ionization (ESI) source and a JEOL JMS-700 fitted with fast atom bombardment (FAB) source. IR spectra were recorded on a Shimadzu IRAffinity-1, and the wave numbers of maximum absorption peaks are reported in cm^{-1}. X-Ray single crystal diffraction analyses were performed on a Rigaku XtaLAB P200 apparatus. UV-vis absorption spectra were recorded on a Shimazu UV-2600. Fluorescence spectra were recorded on a JASCO FP-8600.

2. Preparation of substrates

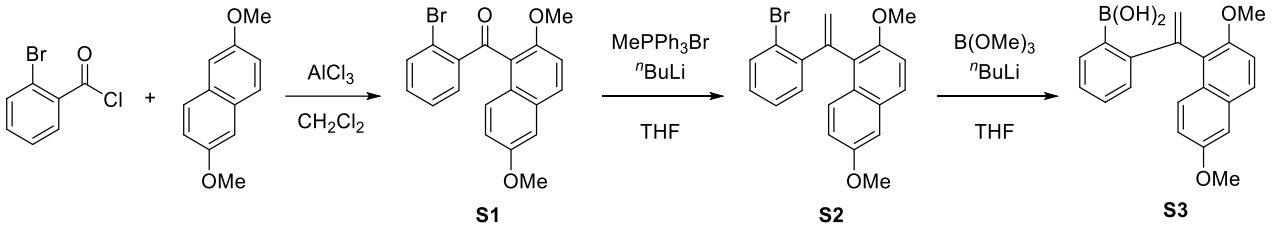

Synthesis of S3[1]

To a stirred solution of 2,6-dimethoxynaphthalene (9.41 g, 50.0 mmol) and $AlCl_3$ (14.6 g, 110 mmol) in dry CH_2Cl_2 (150 mL) was added dropwise 2-bromobenzoylchloride (7.20 mL, 55.1 mmol) at 0 °C under Ar atmosphere. After stirring for 15 min. at room temperature, the reaction mixture was poured into ice/10% HCl aq. The mixture was extracted three times with Et_2O. The combined organic extracts were washed with water, sat. $NaHCO_3$ and brine, dried over Na_2SO_4 and concentrated. Trituration (hexanes) afforded **S1** (18.3 g, 99%) as pale-yellow solids.

S1: R_f 0.18 (hexanes/EtOAc = 5/1, UV); mp. 122–125 °C; ^{1}H NMR (600 MHz, $CDCl_3$) δ 3.66 (s, 3H), 3.91(s, 3H), 7.13 (s, 1H, J = 3.0 Hz), 7.18 (dd, 1H, J = 9.0, 1.8 Hz), 7.21 (d, 1H, J = 9.0 Hz), 7.29 (dt, 2H, J = 9.6, 3.6 Hz), 7.46 (dt, 1H, J = 9.6, 3.6 Hz), 7.65 (dt, 1H, J = 9.6, 3.6 Hz), 7.85 (d, 2H, J = 9.0 Hz) ppm; ^{13}C NMR (151 MHz, $CDCl_3$) δ 55.3, 56.9, 106.2, 114.2, 120.4, 120.7, 123.5, 125.8, 127.1, 127.2, 131.1, 131.4, 131.9, 134.1, 141.4, 154.4, 156.4, 196.9 ppm; IR (neat) 2938, 2835, 1668, 1599, 1258, 1240, 1231 cm^{-1}; HRMS–ESI (*m/z*): $[M+H]^+$ calcd for $C_{19}H_{16}BrO_3$, 371.0277; found, 371.0255.

To a stirred suspension of CH_3PPh_3Br (48.2 g, 135 mmol) in dry THF (230 mL) at 0 °C, ^{n}BuLi (1.6 M in hexanes, 82.0 mL, 131 mmol) was added dropwise under Ar atmosphere. After 1 h, **S1** (16.7 g, 45.0 mmol) in dry THF (150 mL) was added via cannula and stirred for 24 h at 25 °C. The reaction was quenched with water, phases were separated, and the aqueous layer was extracted three times with Et_2O. The combined organic extracts were washed twice over brine, dried over Na_2SO_4 and concentrated. The residue was purified by silica gel column chromatography (hexanes/EtOAc = 5/1–3/1) to give **S2** (12.0 g, 72%) as pale-yellow solids.

S2: R_f 0.36 (hexanes/EtOAc = 5/1, UV); mp. 122–124 °C; ^{1}H NMR (600 MHz, $CDCl_3$) δ 3.67 (s, 3H), 3.91(s, 3H), 5.63 (d, 1H, J = 1.4 Hz), 6.01 (d, 1H, J = 2.1 Hz), 7.04 (td, 1H, J = 7.9, 1.4 Hz), 7.11 (d, 1H, J = 2.1 Hz), 7.12–7.19 (m, 3H), 7.21 (d, 1H, J = 9.0 Hz), 7.58 (dd, 1H, J = 8.3, 1.4 Hz), 7.71 (d, 1H, J = 9.0 Hz), 8.11 (d, 1H, J = 9.0 Hz) ppm; ^{13}C NMR (151 MHz, $CDCl_3$) δ 55.3, 56.9, 105.9, 114.9, 119.3, 121.7, 123.6, 126.3, 126.8, 127.1, 127.9, 128.0, 128.7, 130.3, 133.4, 142.3, 142.9, 152.6, 156.0 (1 signal missing) ppm; IR (neat) 2995, 2930, 2830, 1624, 1589, 1260, 1252, 1233 cm^{-1}; HRMS–ESI (*m/z*): $[M+H]^+$ calcd for $C_{20}H_{17}BrO_2$, 369.0485; found, 369.0460.

To a stirred solution of **S2** (11.1 g, 30.0 mmol) in dry THF (90 mL) at –78°C, ^{n}BuLi (1.6 M in hexanes, 22.5 mL, 36.0 mmol) was added dropwise under Ar atmosphere. After 1 h, $B(OMe)_3$ (27.0 mL, 242 mmol) was added dropwise and stirred for 24 h at 25 °C. The reaction was quenched with sat. aq. NH_4Cl, phases were separated, and the aqueous layer was extracted three times with Et_2O. The combined organic layer was washed three times over brine, dried over Na_2SO_4 and concentrated. Trituration (hexanes) afforded **S3** (7.63 g, 76%) as pale-yellow solids.

S3: mp. 147–151 °C; ^{1}H NMR (600 MHz, acetone-d_6) δ 3.69 (s, 3H), 3.94 (s, 3H), 5.35 (d, 1H, J = 1.0 Hz), 5.72 (d, 1H, J = 1.0 Hz), 6.78 (d, 1H, J = 7.6 Hz), 7.096 (brs, 1H), 7.099 (brs, 1H), 7.13 (t, 1H, J = 7.6 Hz), 7.22 (dd, 1H, J = 9.0, 2.8 Hz), 7.24 (t, 1H, J = 6.9 Hz), 7.34 (d, 1H, J = 2.8 Hz), 7.42 (d, 1H, J = 9.0 Hz), 7.73 (dd, 1H, J = 7.6, 1.4 Hz), 7.88 (d, 1H, J = 9.0 Hz), 8.08 (d, 1H, J = 9.6 Hz) ppm; ^{13}C NMR (151 MHz, acetone-d_6) δ 55.6, 57.2, 106.7, 115.2, 120.7, 122.4, 127.2, 127.37, 127.43, 127.5, 128.9, 129.3, 129.4, 131.6, 135.0, 145.7, 148.1, 152.1, 157.4 (1 signal missing) ppm; IR (neat) 3337, 3067, 3009, 2959, 2835, 1335, 1250, 1072, 1042 cm^{-1}; HRMS–ESI (*m/z*): $[M+H]^+$ calcd for $C_{26}H_{20}BO_4$, 335.1449; found, 335.1423.

Synthesis of S4[1]

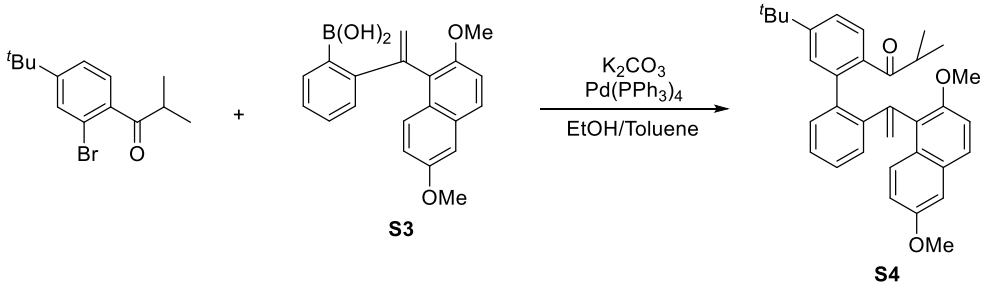

A suspension of 1-[2-bromo-4-(*tert*-butyl)phenyl]-2-methyl-1-propanone[2] (2.88 g, 10.1 mmol), **S3** (3.70 g, 11.1 mmol), K_2CO_3 (5.94 g, 43.0 mmol) and $Pd(PPh_3)_4$ (1.28 g, 1.11 mmol) in a mixed-solution of toluene (20 mL) and EtOH (80 mL) was stirred for 17 h at 95 °C under Ar atmosphere. The reaction mixture was quenched with water, phases were separated, and the aqueous layer was extracted three times with Et_2O. The combined organic layer was washed three times over brine, dried over Na_2SO_4 and concentrated. The residue was purified by silica gel column chromatography (hexanes/EtOAc = 5/1) to afford **S4** (3.08 g, 62%) as pale-yellow amorphous.

S4: R_f 0.35 (hexanes/EtOAc = 5/1, UV); ^{1}H NMR (600 MHz, $CDCl_3$, 50 °C) δ 0.86 (d, 3H, J = 6.9 Hz), 0.93 (d, 3H, J = 6.9 Hz), 1.17 (s, 9H), 2.70 (sep, 1H, J = 6.9 Hz), 3.59 (s, 3H), 3.87 (s, 3H), 5.27 (d, 1H, J = 1.4 Hz), 5.50 (s, 1H), 6.88–7.43 (m, 10H), 7.59 (d, 1H, J = 9.0 Hz), 7.85 (d, 1H, J = 9.0 Hz) ppm; ^{13}C NMR (151 MHz, $CDCl_3$, 50 °C) δ 18.3, 19.4, 31.0, 34.7, 38.8, 55.3, 56.6, 105.8, 114.9, 118.8, 122.9, 123.6, 126.6, 127.1, 127.2, 127.3, 127.6, 128.4, 128.8, 130.1, 130.3, 130.7, 137.4, 139.5, 140.5, 141.4, 142.8, 152.5, 152.8, 156.0, 210.1 ppm (1 additional signal due to its rotation); IR (film) 3055, 2963, 2934, 2903, 2868, 2835, 1682, 1595, 1250, 1234 cm^{-1}; HRMS–ESI (*m/z*): $[M+H]^+$ calcd for $C_{34}H_{37}O_3$, 493.2737; found, 493.2756.

Synthesis of 1b[1]

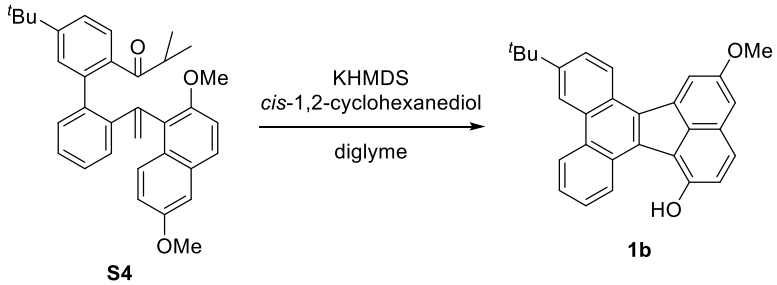

To a stirred solution of **S4** (3.08 g, 6.25 mmol) and *cis*-1,2-cyclohexanediol (144 mg, 1.24 mmol) in dry diglyme (250 mL) was added KHMDS (1.0 M in THF, 19.0 mL, 19.0 mmol). The reaction mixture was evacuated for 15 min

to degas the solvent, refilled with Ar and heated to reflux (180 °C) for 24 h with vigorous stirring. After cooling to room temperature, the reaction was quenched with 10% HCl. The aqueous layer was extracted three times with Et_2O and the combined organic layer was washed three times over brine, dried over Na_2SO_4 and evaporated. The residue was purified by silica gel column chromatography (hexanes/EtOAc = 3/1–1/1), following trituration (hexanes) to afford **1b** (1.53 g, 60%) as yellow solids. Single crystals of **1b** suitable for X-ray crystallographic analysis were successfully grown by slow evaporation of **1b** in acetone at room temperature.

1b: R_f 0.22 ($CHCl_3$, UV); mp. >250 °C; ^{1}H NMR (600 MHz, acetone-d_6) δ 1.56 (s, 9H), 4.04 (s, 3H), 7.40 (s, 1H, J = 2.1 Hz), 7.45 (d, 1H, J = 8.3 Hz), 7.66–7.73 (m, 2H), 7.85 (d, 1H, J = 9.0 Hz), 7.92 (dd, 1H, J = 8.3, 2.1 Hz), 8.40 (s, 1H, J = 2.1 Hz), 8.91 (s, 1H, J = 2.1 Hz), 8.93–9.01 (m, 2H), 10.18–10.24 (m, 1H) ppm; ^{13}C NMR (151 MHz, acetone-d_6) δ 31.7, 35.7, 56.2, 106.6, 118.0, 118.8, 120.0, 123.0, 123.8, 125.4, 126.0, 126.4, 126.9, 127.0, 128.6, 129.8, 130.2, 130.4, 131.0, 131.2, 131.4, 131.8, 137.2, 137.9, 149.2, 152.5, 159.1 ppm; IR (film) 3310, 2951, 2905, 2866, 1701, 1605 cm^{-1}; HRMS–ESI (*m/z*): $[M+H]^+$ calcd for $C_{29}H_{25}O_2$, 405.1849; found, 405.1845.

Synthesis of 1a[3]

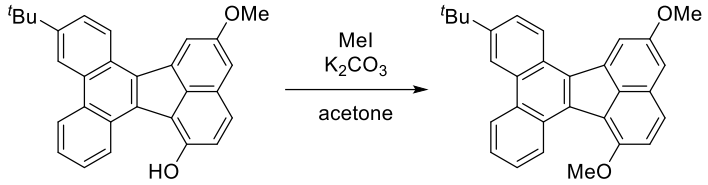

1b **1a**

To a solution of **1b** (406 mg, 1.00 mmol) and K_2CO_3 (416 mg, 3.01 mmol) in acetone (20 mL) was added MeI (200 µL, 3.21 mmol) at room temperature under Ar atmosphere. After refluxing for 2.5 h, the reaction was quenched with water. The mixture was extracted three times with EtOAc. The combined organic extracts were washed three times with brine, dried over Na_2SO_4 and concentrated. The residue was purified by silica gel column chromatography (hexanes/$CHCl_3$ = 1/2) to give **1a** (408 mg, 97%) as yellow solids. Single crystals of **1a** suitable for X-ray crystallographic analysis were successfully grown by slow evaporation of **1a** in $CHCl_3$ at room temperature.

1a: R_f 0.80 ($CHCl_3$, UV); mp. 201–202 °C; ^{1}H NMR (600 MHz, $CDCl_3$) δ 1.54 (s, 9H), 4.01 (s, 3H), 4.17 (s, 3H), 7.14 (d, 1H, J = 1.8 Hz), 7.37 (d, 1H, J = 8.4 Hz), 7.65–7.70 (m, 2H), 7.77 (d, 1H, J = 9.0 Hz), 7.78 (dd, 1H, J = 9.0, 1.2 Hz), 8.29 (d, 1H, J = 3.2 Hz), 8.77 (d, 1H, J = 1.2 Hz), 8.79–8.84 (m, 2H), 9.75–9.79 (m, 1H) ppm; ^{13}C NMR (151 MHz, $CDCl_3$) δ 31.5, 35.2, 55.9, 56.8, 104.8, 117.0, 118.1, 119.1, 121.7, 122.9, 124.5, 125.2, 125.3, 126.0, 126.1, 127.7, 128.8, 128.9, 129.5, 129.8, 130.5, 131.1, 131.3, 136.3, 137.8, 148.4, 153.3, 158.4 ppm; IR (neat) 2959, 2936, 2905, 2866, 2835, 1581 cm^{-1}; HRMS–ESI (*m/z*): $[M+H]^+$ calcd for $C_{30}H_{27}O_2$, 419.2006; found, 419.2026.

Synthesis of 1d[1]

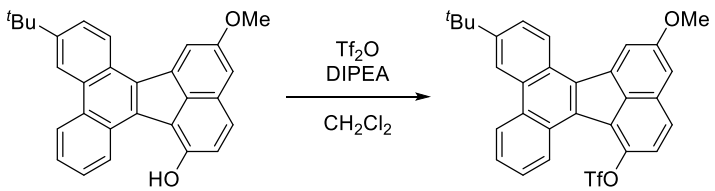

1b **1d**

To a solution of **1b** (209 mg, 0.498 mmol) and DIPEA (130 µL, 0.764 mmol) in dry CH_2Cl_2 (10 mL) was added dropwise Tf_2O (130 µL, 0.774 mmol) at 0 °C under Ar atmosphere. After stirring for 6 h at room temperature, the

reaction was quenched with sat. NH_4Cl aq. The mixture was extracted from EtOAc. The combined organic extracts were washed with brine, dried over Na_2SO_4 and concentrated. The residue was purified by silica gel column chromatography ($CHCl_3$) to give **1d** (259 mg, 97%) as orange solids. Single crystals of **1d** suitable for X-ray crystallographic analysis were successfully grown by slow evaporation of **1d** in $CHCl_3$ at room temperature.

1d: R_f 0.83 ($CHCl_3$, UV); mp. 200–202 °C; ^{1}H NMR (600 MHz, $CDCl_3$) δ 1.54 (s, 9H), 3.98 (s, 3H), 7.05 (d, 1H, J = 2.4 Hz), 7.45 (d, 1H, J = 9.0 Hz), 7.67–7.72 (m, 2H), 7.73 (d, 1H, J = 9.0 Hz), 7.77 (dd, 1H, J = 9.0, 1.8 Hz), 8.15 (d, 1H, J = 1.8 Hz), 8.65 (d, 1H, J = 9.0 Hz), 8.75 (d, 1H, J = 1.8 Hz), 8.76–8.79 (m, 1H), 8.86–8.90 (m, 1H) ppm; ^{13}C NMR (151 MHz, $CDCl_3$) δ 31.4, 35.3, 55.9, 104.4, 118.6 ($J_{C–F}$ = 322 Hz), 119.3, 119.8, 123.1, 123.3, 124.6, 125.7, 126.7, 126.8, 127.2, 128.0, 128.2, 128.8, 129.0, 131.2, 131.5, 133.7, 134.1, 139.2, 140.7, 149.8, 160.5 (2 signals missing) ppm; IR (neat) 2947, 2905, 2866, 1616, 1466, 1416, 1204, 1138 cm^{-1}; HRMS–ESI (*m/z*): $[M+K]^+$ calcd for $C_{30}H_{23}F_3KO_4S$, 575.0901; found, 575.0885.

Synthesis of 1c[1]

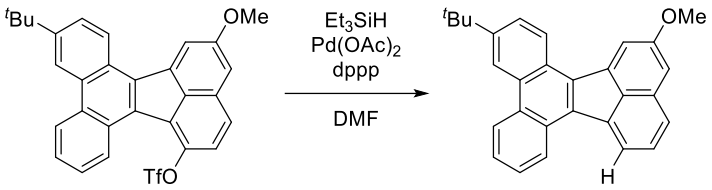

1d **1c**

1d (268 mg, 0.500 mmol), $Pd(OAc)_2$ (11.2 mg, 0.0499 mmol) and dppp (20.8 mg, 0.0504 mmol) were dissolved in dry DMF (8.0 mL) and degassed by three cycles of evacuation and Ar back-filling. Et_3SiH (210 µL, 1.32 mmol) was added at room temperature, and the mixture was heated to 60 °C and stirred for 4 h. After cooling to room temperature, the reaction was quenched with water, and the resulting precipitate collected by filtration and washed with H_2O and hexanes. The crude material was applied to a short silica pad and eluted with $CHCl_3$; the combined eluates were concentrated under reduced pressure to afford **1c** (191 mg, 98%) as yellow solids. Single crystals of **1c** suitable for X-ray crystallographic analysis were successfully grown by slow evaporation of **1c** in $CHCl_3$ at room temperature.

1c: R_f 0.76 (hexanes/EtOAc = 2/1, UV); mp. 218–220 °C; ^{1}H NMR (600 MHz, $CDCl_3$) δ 1.54 (s, 9H), 4.03 (s, 3H), 7.13 (s, 1H), 7.62 (td, 1H, J = 7.8, 3.0 Hz), 7.65–7.76 (m, 3H), 7.80 (d, 1H, J = 8.4 Hz), 8.16 (s, 1H), 8.31–8.38 (m, 1H), 8.73 (dd, 1H, J = 9.0, 3.6 Hz), 8.76 (s, 1H), 8.79 (d, 1H, J = 8.4 Hz), 8.84 (d, 1H, J = 7.2 Hz) ppm; ^{13}C NMR (151 MHz, $CDCl_3$) δ 31.5, 35.2, 55.9, 104.7, 118.4, 119.2, 122.5, 123.5, 124.5, 125.1, 125.6, 126.1, 126.4, 126.9, 127.6, 127.7, 128.3, 129.6, 129.9, 130.5, 131.1, 132.9, 134.4, 137.5, 139.1, 148.9, 160.0 ppm; IR (neat) 3046, 2955, 2899, 2862, 2826, 1614, 1467, 1234 cm^{-1}; HRMS–FAB (*m/z*): $[M+H]^+$ calcd for $C_{29}H_{25}O$, 389.1905; found, 389.1898

Synthesis of 1e[3]

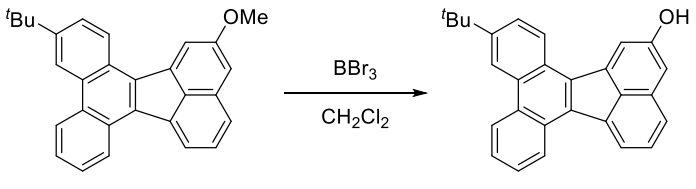

1c **1e**

To a solution of **1c** (38.6 mg, 0.0993 mmol) in CH_2Cl_2 (1.0 mL) was added dropwise BBr_3 (1.0 M in CH_2Cl_2, 0.15 mL, 0.15 mmol) at 0 °C under Ar atmosphere. After stirring for 3 h at room temperature, the reaction was quenched

with ice water. The mixture was extracted three times with EtOAc. The combined organic extracts were washed with brine, dried over Na_2SO_4 and concentrated. The crude product was purified by preparative TLC (silica gel, $CHCl_3$) to afford **1e** (35.9 mg, 97%) as brownish-yellow solids.

1e: R_f 0.30 ($CHCl_3$, UV); mp. 139–143 °C; ^{1}H NMR (600 MHz, $CDCl_3$) δ 1.49 (s, 9H), 5.65 (brs, 1H), 7.04 (s, 1H), 7.47 (t, 1H, J = 7.6 Hz), 7.54 (d, 1H, J = 8.3 Hz), 7.57–7.64 (m, 2H), 7.66 (d, 1H, J = 9.0 Hz), 7.97 (s, 1H), 8.15 (d, 1H, J = 6.9 Hz), 8.52 (d, 1H, J = 8.3 Hz), 8.63–8.73 (m, 3H) ppm; ^{13}C NMR (151 MHz, $CDCl_3$) δ 31.4, 35.2, 108.8, 116.8, 119.1, 122.7, 123.3, 124.3, 124.9, 125.4, 126.0, 126.1, 126.8, 127.4, 128.3, 129.5, 129.8, 130.4, 131.0, 132.7, 134.2, 137.4, 139.5, 148.7, 155.4 (1 signal missing) ppm; IR (neat) 3287, 2953, 2903, 2864, 1614, 1595, 1418, 1144 cm^{-1}; HRMS–FAB (m/z): $[M+H]^+$ calcd for $C_{28}H_{23}O$, 375.1749; found, 375.1744.

Synthesis of 3f[4]

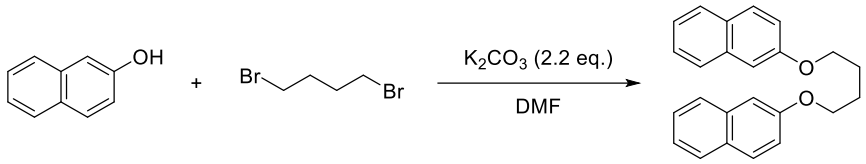

3f

2-Naphthol (216 mg, 1.50 mmol) and K_2CO_3 (456 mg, 3.30 mmol) were stirred in dry DMF (7.5 mL) at 80 °C under Ar atmosphere. 1,4-Dibromobutane (356 mg, 1.65 mmol) in dry DMF (5.0 mL) was added dropwise after which it was stirred at 80 °C for 17 h. The reaction mixture was then poured into water and extracted with $CHCl_3$. The organic layer was washed with water and brine, dried over Na_2SO_4 and concentrated. The crude product was purified by silica gel column chromatography ($CHCl_3$/hexane = 1/2–1/1) to afford **3f** (99.0 mg, 39%) as white solids.

3f: R_f 0.47 (hexanes/$CHCl_3$ = 1/1, UV); mp. 184–186 °C; ^{1}H NMR (600 MHz, $CDCl_3$) δ 2.07–2.13 (m, 4H), 4.16–4.24 (m, 4H), 7.13–7.19 (m, 4H), 7.33 (t, 2H, J = 7.8 Hz), 7.43 (t, 2H, J = 7.8 Hz), 7.72 (d, 2H, J = 7.8 Hz), 7.74 (d, 2H, J = 9.6 Hz), 7.77 (d, 2H, J = 8.4 Hz) ppm; ^{13}C NMR (151 MHz, $CDCl_3$) δ 26.0, 67.4, 106.6, 118.9, 123.5, 126.3, 126.7, 127.6, 128.9, 129.4, 134.6, 156.9 ppm; IR (neat) 3059, 3032, 2936, 2882, 2855, 1624, 1597, 1258, 1215, 1177, 1049 cm^{-1}; HRMS–ESI (*m/z*): $[M+H]^+$ calcd for $C_{24}H_{23}O_2$, 343.1693; found, 343.1681.

3. Optimization of reaction condition

3-1. General reaction setup

Reaction setup A

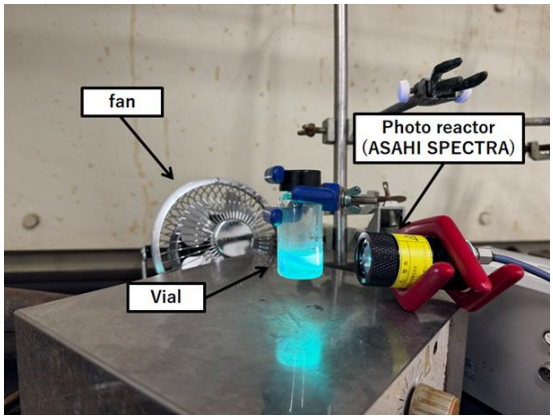

Reaction setup B

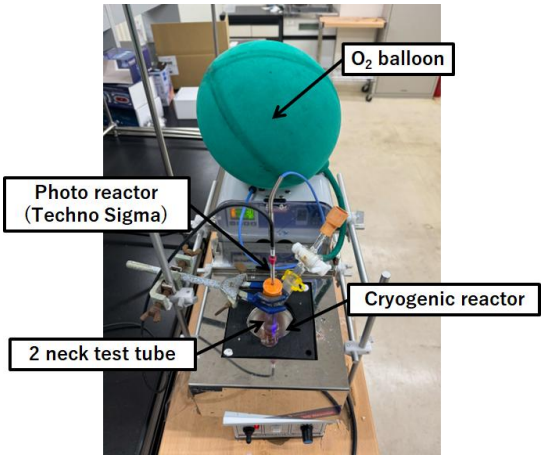

3-2. Dibenzo[*j*,*l*]fluoranthene **1a** as a model substrate (**Reaction setup B**)

Table S1. Optimization of solvent

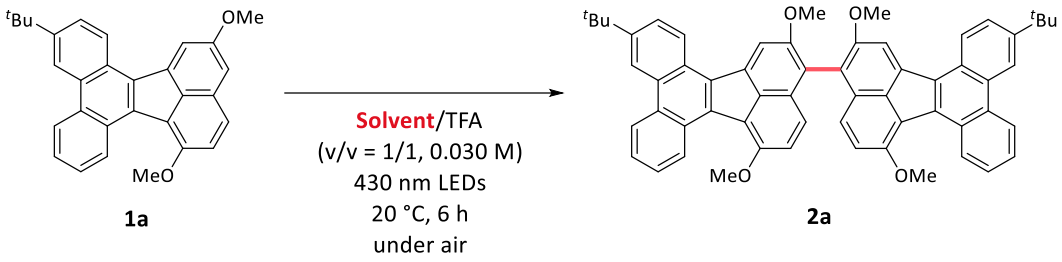

		Yield [%]*	
Entry	**Solvent**	**2a**	**1a** (recovered)
1	Toluene	84	0
2	Et_2O	19	64
3	**CH_2Cl_2**	**92**	**0**
4	$(CH_2Cl)_2$	94	0
5	MeCN	trace	96
6	DMSO	0	95
7	MeOH	0	>99
8	HFIP	20	75

*Reaction yields were determined by ^{1}H NMR analysis using Ph_3CH as an internal standard. HFIP, 1,1,1,3,3,3-hexafluoro-2-propanol

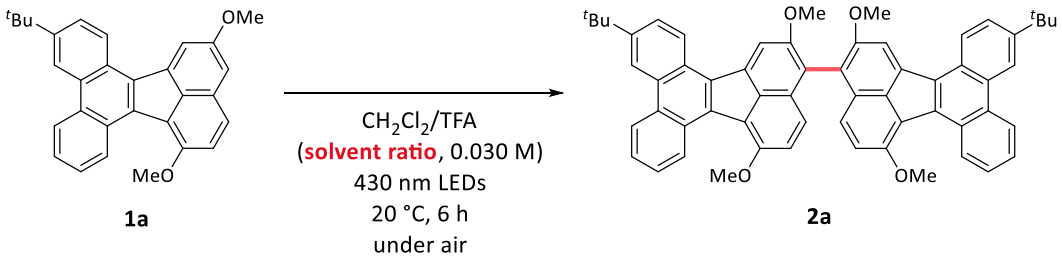

Table S2. Optimization of solvent ratio of CH_2Cl_2 and TFA as a mixed-solvent

		Yield [%]*	
Entry	**CH_2Cl_2/TFA ratio**	**2a**	**1a** (recovered)
1	99.995/0.005	0	85
2	99/1	36	60
3	**90/10**	**90(85)**	**0**
4	50/50	92	0

*Reaction yields were determined by ^{1}H NMR analysis using Ph_3CH as an internal standard. Isolated yield was shown in parentheses.

Table S3. Optimization of acids

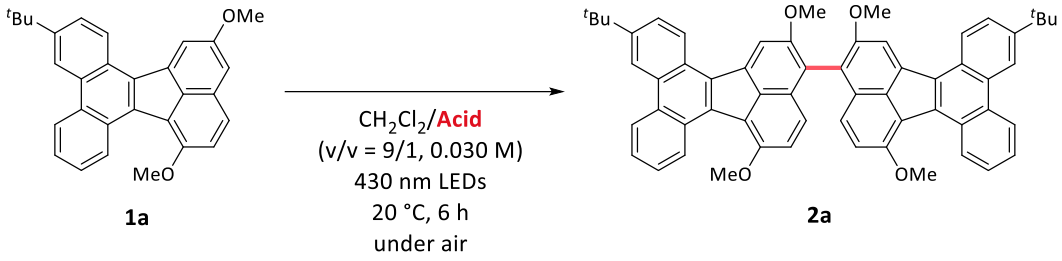

Entry	Acid	Yield [%]*	
		2a	**1a** (recovered)
1	AcOH	0	93
2	**TFA**	**90(85)**	**0**
3	MsOH	90	0
4	TfOH	0	0

*Reaction yields were determined by ^{1}H NMR analysis using Ph_3CH as an internal standard. Isolated yield was shown in parentheses.

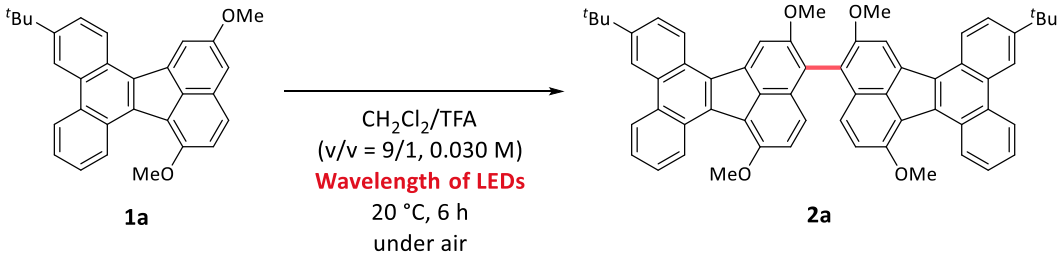

Table S4. Optimization of wavelength of LEDs

Entry	Wavelength of LEDs [nm]	Yield [%]*	
		2a	**1a** (recovered)
1	365	82	0
2	**405**	**90(85)**	**0**
3	505	99	Trace
4	568	74	10
5	615	11	93
6	730	10	78
7	white	55	40
8	white**	98	0

*Reaction yields were determined by ^{1}H NMR analysis using Ph_3CH as an internal standard. Isolated yield was shown in parentheses. **Reaction was run for 24 h.

Table S5. Oxidative biaryl coupling using known conditions

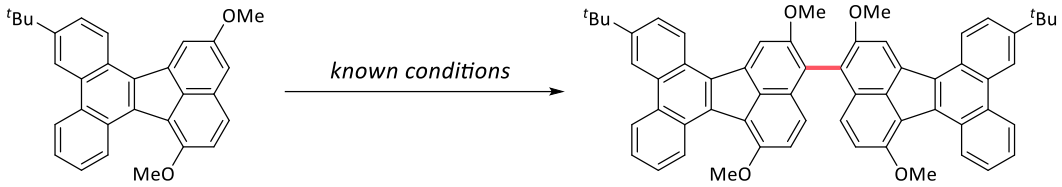

1a **2a**

Entry	conditions	Yield [%]*	
		2a	**1a** (recovered)
1[a]	$CuSO_4/Al_2O_3$, PhCl, 140 °C, 24 h	0	99
2[b]	$[Cu(TMEDA)(OH)]_2Cl_2$, CH_2Cl_2, 20 °C, 24 h	0	96
3[c]	$VO(acac)_2$, CH_2Cl_2, 20 °C, 24 h, O_2	0	88
4[d]	$FeCl_3$, EtOH, reflux, 24 h	(8)	(87)
5[e]	DDQ and TfOH, CH_2Cl_2, 0 °C, 10 min.	21	3

*Reaction yields were determined by ^{1}H NMR analysis using Ph_3CH as an internal standard. Isolated yield was shown in parentheses. Reaction conditions: [a]**1a** (0.050 mmol) and $CuSO_4/Al_2O_3$ (0.010 mmol) in PhCl (1.0 mL) at 140 °C for 24 h[5]; [b]**1a** (0.050 mmol) and $[Cu(TMEDA)(OH)]_2Cl_2$ (0.0050 mmol) in CH_2Cl_2 (5.0 mL) at 20 °C for 24 h[6]; [c]**1a** (0.050 mmol) and $VO(acac)_2$ (0.0050 mmol) in CH_2Cl_2 (1.0 mL) at 20 °C for 24 h[7]; [d]**1a** (0.050 mmol) and $FeCl_3$ (0.20 mmol) in EtOH (1.4 mL) at 95 °C (reflux) for 15 h[8]; [e]**1a** (0.050 mmol), DDQ (0.10 mmol) and TfOH (0.30 mmol) in CH_2Cl_2 (5.0 mL) at 0 °C for 10 min.[9]

3-3. 2-Naphthol (**3d**) as a model substrate (**Reaction setup A**)

Table S6. Optimization of reaction temperature

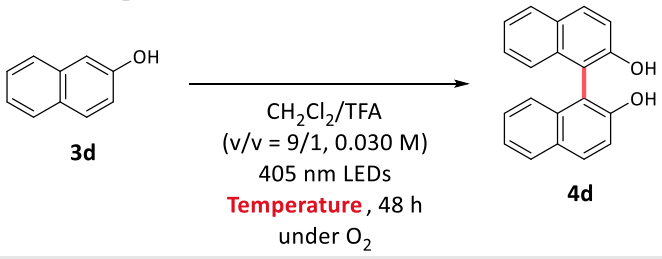

3d **4d**

Entry	Temperature [°C]	Yield [%]*	
		4d	**3d** (recovered)
1	20	37	0
2	10	33	0
3	0	43	0
4	–10	44	0
5	**–30**	**46**	**10**

*Reaction yields were determined by ^{1}H NMR analysis using Ph_3CH as an internal standard.

Table S7. Concentration effect

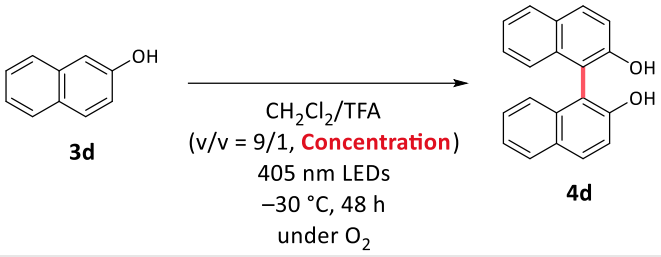

		Yield [%]*	
Entry	**Concentration [M]**	**4d**	**3d** (recovered)
1	0.030	46	10
2	**0.10**	**22**	**64**

*Reaction yields were determined by ^{1}H NMR analysis using Ph_3CH as an internal standard.

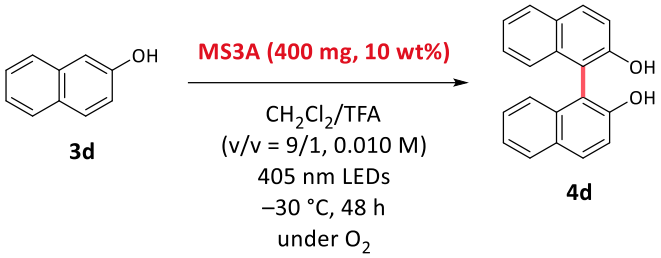

Table S8. The effect of molecular sieves

		Yield [%]*	
Entry	**deviation**	**4d**	**3d** (recovered)
1	w/o MS3A	22	64
2	**none**	**30**	**50**
3	w/o TFA	5	42
4	w/o TFA and 405 nm LEDs	5	57

*Reaction yields were determined by ^{1}H NMR analysis using Ph_3CH as an internal standard.

The effect of molecular sieves (MS) 3A is summarized in Table S8. Addition of MS3A (10 wt%) afforded a slight increase in yield, likely due to the removal of residual water and the generated H_2O_2 by MS3A (entry 1 and 2).[10] Control experiments without TFA and/or light showed the reaction to be effectively suppressed, indicating that MS3A does not facilitate a background pathway (entry 3 and 4).

Table S9. Optimization of solvent ratio of CH_2Cl_2 and TFA as a mixed-solvent

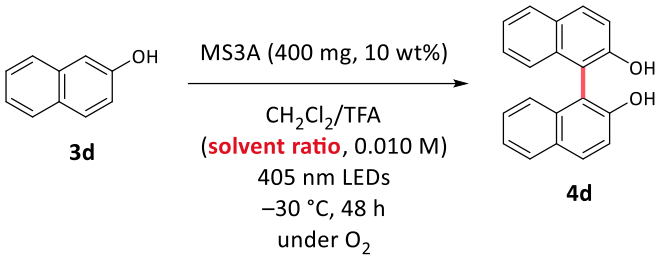

Entry	CH_2Cl_2/TFA ratio	Yield [%]*	
		4d	**3d** (recovered)
1	9/1	30	50
2	**1/1**	**78 (70)**	**0**

*Reaction yields were determined by ^{1}H NMR using triphenylmethane as an internal standard. Isolated yield was shown in parentheses.

3-4. Optimization for substrate **3** (**Reaction setup A**)

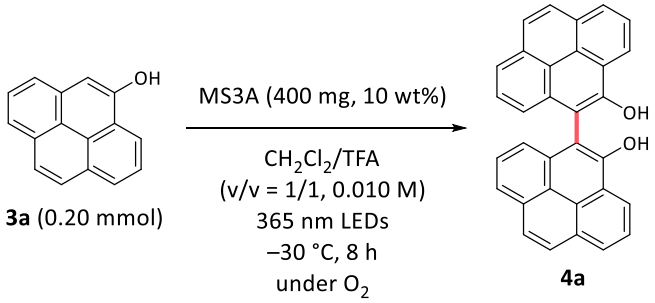

Table S10. Optimization for **3a**

Entry	**deviation**	Yield [%]*	
		4b	**3b** (recovered)
1	none	82	0
2	0 °C instead of –30 °C 48 h instead of 8 h	31	0
3	48 h instead of 8 h	38	0

*Isolated yield.

Table S11. Optimization for **3b**

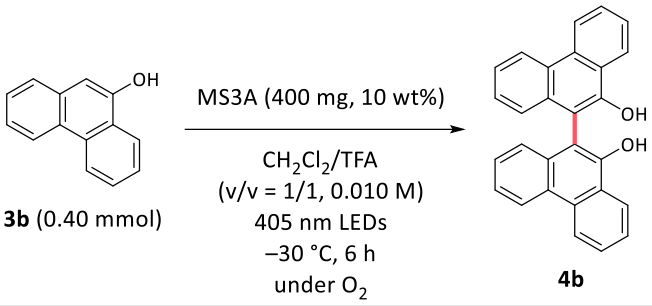

3b (0.40 mmol)

4b

Entry	**deviation**	Yield [%]*	
		4b	**3b** (recovered)
1	none	76	0
2	365 nm instead of 405 nm LEDs 48 h instead of 6 h	complex mixture	
3	24 h instead of 6 h	46	0

*Isolated yield.

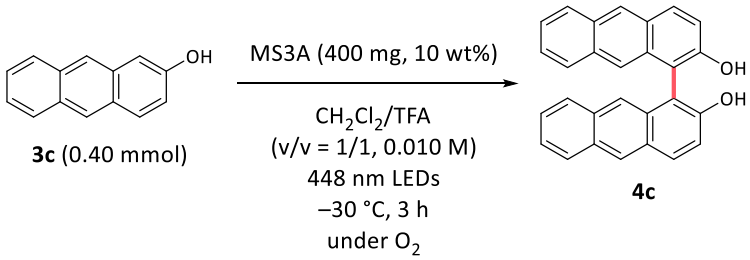

3c (0.40 mmol)

4c

Table S12. Optimization for **3c**

Entry	**deviation**	Yield [%]**	
		4c	**3c** (recovered)
1	none	48	0
2*	none	43	0
3*	365 nm instead of 448 nm LEDs 6 h instead of 3 h	<29	0
4*	405 nm instead of 448 nm LEDs	41	0

*0.20 mmol of **3c**; **Isolated yield.

Table S13. Optimization for **3g**

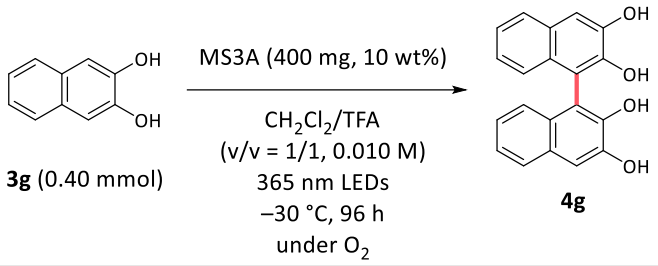

Entry	deviation	Yield [%]*	
		4g	**3g** (recovered)
1	none	(53)	0
2	405 nm instead of 365 nm LEDs 48 h instead of 96 h	56	11
3	48 h instead of 96 h	14	40

*Reaction yields were determined by ^{1}H NMR using triphenylmethane as an internal standard. Isolated yield was shown in parentheses.

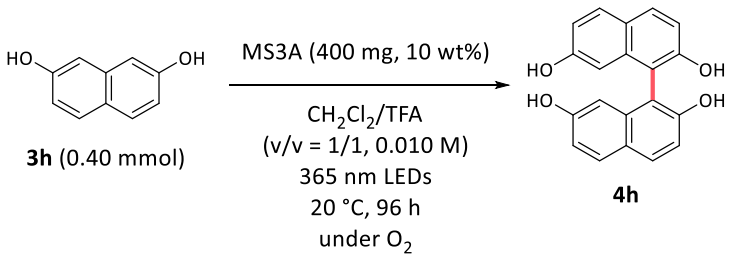

Table S14. Optimization for **3h**

Entry	deviation	Yield [%]*	
		4h	**3h** (recovered)
----------**reaction setup B**----------			
1	none	(58)	(23)
2	405 nm instead of 365 nm LEDs 48 h instead of 96 h	32	54
----------**reaction setup A**----------			
3	405 nm instead of 365 nm LEDs (reaction setup B)	43	10
4	395 nm instead of 365 nm LEDs (reaction setup B)	58	22
5	395 nm instead of 365 nm LEDs (reaction setup B) 48 h instead of 96 h	50	12
6	365 nm instead of 365 nm LEDs (reaction setup B)	50	23

*Reaction yields were determined by ^{1}H NMR using triphenylmethane as an internal standard. Isolated yield was shown in parentheses.

4. Photo-induced oxidative biaryl coupling of polycyclic aromatic hydrocarbons

General procedure for substrate 1 (reaction setup A)

To a 4 mL vial equipped with a magnetic stir bar were added the substrate **1** and CH_2Cl_2/TFA (v/v = 9/1) under air. The mixture was irradiated with an appropriate LED light while being stirred at room temperature under fan cooling until completion, as monitored by TLC. The reaction was quenched by pouring the mixture into sat. $NaHCO_3$ aq. The aqueous phase was extracted three times with EtOAc; the combined organic layers were washed three times with brine, dried over Na_2SO_4, filtered, and concentrated under reduced pressure. The crude product was purified by preparative TLC (silica gel) to afford the biaryl compound **2**.

Synthesis of 2a

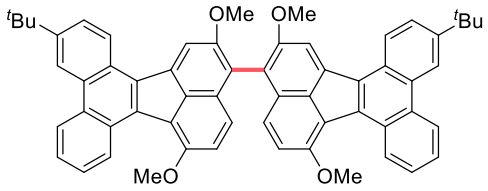

The general procedure using **1a** (12.8 mg, 0.0306 mmol; 0.030 M) afforded **2a** (10.9 mg, 85%) as orange solids. [Reaction time: 6 h, 430 nm LED, preparative TLC (hexanes/$CHCl_3$ = 4/1)] Single crystals of **2a** suitable for X-ray crystallographic analysis were successfully grown by slow diffusion of hexanes into the solution of **2a** in $CHCl_3$ at room temperature.

2a: R_f 0.43 (hexanes/$CHCl_3$ = 1/1, UV); mp. >250 °C; ^{1}H NMR (600 MHz, $CDCl_3$) δ 1.58 (s, 18H), 4.00 (s, 6H), 4.18 (s, 6H), 7.28 (d, 2H, J = 9.0 Hz), 7.41 (d, 2H, J = 9.0 Hz), 7.67–7.74 (m, 4H), 7.89 (dd, 2H, J = 9.0, 2.4 Hz), 8.63 (s, 2H), 8.84 (s, 2H, J = 1.8 Hz), 8.84–8.88 (m, 2H), 8.95 (d, 2H, J = 9.0 Hz), 9.79–9.84 (m, 2H) ppm; ^{13}C NMR (151 MHz, $CDCl_3$) δ 31.5, 35.2, 56.8, 58.2, 114.6, 117.3, 119.3, 120.4, 121.4, 122.9, 124.3, 125.5, 125.9, 126.1, 127.7, 128.82, 128.84, 129.7, 129.9, 130.6, 131.1, 131.6, 135.9, 137.7, 148.4, 153.8, 156.0 (1 signal missing) ppm; IR (neat) 2951, 2905, 2862, 2839, 1578 cm^{-1}; HRMS–FAB (m/z): $[M+H]^+$ calcd for $C_{60}H_{51}O_4$, 835.3787; found, 835.3771

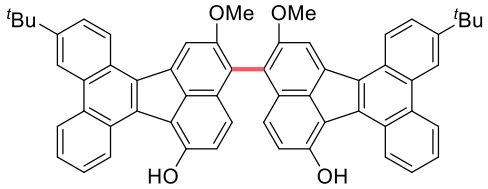

Synthesis of 2b

The general procedure using **1b** (12.8 mg, 0.0306 mmol; 0.030 M) afforded **2b** (12.7 mg, 99%) as yellow solids. [Reaction time: 6 h, 385 nm LED, preparative TLC ($CHCl_3$)]

2b: R_f 0.09 ($CHCl_3$, UV); mp. >250 °C; ^{1}H NMR (600 MHz, acetone-d_6) δ 1.60 (s, 18H), 4.04 (s, 6H), 7.30 (s, 4H), 7.69–7.75 (m, 4H), 7.95 (dd, 2H, J = 8.4, 1.2 Hz), 8.82 (s, 2H), 8.97 (s, 2H, J = 2.4 Hz), 8.98–9.02 (m, 2H), 9.16 (d, 2H, J = 7.8 Hz), 10.20–10.24 (m, 2H), 10.25 (brs, 2H) ppm; ^{13}C NMR (151 MHz, acetone-d_6) δ 31.8, 35.8, 57.9, 114.5, 118.5, 120.1, 121.6, 123.2, 123.9, 125.6, 126.5, 126.7, 126.9, 127.0, 128.7, 129.7, 130.1, 130.5, 130.6, 131.3,

131.81, 131.84, 136.6, 137.7, 149.3, 152.8, 156.8 ppm; IR (neat) 3281, 2953, 2907, 2860, 1589, 1479, 1356, 1260 cm^{-1}; HRMS–FAB (*m*/*z*): $[M+H]^+$ calcd for $C_{58}H_{47}O_4$, 807.3474; found, 807.3467.

Synthesis of 2c

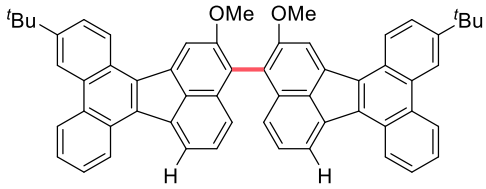

The general procedure using **1c** (11.2 mg, 0.0288 mmol; 0.030 M) afforded **2c** (8.6 mg, 77%) as orange solids. [Reaction time: 24 h, 385 nm LED, preparative TLC (hexanes/$CHCl_3$ = 3/1)]

2c: R_f 0.52 (hexanes/$CHCl_3$ = 1/1, UV); mp. >250 °C; ^{1}H NMR (600 MHz, $CDCl_3$) δ 1.58 (s, 18H), 4.02 (s, 6H), 7.35 (d, 2H, *J* = 7.8 Hz), 7.49 (t, 2H, *J* = 7.8 Hz), 7.70 (t, 2H, *J* = 7.2 Hz), 7.74 (t, 2H, *J* = 7.2 Hz), 7.90 (dd, 2H, *J* = 9.0, 1.8 Hz), 8.41 (d, 2H, *J* = 6.6 Hz), 8.51 (s, 2H), 8.83 (s, 2H, *J* = 1.2 Hz), 8.85 (d, 2H, *J* = 8.4 Hz), 8.87 (d, 2H, *J* = 9.0 Hz), 8.91 (d, 2H, *J* = 7.8 Hz) ppm; ^{13}C NMR (151 MHz, $CDCl_3$) δ 31.5, 35.3, 58.0, 114.3, 119.4, 120.4, 123.3, 123.6, 124.4, 125.1, 125.7, 126.1, 126.2, 127.1, 127.7, 128.4, 130.1, 130.4, 130.7, 131.1, 133.2, 134.1, 137.8, 139.3, 148.9, 157.5 (1 signal missing) ppm; IR (neat) 3063, 2951, 2901, 2862, 2839, 1593, 1462 cm^{-1}; HRMS–FAB (*m*/*z*): $[M+H]^+$ calcd for $C_{58}H_{47}O_2$, 775.3576; found, 775.3571.

Synthesis of 2d

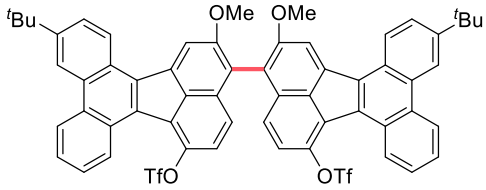

The general procedure using **1d** (16.2 mg, 0.0302 mmol; 0.030 M) afforded **2d** (4.5 mg, 28%) as orange solids. [Reaction time: 6 h, 385 nm LED, preparative TLC (hexanes/$CHCl_3$ = 5/1)] Single crystals of **2d** suitable for X-ray crystallographic analysis were successfully grown by slow diffusion of hexanes into the solution of **2d** in EtOAc at room temperature.

2d: R_f 0.16 (hexanes/$CHCl_3$ = 3/1, UV); mp. >250 °C; ^{1}H NMR (600 MHz, acetone-d_6) δ 1.60 (s, 18H), 4.15 (s, 6H), 7.59 (d, 2H, *J* = 9.0 Hz), 7.62 (d, 2H, *J* = 9.0 Hz), 7.77–7.83 (m, 4H), 7.99 (dd, 2H, *J* = 9.0, 1.8 Hz), 8.90 (s, 2H), 8.95 (dt, 2H, *J* = 10.2, 2.4 Hz), 8.99 (s, 2H, *J* = 1.8 Hz), 9.04 (dt, 2H, *J* = 9.6, 2.4 Hz), 9.11 (d, 2H, *J* = 9.0 Hz) ppm; ^{13}C NMR (151 MHz, acetone-d_6) δ 31.6, 36.0, 57.7, 116.5, 119.5 (J_{C-F} = 321 Hz), 120.3, 120.5, 124.5, 124.7, 126.1, 127.1, 127.6, 127.8, 127.88, 127.93, 128.8, 129.2, 129.3, 130.2, 130.4, 132.1, 132.7, 133.9, 135.6, 140.1, 142.1, 151.3, 159.3 ppm; IR (neat) 2953, 2905, 2860, 1591, 1423, 1207, 1140 cm^{-1}; HRMS–FAB (*m*/*z*): $[M+H]^+$ calcd for $C_{60}H_{45}F_6O_8S_2$, 1071.2460; found,1071.2457.

Synthesis of 2e

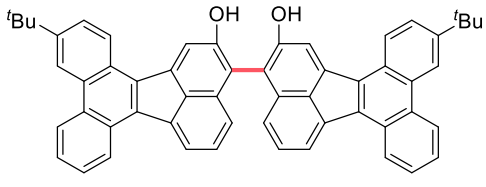

The general procedure using **1e** (11.2 mg, 0.0298 mmol; 0.030 M) afforded **2e** (7.1 mg, 64%) as yellow solids. [Reaction time: 6 h, 430 nm LED, preparative TLC (hexanes/$CHCl_3$ = 1/1)]

2e: R_f 0.15 (hexanes/$CHCl_3$ = 1/1, UV); mp. >250 °C; ^{1}H NMR (600 MHz, $CDCl_3$) δ 1.57 (s, 18H), 5.58 (brs, 2H), 7.37 (d, 2H, *J* = 8.4 Hz), 7.54 (t, 2H, *J* = 7.2 Hz), 7.68–7.77 (m, 4H), 7.86 (d, 2H, *J* = 9.0 Hz), 8.39 (d, 2H, *J* = 7.2 Hz), 8.44 (s, 2H), 8.77–8.91 (m, 8H) ppm; ^{13}C NMR (151 MHz, $CDCl_3$) δ 31.5, 35.3, 110.8, 117.0, 119.4, 123.2, 123.6, 124.4, 124.9, 125.1, 125.8, 126.4, 127.1, 127.5, 127.9, 129.4, 129.7, 129.8, 130.7, 131.4, 132.7, 134.7, 138.2, 140.9, 149.2, 154.8 ppm; IR (neat) 3480, 2953, 2905, 2862, 1595 cm^{-1}; HRMS–FAB (*m*/*z*): $[M+H]^+$ calcd for $C_{56}H_{43}O_2$, 747.3263; found, 747.3256.

Synthesis of 2f

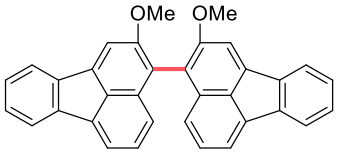

The general procedure using **1f** (46.4 mg, 0.200 mmol; 0.10 M) afforded **2f** (34.2 mg, 74%) as orangish yellow solids. [MsOH instead of TFA, O_2 saturated, not air, reaction time: 24 h, 365 nm LED, preparative TLC (hexanes/$CHCl_3$ = 1/1)] Single crystals of **2f** suitable for X-ray crystallographic analysis were successfully grown by slow evaporation of **2f** in $CHCl_3$ at room temperature.

2f: R_f 0.14 (hexanes/$CHCl_3$ = 1/1, UV); mp. 135–137 °C; ^{1}H NMR (600 MHz, $CDCl_3$) δ 3.90 (s, 6H), 7.21 (d, 2H, *J* = 8.3 Hz), 7.37–7.44 (m, 6H), 7.79 (d, 2H, *J* = 6.9 Hz), 7.89–7.93 (m, 4H), 7.94–7.98 (m, 2H) ppm; ^{13}C NMR (151 MHz, $CDCl_3$) δ 57.5, 108.9, 118.2, 119.7, 121.3, 121.5, 125.4, 127.4, 127.7, 128.0, 128.4, 131.0, 136.7, 138.1, 139.2, 140.2, 157.6 ppm; IR (neat) 3055, 3001, 2963, 2932, 2847, 1609, 1439 cm^{-1}; HRMS–ESI (*m*/*z*): $[M+H]^+$ calcd for $C_{34}H_{23}O_2$, 463.1693; found, 463.1695.

General procedure for substrate 3 (reaction setup B)

A 10 mL two-necked test tube containing MS3A (0.1 g/0.1 mmol of substrate **3**) was activated in a microwave oven (500 W) for 1 min, three times, then evacuated and allowed to return to room temperature. A stir bar and substrate **3** were added, an O_2 balloon was attached, and the vessel was evacuated and backfilled with O_2 three times. CH_2Cl_2/TFA (v/v = 1/1) was then added at room temperature. The mixture was irradiated with appropriate LEDs at the designated temperature and stirred. The reaction was quenched by pouring the mixture into sat. $NaHCO_3$ aq. The aqueous phase was extracted three times with EtOAc; the combined organic layers were washed three times with brine, dried over Na_2SO_4, filtered, and concentrated under reduced pressure. The crude product was purified by preparative TLC (silica gel) to afford the biaryl compound **4**.

Synthesis of 4a

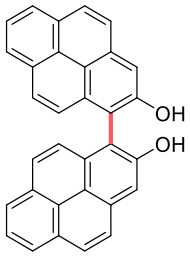

The general procedure using **3a** (43.6 mg, 0.200 mmol; 0.10 M) afforded **4a** (35.6 mg, 82%) as brown solids. [Reaction time and temperature: 8 h, –30 °C, 365 nm LED, preparative TLC ($CHCl_3$)] Single crystals of **4a** suitable for X-ray crystallographic analysis were successfully grown by slow diffusion of hexanes into the solution of **4a** in EtOAc at room temperature.

4a: R_f 0.13 ($CHCl_3$, UV); mp. 242–245 °C; ^{1}H NMR (600 MHz, $CDCl_3$) δ 5.30 (brs, 2H), 7.41 (d, 2H, J = 9.0 Hz), 7.91 (d, 2H, J = 9.0 Hz), 7.97 (t, 2H, J = 7.6 Hz), 8.01 (s, 2H), 8.11 (d, 2H, J = 9.0 Hz), 8.14 (d, 2H, J = 6.9 Hz), 8.17 (d, 2H, J = 9.0 Hz), 8.23 (d, 2H, J = 7.6 Hz) ppm; ^{13}C NMR (151 MHz, $CDCl_3$) δ 112.1, 113.7, 120.5, 124.0, 124.6, 125.4, 125.9, 126.0, 126.7, 129.0, 129.4, 129.9, 130.3, 132.1, 133.9, 152.9 ppm; IR (neat) 3418, 3040, 2955, 2916, 1582, 1539 cm^{-1}; HRMS–FAB (m/z): $[M+H]^+$ calcd for $C_{32}H_{19}O_2$, 435.1385; found, 435.1390.

Synthesis of 4b

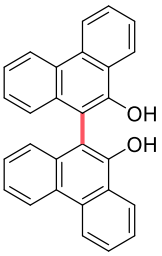

The general procedure using **3b** (77.3 mg, 0.398 mmol; 0.10 M) afforded **4b** (58.5 mg, 76%) as pale-yellow solids. [Reaction time and temperature: 6 h, –30 °C, 405 nm LED, preparative TLC (hexanes/$CHCl_3$ = 1/1)] Spectral data were in full agreement with reported data.[11]

Scale-up experiment

A 30 mL two-necked flask containing MS3A (1.0 g) was activated in a microwave oven (500 W) for 1 min, three times, then evacuated and allowed to return to room temperature. A stir bar and **3b** (194 mg, 1.00 mmol) were added, an O_2 balloon was attached, and the vessel was evacuated and backfilled with O_2 three times. CH_2Cl_2/TFA (v/v = 1/1, 10 mL) was then added at room temperature. The mixture was irradiated with 405 nm LEDs at –30 °C and stirred for 12 h. The reaction was quenched by pouring the mixture into sat. $NaHCO_3$ aq. The aqueous phase was extracted three times with EtOAc; the combined organic layers were washed three times with brine, dried over Na_2SO_4, filtered, and concentrated under reduced pressure. The crude product was purified by silica gel column chromatography (hexanes/$CHCl_3$ = 1/1–1/2) to afford the biaryl compound **4b** (164 mg, 85%).

Synthesis of 4c

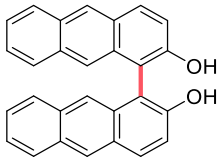

The general procedure using **3c** (77.9 mg, 0.401 mmol; 0.10 M) afforded **4c** (36.9 mg, 48%) as pale-yellow solids. [Reaction time and temperature: 3 h, –30 °C, 448 nm LED, preparative TLC ($CHCl_3$)] Spectral data were in full agreement with reported data.[12]

Synthesis of 4d

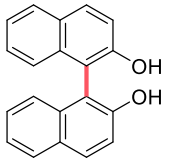

The general procedure using **3d** (77.3 mg, 0.398 mmol; 0.10 M) afforded **4d** (58.5 mg, 76%) as pale-yellow solids. [Reaction time and temperature: 48 h, –30 °C, 405 nm LED, preparative TLC (hexanes/$CHCl_3$ = 1/1)] Spectral data were in full agreement with reported data.[11]

Synthesis of 4e

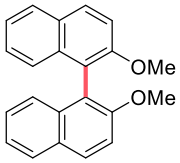

The general procedure using **3e** (62.9 mg, 0.398 mmol; 0.10 M) afforded **4e** (7.4 mg, 12%) as white solids; substrate **3e** was recovered (43.8 mg, 70%). [Reaction time and temperature: 48 h, –30 °C, 405 nm LED, preparative TLC (hexanes/$CHCl_3$ = 3/1)] Spectral data were in full agreement with reported data.[13]

Synthesis of 4g

The general procedure using **3g** (64.6 mg, 0.403 mmol; 0.10 M) afforded **4g** (33.9 mg, 53%) as white solids. [Reaction time and temperature: 96 h, –30 °C, 365 nm LED, preparative TLC ($CHCl_3$/MeOH = 20/1)] Spectral data were in full agreement with reported data.[11]

Synthesis of 4h

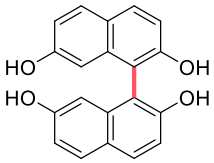

The general procedure using **3h** (63.6 mg, 0.397 mmol; 0.10 M) afforded **4h** (36.5 mg, 58%) as pale-yellow solids; substrate **3h** was recovered (14.9 mg, 23%). [Reaction time and temperature: 96 h, 20 °C, 365 nm LED, preparative TLC (hexanes/EtOAc = 3/1)] Spectral data were in full agreement with reported data.[11]

Synthesis of 4i

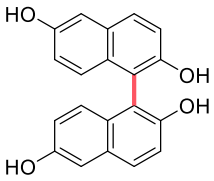

The general procedure using **3i** (64.1 mg, 0.400 mmol; 0.10 M) afforded **4i** (46.7 mg, 72%) as pale-yellow solids. [Reaction time and temperature: 48 h, 20 °C, 405 nm LED, preparative TLC ($CHCl_3$/MeOH = 10/1)] Spectral data were in full agreement with reported data.[14]

Synthesis of 4j and 4j'

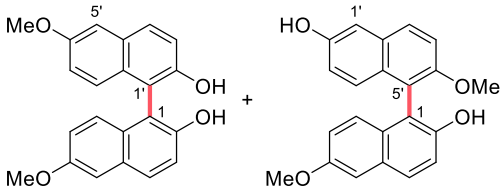

4j **4j'**

The general procedure using **3j** (20.9 mg, 0.120 mmol; 0.030 M) afforded **4j** (11.2 mg, 54%) as white solids and **4j'** (1.6 mg, 7.7%) as white solids; substrate **3j** was recovered (2.6 mg, 12%). [Reaction time and temperature: 24 h, 20 °C, 405 nm LED, preparative TLC (hexanes/EtOAc = 2/1)] Spectral data of **4j** were in full agreement with reported data.[11]

4j': R_f 0.27 (hexanes/EtOAc = 2/1, UV); mp. >250 °C; ^{1}H NMR (600 MHz, $CDCl_3$) δ 3.77 (s, 3H), 3.90 (s, 3H), 4.79 (brs, 1H), 4.91 (brs, 1H), 6.90 (dd, 1H, J = 9.0, 2.8 Hz), 6.91 (dd, 1H, J = 9.0, 2.8 Hz), 6.96 (d, 1H, J = 9.0 Hz), 7.08 (d, 1H, J = 9.0 Hz), 7.18 (d, 1H, J = 2.8 Hz), 7.22 (d, 1H, J = 2.1 Hz), 7.32 (d, 1H, J = 9.0 Hz), 7.44 (d, 1H, J = 9.0 Hz), 7.79 (d, 1H, J = 9.0 Hz), 7.87 (d, 1H, J = 9.0 Hz) ppm; ^{13}C NMR (151 MHz, $CDCl_3$) δ 55.3, 56.9, 106.4, 109.8, 114.9, 115.4, 115.9, 117.8, 118.9, 119.2, 126.4, 127.0, 128.4, 129.0, 129.20, 129.25, 129.9, 130.5, 149.6, 152.2, 154.3, 155.8 ppm; IR (film) 3387, 2963, 2936, 2839, 1601, 1512, 1258, 1234 cm^{-1}; HRMS–ESI (m/z): $[M+H]^+$ calcd for $C_{22}H_{19}O_4$, 347.1278; found, 347.1273.

Synthesis of 4k

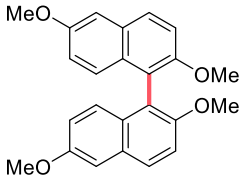

The general procedure using **3k** (22.6 mg, 0.120 mmol; 0.030 M) afforded **4k** (5.6 mg, 25%) as pale-yellow solids; substrate **3k** was recovered (6.2 mg, 27%). [Reaction time and temperature: 24 h, 20 °C, 365 nm LED, preparative TLC (hexanes/$CHCl_3$ = 1/1)] Spectral data of **4k** were in full agreement with reported data.[15]

5. X-ray crystallographic data

CCDC 2498496–2498502 contain supplementary crystallographic data for this paper. These data can be obtained free of charge from The Cambridge Crystallographic Data Centre via www.ccdc.cam.ac.uk/data_request/cif

Table S15. Summary of crystallographic data of **1a** (CCDC: 2498496).

Empirical formula	$C_{30}H_{26}O_2$
Formula weight	418.51
Temperature/K	93
Crystal system	triclinic
Space group	P-1
a/Å	7.6823(4)
b/Å	10.0325(5)
c/Å	14.5626(6)
α/°	75.757(4)
β/°	79.327(4)
γ/°	76.421(4)
Volume/Å^3	1047.75(9)
Z	2
ρ_{calc}g/cm^3	1.327
μ/mm^{-1}	0.634
F(000)	444.0
Crystal size/mm^3	0.2 × 0.2 × 0.2
Radiation	Cu Kα (λ = 1.54184)
2Θ range for data collection/°	6.32 to 152.378
Index ranges	-9 ≤ h ≤ 9, -10 ≤ k ≤ 12, -17 ≤ l ≤ 17
Reflections collected	13654
Independent reflections	3974 [R_{int} = 0.0491, R_{sigma} = 0.0395]
Data/restraints/parameters	3974/0/295
Goodness-of-fit on F^2	1.049
Final R indexes [I>=2σ (I)]	R_1 = 0.0507, wR_2 = 0.1526
Final R indexes [all data]	R_1 = 0.0561, wR_2 = 0.1617
Largest diff. peak/hole / e Å^{-3}	0.33/-0.28

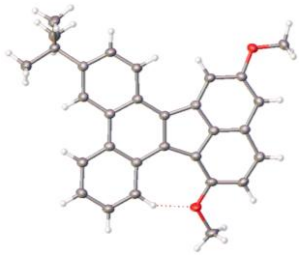

Figure S1. X-ray crystallographic structure of **1a**. Ellipsoids shown with 50% probability.

Table S16. Summary of crystallographic data of **1b** (CCDC: 2498498).

Empirical formula	$C_{32}H_{30}O_3$
Formula weight	462.56
Temperature/K	93
Crystal system	monoclinic
Space group	$P2_1/c$
a/Å	17.3008(3)
b/Å	7.44911(16)
c/Å	18.6556(3)
α/°	90
β/°	90.8618(17)
γ/°	90
Volume/Å^3	2403.98(8)
Z	4
ρ_{calc}g/cm^3	1.278
μ/mm^{-1}	0.634
F(000)	984.0
Crystal size/mm^3	0.4 × 0.1 × 0.03
Radiation	Cu Kα (λ = 1.54184)
2Θ range for data collection/°	5.108 to 143.434
Index ranges	-16 ≤ h ≤ 21, -8 ≤ k ≤ 8, -22 ≤ l ≤ 22
Reflections collected	18264
Independent reflections	4616 [R_{int} = 0.0361, R_{sigma} = 0.0339]
Data/restraints/parameters	4616/0/324
Goodness-of-fit on F^2	1.044
Final R indexes [I>=2σ (I)]	R_1 = 0.0407, wR_2 = 0.1065
Final R indexes [all data]	R_1 = 0.0475, wR_2 = 0.1112
Largest diff. peak/hole / e Å^{-3}	0.21/-0.21

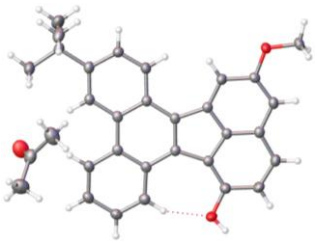

Figure S2. X-ray crystallographic structure of **1b**. Ellipsoids shown with 50% probability.

Table S17. Summary of crystallographic data of **1d** (CCDC: 2498499).

Empirical formula	$C_{30}H_{23}F_3O_4S$
Formula weight	536.54
Temperature/K	93
Crystal system	monoclinic
Space group	$P2_1/c$
a/Å	10.36770(10)
b/Å	13.9097(2)
c/Å	16.4888(2)
α/°	90
β/°	95.5040(10)
γ/°	90
Volume/Å^3	2366.91(5)
Z	4
ρ_{calc}g/cm^3	1.506
μ/mm^{-1}	1.756
F(000)	1112.0
Crystal size/mm^3	0.2 × 0.2 × 0.2
Radiation	Cu Kα (λ = 1.54184)
2Θ range for data collection/°	10.674 to 146.342
Index ranges	-12 ≤ h ≤ 12, -16 ≤ k ≤ 17, -14 ≤ l ≤ 20
Reflections collected	16950
Independent reflections	4664 [R_{int} = 0.0470, R_{sigma} = 0.0310]
Data/restraints/parameters	4664/0/348
Goodness-of-fit on F^2	1.015
Final R indexes [I>=2σ (I)]	R_1 = 0.0407, wR_2 = 0.1137
Final R indexes [all data]	R_1 = 0.0412, wR_2 = 0.1143
Largest diff. peak/hole / e Å^{-3}	0.41/-0.41

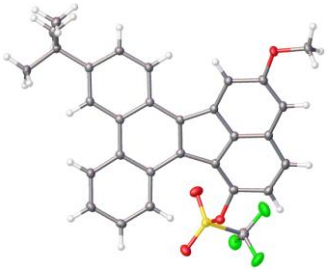

Figure S3. X-ray crystallographic structure of **1d**. Ellipsoids shown with 50% probability.

Table S18. Summary of crystallographic data of **2a** (CCDC: 2498497).

Empirical formula	$C_{30.75}H_{25.75}Cl_{2.25}O_2$
Formula weight	507.02
Temperature/K	93
Crystal system	monoclinic
Space group	$P2_1/n$
a/Å	19.8054(5)
b/Å	23.0253(5)
c/Å	25.2516(6)
α/°	90
β/°	105.763(2)
γ/°	90
Volume/Å^3	11082.3(5)
Z	16
ρ_{calc}g/cm^3	1.216
μ/mm^{-1}	2.516
F(000)	4232.0
Crystal size/mm^3	0.4 × 0.2 × 0.2
Radiation	Cu Kα (λ = 1.54184)
2Θ range for data collection/°	5.288 to 145.626
Index ranges	-24 ≤ h ≤ 16, -27 ≤ k ≤ 19, -30 ≤ l ≤ 31
Reflections collected	84896
Independent reflections	21400 [R_{int} = 0.0693, R_{sigma} = 0.0693]
Data/restraints/parameters	21400/24/1285
Goodness-of-fit on F^2	1.078
Final R indexes [I>=2σ (I)]	R_1 = 0.0901, wR_2 = 0.2731
Final R indexes [all data]	R_1 = 0.1139, wR_2 = 0.2926
Largest diff. peak/hole / e Å^{-3}	0.89/-0.71

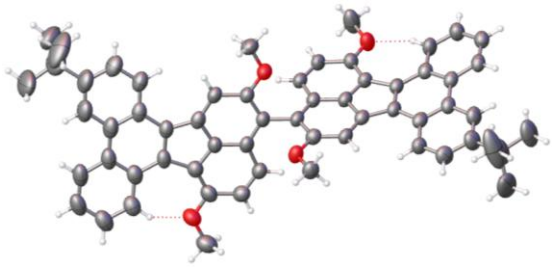

Figure S4. X-ray crystallographic structure of **2a**. Ellipsoids shown with 50% probability. Two disordered solvent molecules were removed using OLEX solvent mask.

Table S19. Summary of crystallographic data of **2d** (CCDC: 2498500).

Empirical formula	$C_{60}H_{44}F_6O_8S_2$
Formula weight	1071.07
Temperature/K	93
Crystal system	triclinic
Space group	P-1
a/Å	11.2328(4)
b/Å	11.3152(5)
c/Å	24.1172(8)
α/°	97.562(3)
β/°	99.303(3)
γ/°	91.481(3)
Volume/Å^3	2995.2(2)
Z	2
ρ_{calc}g/cm^3	1.188
μ/mm^{-1}	1.388
F(000)	1108.0
Crystal size/mm^3	0.3 × 0.3 × 0.3
Radiation	Cu Kα (λ = 1.54184)
2Θ range for data collection/°	7.5 to 151.55
Index ranges	-13 ≤ h ≤ 13, -8 ≤ k ≤ 13, -29 ≤ l ≤ 29
Reflections collected	41223
Independent reflections	11291 [R_{int} = 0.0845, R_{sigma} = 0.0652]
Data/restraints/parameters	11291/0/694
Goodness-of-fit on F^2	0.849
Final R indexes [I>=2σ (I)]	R_1 = 0.0877, wR_2 = 0.2568
Final R indexes [all data]	R_1 = 0.1112, wR_2 = 0.2774

Largest diff. peak/hole / e Å^{-3}	0.63/-0.66

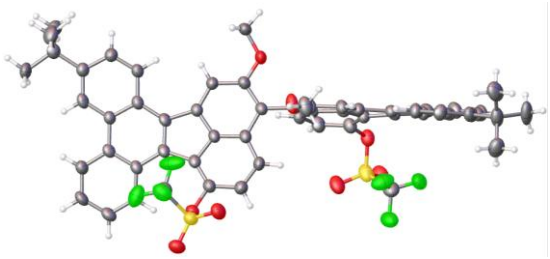

Figure S5. X-ray crystallographic structure of **2d**. Ellipsoids shown with 50% probability. Two disordered solvent molecules were removed using OLEX solvent mask.

Table S20. Summary of crystallographic data of **2f** (CCDC: 2498501).

Empirical formula	$C_{35}H_{23}Cl_3O_2$
Formula weight	581.88
Temperature/K	93
Crystal system	monoclinic
Space group	$P2_1/c$
a/Å	13.3054(3)
b/Å	17.9492(3)
c/Å	12.5807(3)
α /°	90
β /°	116.469(3)
γ /°	90
Volume/Å^3	2689.59(12)
Z	4
ρ_{calc}g/cm^3	1.437
μ /mm^{-1}	3.345
F(000)	1200.0
Crystal size/mm^3	0.2 × 0.2 × 0.2
Radiation	Cu Kα (λ = 1.54184)
2Θ range for data collection/°	8.91 to 144.378
Index ranges	-15 ≤ h ≤ 16, -21 ≤ k ≤ 21, -14 ≤ l ≤ 15
Reflections collected	19869
Independent reflections	5211 [R_{int} = 0.0886, R_{sigma} = 0.0461]
Data/restraints/parameters	5211/0/364
Goodness-of-fit on F^2	1.076

Final R indexes [I>=2 σ (I)]	R_1 = 0.0567, wR_2 = 0.1649
Final R indexes [all data]	R_1 = 0.0593, wR_2 = 0.1677
Largest diff. peak/hole / e Å^{-3}	0.97/-0.75

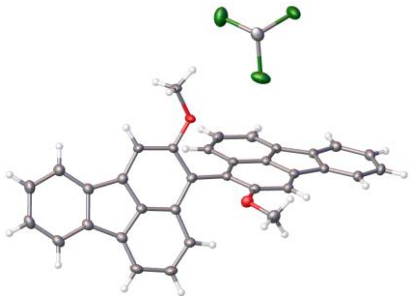

Figure S6. X-ray crystallographic structure of **2f** and $CHCl_3$ as a solvent. Ellipsoids shown with 50% probability.

Table S21. Summary of crystallographic data of **4a** (CCDC: 2498502).

Empirical formula	$C_{36}H_{26}O_4$
Formula weight	522.57
Temperature/K	93
Crystal system	triclinic
Space group	P-1
a/Å	8.01237(13)
b/Å	11.7893(2)
c/Å	14.1489(3)
α/°	108.7875(18)
β/°	98.5955(15)
γ/°	94.2027(15)
Volume/Å^3	1240.52(4)
Z	2
ρ_{calc}g/cm^3	1.399
μ/mm^{-1}	0.721
F(000)	548.0
Crystal size/mm^3	0.2 × 0.2 × 0.2
Radiation	Cu Kα (λ = 1.54184)
2Θ range for data collection/°	6.712 to 144.064
Index ranges	-9 ≤ h ≤ 9, -14 ≤ k ≤ 10, -15 ≤ l ≤ 17
Reflections collected	18236
Independent reflections	4699 [R_{int} = 0.0392, R_{sigma} = 0.0273]

Data/restraints/parameters	4699/0/366
Goodness-of-fit on F^2	1.076
Final R indexes [I>=2 σ (I)]	R_1 = 0.0386, wR_2 = 0.1161
Final R indexes [all data]	R_1 = 0.0408, wR_2 = 0.1187
Largest diff. peak/hole / e $Å^{-3}$	0.24/-0.21

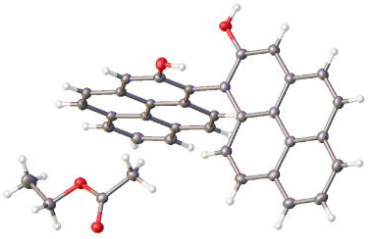

Figure S7. X-ray crystallographic structure of **4a** and EtOAc as a solvent. Ellipsoids shown with 50% probability.

6. Chiroptical and photophysical properties

6-1. Optical resolution of **2a**

Racemic mixtures of **2a** were separated by preparative chiral HPLC (column: YMC CHIRAL Amylose-SA, eluent: hexanes/$CHCl_3$ = 100/0–30/70), flow rate: 5.0 mL/min, detection: UV 340 nm). Analytical HPLC (column: YMC CHIRAL Amylose-SA, eluent: hexanes/$CHCl_3$ = 70/30, flow rate: 1.0 mL/min, detection: PDA 340 nm, temperature: 20 °C) (+)-**2a** 5.5 min, (–)-**2a** 7.6 min. $[\alpha]^{24}_{D}$ +2.70×10^4 (c 0.0010, $CHCl_3$, >99% ee).

Chromatogram of *rac*-2a

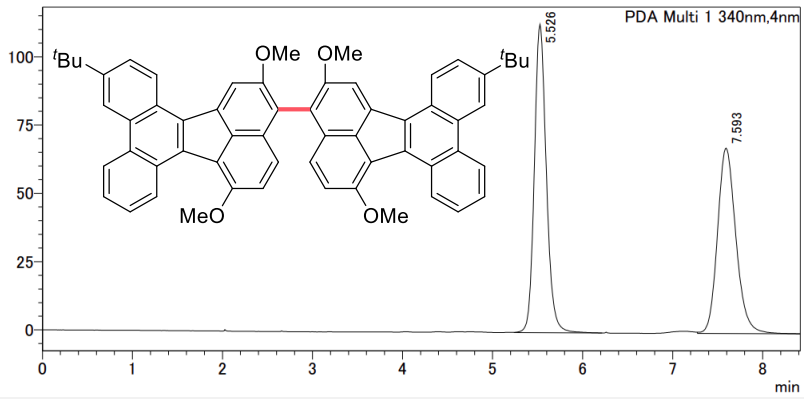

peak#	retention time	area	height	area%
1	5.526	1047692	112846	52.052
2	7.593	965104	67898	47.948
sum		2012796	180744	100.000

Chromatogram of (+)-2a (>99% ee)

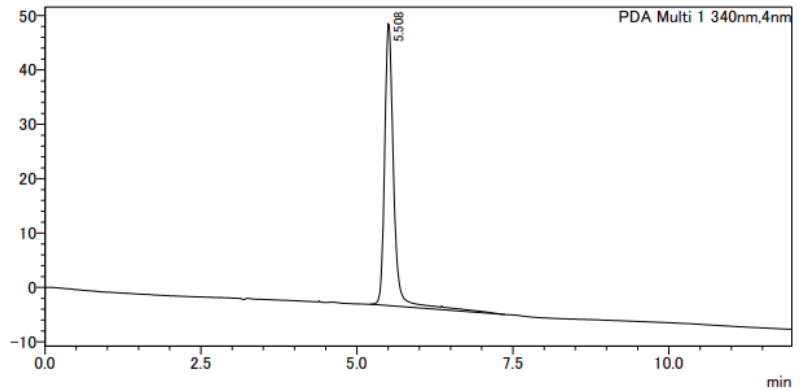

peak#	retention time	area	height	area%
1	5.508	532775	51781	100.000
sum		532775	51781	100.000

Chromatogram of (–)-2a (>99% ee)

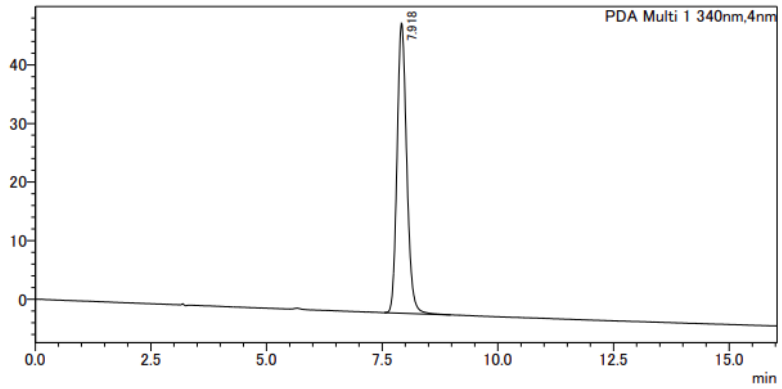

peak#	retention time	area	height	area%
1	7.918	719451	49455	100.000
sum		719451	49455	100.000

6-2. CD spectra of **2a**

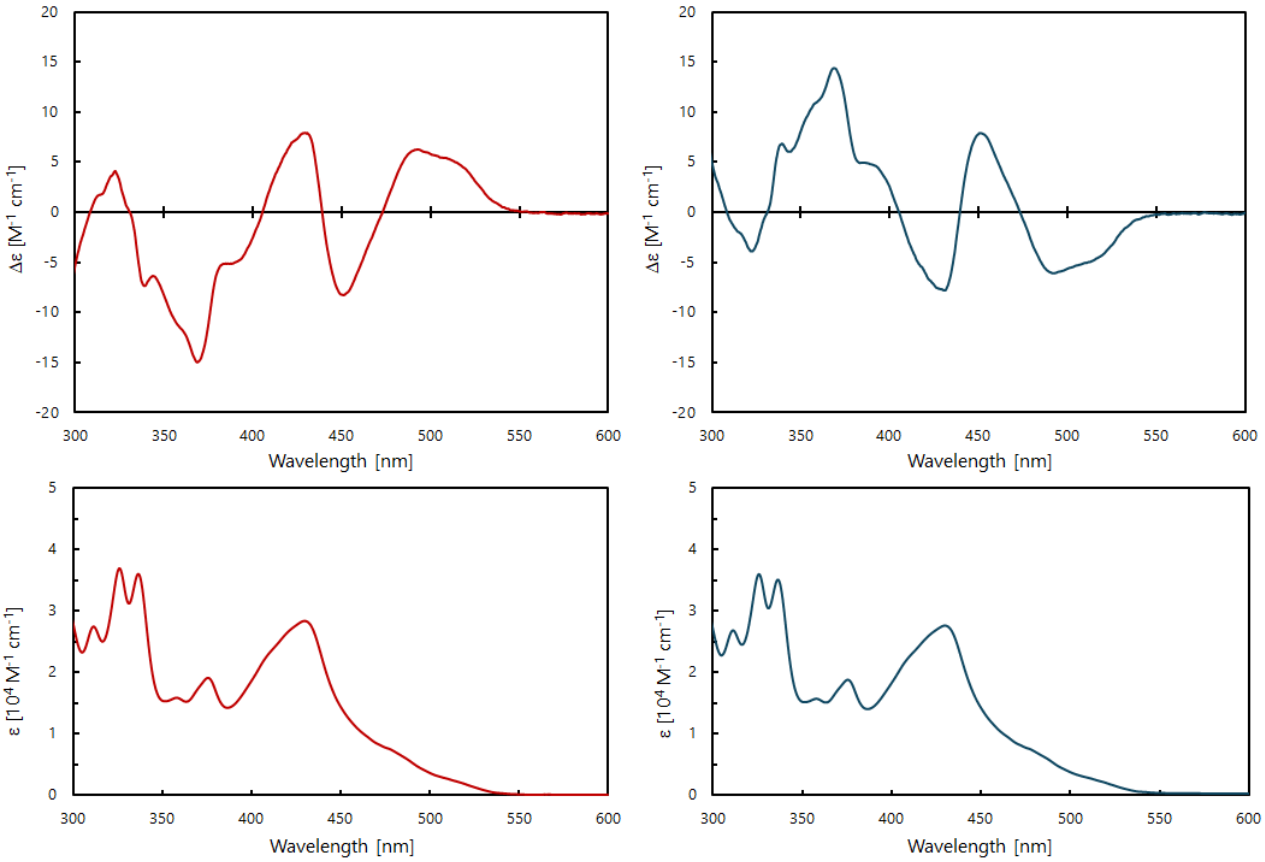

Figure S8. CD (top) and absorption (bottom) spectra of (+)-**2a** (left) and (–)-**2a** (right) in $CHCl_3$ at 298 K.

6-3. Experimental determination of the racemization barrier of **2a**

Thermal racemization experiment was conducted with (+)-**2a** in diphenyl ether at 198 °C (T = 471 K). The isomerization process was traced using chiral HPLC (condition: same as above) and the area% of both enantiomers is summarized in Table S17. The plot of HPLC-based conversion ratio of (+)-**2a** at time (t) is shown in Figure S9. From these analyses, the observed rate constant (k_{obs}) was obtained by fitting the data to a reversible first order reaction with the equation: $t = (1/k_{obs})\ln\{ee(t)\}$, giving 1.460×10^{-4} s^{-1}. The Gibbs activation energy can be determined as $\Delta G^{\ddagger}(T) = -RT\ln(k_{obs}h/2\kappa k_B T)$. R is the gas constant (R = 8.314 m^2 kg/(s^2 K mol)); h is the Planck constant (h = 6.626×10^{-34} m^2 kg/s); k_B is the Boltzmann constant ($k_B = 1.381 \times 10^{-23}$ m^2 kg/(s^2 K)); κ is the transmission coefficient (κ = 1). As a result, the isomerization energy was determined as $\Delta G^{\ddagger} = 1.545 \times 10^5$ J/mol = 36.93 kcal/mol. $t_{1/2} = \ln 2/k_{obs} = 4.748 \times 10^3$ s = 79.14 min.

Table S22. The area% of both enantiomers in each time

Time [s]	Area% of (+)-**2a**	Area% of (–)-**2a**	ee (t)
0	100	0	100
340	97.342	2.658	94.684
636	95.663	4.337	91.326
1579	89.630	10.370	79.260
3639	79.135	20.865	58.270
7719	66.281	33.719	32.562

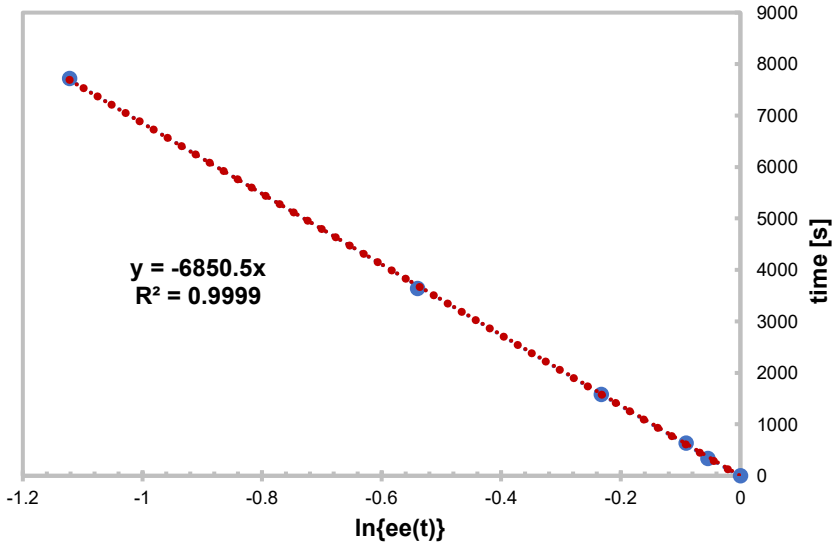

Figure S9. Plots of ln{ee(t)} vs time at 471 K.

6-4. UV-vis and fluorescence spectra of **1a**–**1d** and **2a**–**2d**

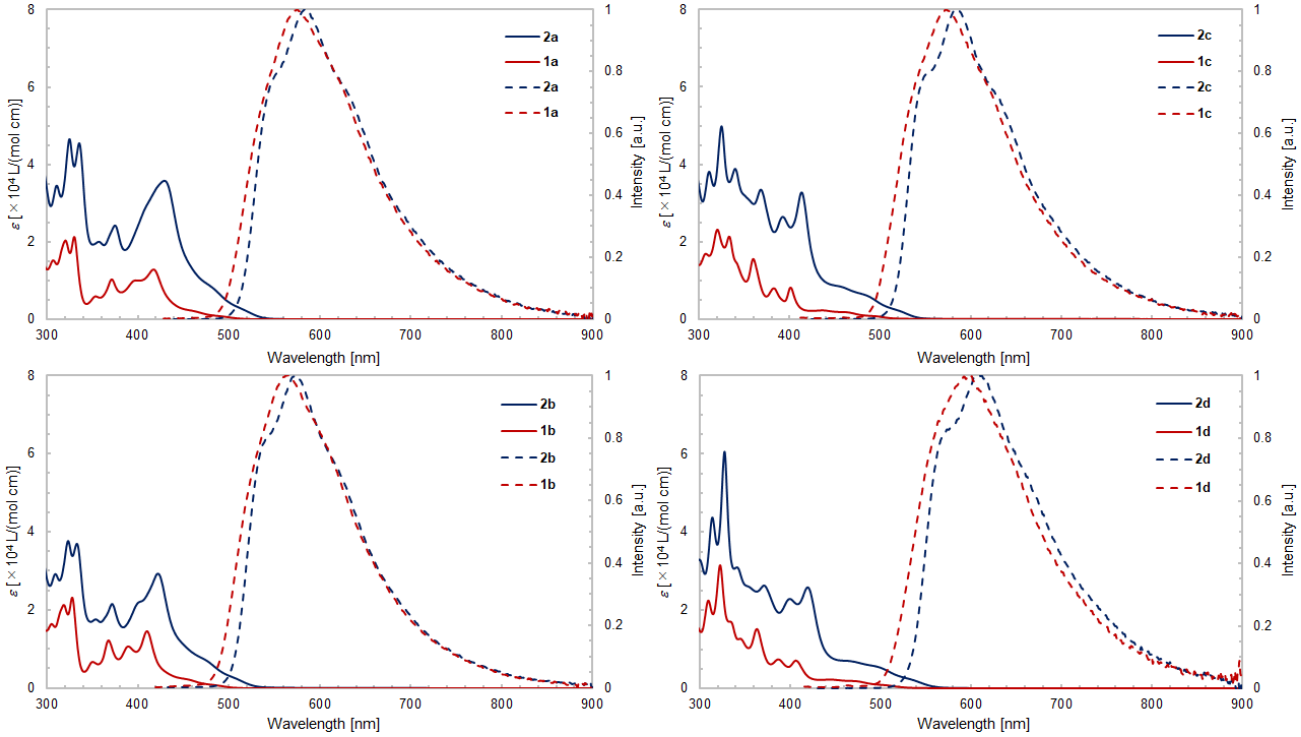

Figure S10. UV-vis absorption (solid line) and fluorescence (dashed line) spectra of **1a**–**1d** and **2a**–**2d** in CH_2Cl_2 at 298 K.

Table S23. Physical properties of **1a**–**1d** and **2a**–**2d** in CH_2Cl_2[a]

Compounds	λ_{abs} [nm] (ε [10^4 L (mol cm)$^{-1}$])	λ_{ex} [nm]	λ_{em} [nm]	Φ [%][b]
1a	398 (1.00), 418 (1.28)	418	575	1.7
2a	375 (2.42), 430 (3.57)	430	584	2.6
1b	390 (1.07), 410 (1.46)	410	566	2.4
2b	373 (2.15), 423 (2.93)	423	575	3.7
1c	383 (0.79), 402 (0.81)	402	573	2.0
2c	393 (2.64), 414 (3.28)	414	586	2.7
1d	387 (0.74), 406 (0.70)	406	597	1.0
2d	400 (2.28), 420 (2.58)	420	608	1.6

[a] Both absorption and emission spectra were recorded in solution ($c = 5.0 \times 10^{-5}$ M) at 298 K. [b] Quinine sulfate was used as a reference dye (λ_{ex} = 366 nm, Φ = 55%).[16]

7. Mechanistic experiments

7-1. UV-vis absorption spectra

For **3d**, the spectrum in CH_2Cl_2/TFA (black line, Figure S11) was similar with that in CH_2Cl_2 (gray line). When irradiation with 365 nm LED light, the new broad absorption over 800 nm was observed (red line). It suggests that the generation of new species with longer absorption spectra such as a radical species.

Procedure: In two reaction vials were added respectively **3d** (8.4 mg, 0.058 mmol) and CH_2Cl_2 (2.0 mL) in the first, and **3d** (8.6 mg, 0.060 mmol), CH_2Cl_2 (1.8 mL) and TFA (0.2 mL) in the second. The stock solutions (0.03 M) were transferred to the quartz cuvette (10 × 10 mm light path) and then measured (gray or black line). The solution including TFA was irradiated with 365 nm LED for 10 minutes and immediately measured (red line).

For **1a**, the spectrum in CH_2Cl_2 was measured (black line, Figure S11). When only addition of TFA, the new broad absorption over 800 nm was observed as in the case of **3d** (blue line). After the irradiation of 430 nm LEDs, the absorbance in ca. 640 nm was increased (blue line).

Procedure: In two reaction vials were added respectively the **1a** (27.7 mg, 0.066 mmol) and CH_2Cl_2 (2.0 mL) in the first, and **1a** (27.7 mg, 0.066 mmol), CH_2Cl_2 (1.8 mL) and TFA (0.2 mL) in the second. The stock solutions (0.033 M) were transferred to the quartz cuvette (10 × 10 mm light path) and then measured (gray or black line). The solution including TFA was irradiated with 430 nm LED for 10 minutes and immediately measured (red line).

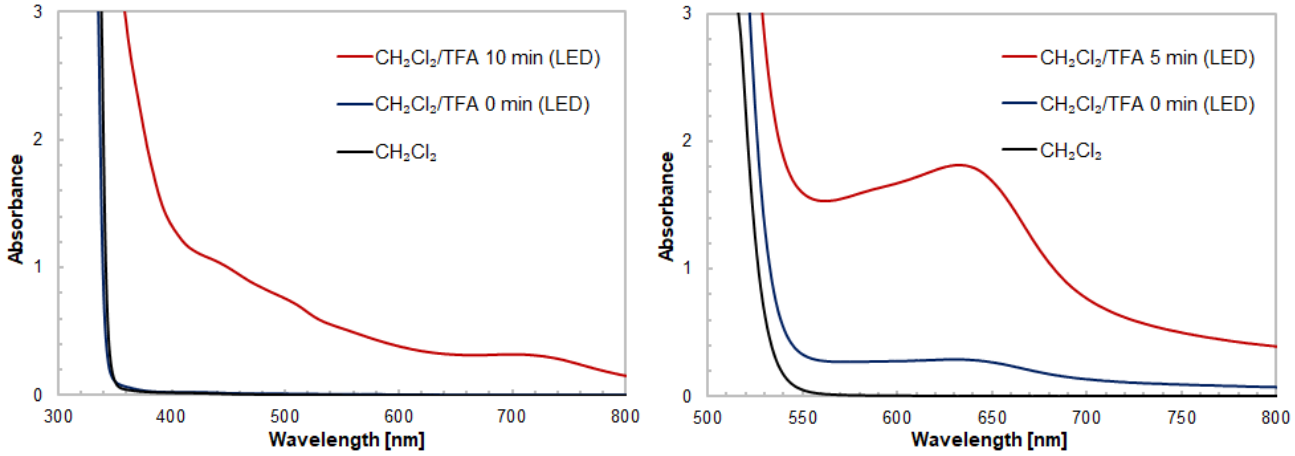

Figure S11. UV-vis absorption spectra of reaction mixture of **3d** (left) and **1a** (right) in CH_2Cl_2 or CH_2Cl_2/TFA (v/v = 9/1) at 298 K.

For **1a**, UV-vis absorption spectra titrated with Magic Blue were measured in CH_2Cl_2 (gray and purple lines). Upon addition of Magic Blue, a new band appeared at ca. 650 nm which originated from the radical cation $\mathbf{1a}^{\bullet+}$. In line with this, the new absorption near 640 nm observed in Figure S11 (right) is suggested to arise from the radical cation $\mathbf{1a}^{\bullet+}$.

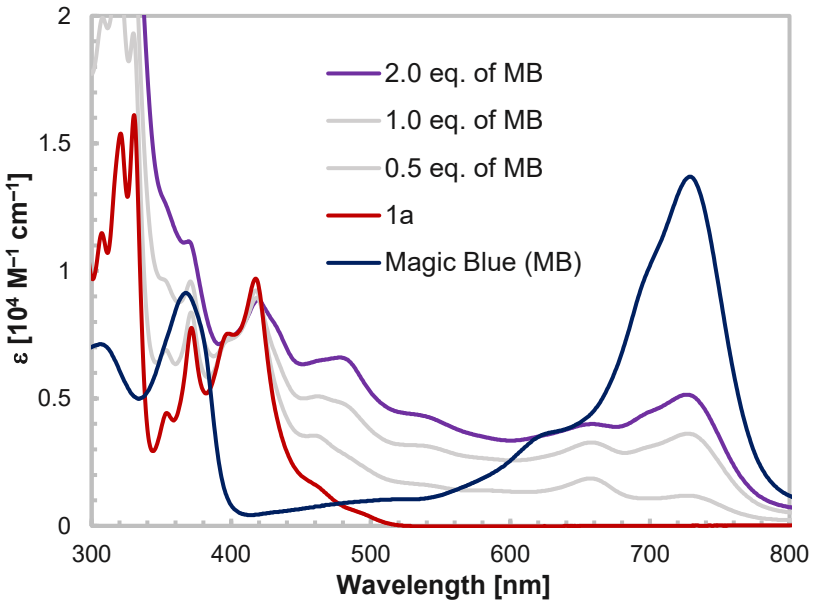

Figure S12. UV-vis absorption spectra of **1a** in CH_2Cl_2, titrated with Magic Blue (0–2.0 eq.) at 298 K.

7-2. Biaryl coupling reaction using TEMPO as a single electron oxidant

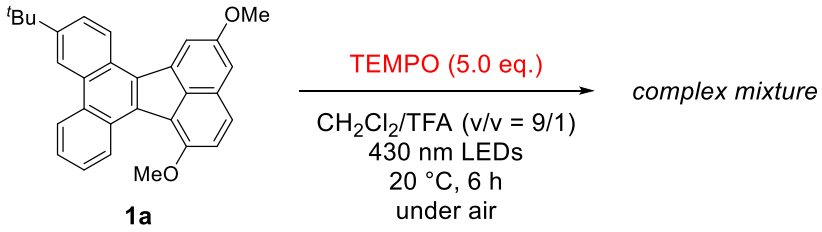

To a 4 mL vial equipped with a magnetic stir bar were added the substrate **1a** (12.2 mg, 0.0291 mmol), 2,2,6,6-tetramethylpiperidine 1-oxyl free radical (TEMPO, 23.5 mg, 0.150 mmol) and CH_2Cl_2/TFA (v/v = 9/1, 1.0 mL) under air. The mixture was irradiated with 430 nm LEDs while being stirred at room temperature under fan cooling for 6 h. The reaction was quenched by pouring the mixture into sat. $NaHCO_3$ aq. The aqueous phase was extracted three times with EtOAc; the combined organic layers were washed three times with brine, dried over Na_2SO_4, filtered, and concentrated under reduced pressure. The crude product was analyzed by ^1H NMR in $CDCl_3$.

7-3. Electron spin resonance (ESR) experiments

The spectral data were collected at 298 K with the following spectrometer settings: microwave power = 2.000 mW; center field = 3500.000 G, sweep width = 100.000 G, sweep time = 20.972 s, modulation frequency = 100.000 KHz, modulation amplitude = 1.000 G, power attenuation = 20.00 dB, time constant = 20.480 ms, conversion time = 20.480 ms

For **3d**, an extremely weak single signal was observed in CH_2Cl_2 (gray line, Figure S13) and CH_2Cl_2/TFA (v/v = 9/1, black line). When irradiating with 405 nm LEDs, the intensity of ESR signal at 3516.8 G (g-values = 2.0055) increased with the irradiation time (5 min.; blue line, 10 min.; red line). These results suggest that light helps the generation of radical species.

Procedure: 3d (43.5 mg, 0.30 mmol) and CH_2Cl_2 (2.7 mL) were added to a vial. Then, the solution (0.9 mL) was taken into two vials and CH_2Cl_2 (0.1 mL) and TFA (0.1 mL) were added to each, respectively. The stock solutions (0.10 M) were transferred to the capillary tube and then measured (gray or black line). The tube was irradiated with 405 nm LED for 5 minutes and immediately measured (blue line). It was further irradiated for another 5 minutes and measured again (red line).

For **1a**, no signal was observed in CH_2Cl_2 (gray line, Figure S13). In contrast to **3d**, when addition of TFA (black line), the single clean ESR signal was observed at 3519.0 G (g-values = 2.0045). These results suggest that radical species of **1a** is generated easier than that of **3d**. When irradiating with 430 nm LEDs, the intensity of ESR signal with the irradiation time (5 min.; blue line, 10 min.; red line). The trend of change of **1a** was same as that of **3d**.

Procedure: 1a (38.1 mg, 0.091 mmol) and CH_2Cl_2 (2.7 mL) were added to a vial. Then, the solution (0.9 mL) was taken into two vials and CH_2Cl_2 (0.1 mL) and TFA (0.1 mL) were added to each, respectively. The stock solutions (0.030 M) were transferred to the capillary tube and then measured (gray or black line). The tube was irradiated with 430 nm LED for 5 minutes and immediately measured (blue line). It was further irradiated for another 5 minutes and measured again (red line).

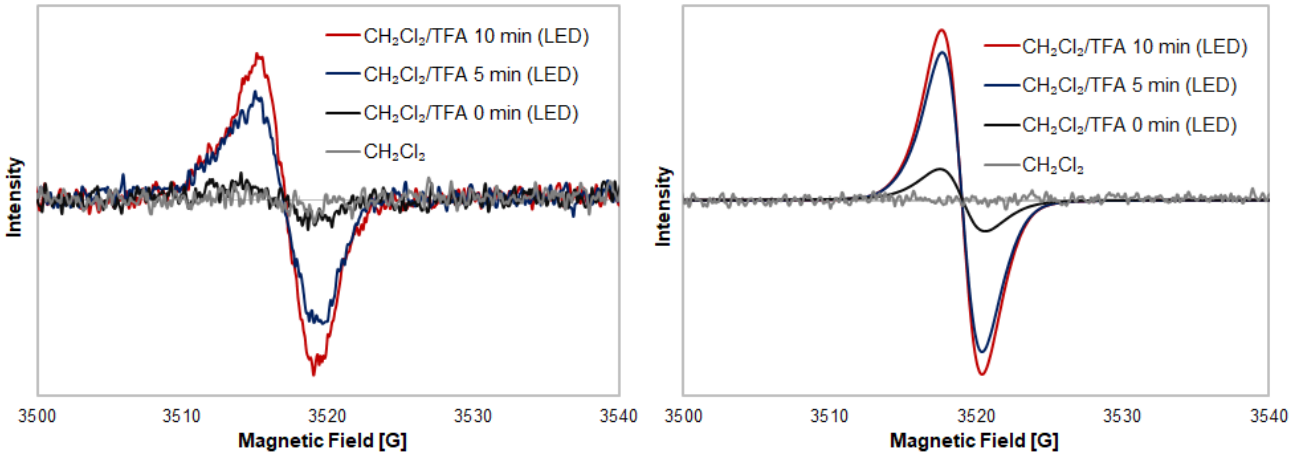

Figure S13. ESR spectra of reaction mixture of **3d** (g-values = 2.0055) and **1a** (g-values = 2.0045) in CH_2Cl_2 or CH_2Cl_2/TFA (v/v = 9/1) at 298 K.

7-4. Biaryl coupling reaction using Magic Blue as a single electron oxidant

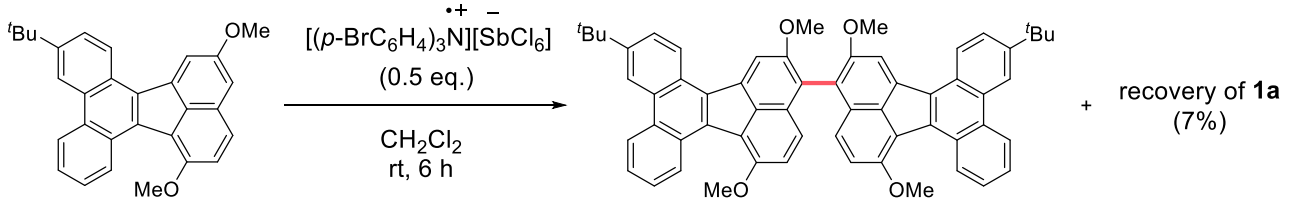

1a **2a** (39%)

To a 4 mL vial equipped with a magnetic stir bar were added the substrate **1a** (12.4 mg, 0.0296 mmol), tris(4-bromophenyl)ammoniumyl hexachloroantimonate (Magic Blue, 12.3 mg, 0.0150 mmol) and CH_2Cl_2 (1.0 mL) under air. The mixture was stirred at room temperature for 6 h. The reaction mixture was filtered through silica gel, washed

with $CHCl_3$, and concentrated under reduced pressure. The yields of **1a** and **2a** were determined by ^1H NMR analysis using Ph_3CH as an internal standard.

8. Computational studies

All DFT calculations were performed using the GRRM17[17,18] program combined with Gaussian 16 program.[19]

8-1. Exploration of possible CT complex geometries of two 2-naphthols and TFA

Conformational searches for CT complex were performed using the MMFF94s force field and CONFLEX 9 Rev. C software.[20–24] The selected geometries were optimized at the B3LYP-D3/6-311G+(d,p)-CPCM(CH_2Cl_2) level of theory. Electronic transitions were simulated by time-dependent (TD) DFT calculations at the B3LYP-D3/6-311+G(d,p)-CPCM(CH_2Cl_2) level of theory, using geometries optimized at the same level of theory. In addition, the nature of the excited states was explored using the natural transition orbital (NTO) analysis. Non-covalent interaction (NCI) plots were obtained from wavefunctions generated at the B3LYP-D3/6-311+G(d,p)-CPCM(CH_2Cl_2) level of theory and visualized using the VMD program. NCI plots are displayed with a reduced density gradient (RDG) surfaces = 0.5 a.u. and the color range blue (attractive)-green-red (repulsive).

Three possible CT complexes were identified, and their optimized geometries and their corresponding binding energies are summarized in Figure S14. In **CT1**, the carboxylic acid moiety of TFA bridges the two 2-naphthol molecules. In **CT2**, one 2-naphthol interacts with the protonated counterpart without involvement of the TFA bridge. In **CT3**, the hydroxy group of TFA bridges the two 2-naphthol molecules. Binding energy calculations indicate that **CT1** is the most stable structure. NCI plot, TD-DFT calculation and NTO analysis of **CT1** are shown in Figures S15–S17 and Table S19, respectively.

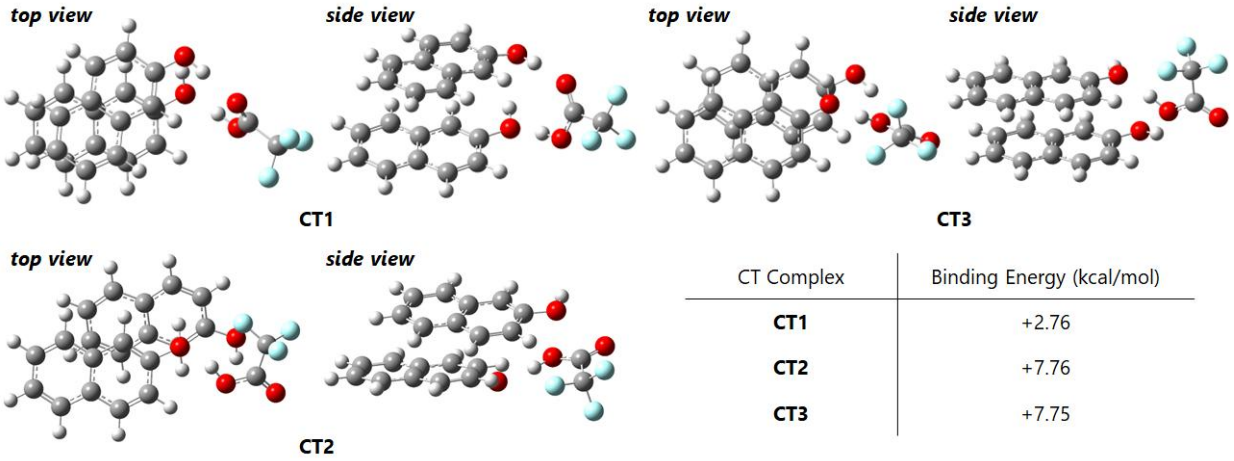

CT Complex	Binding Energy (kcal/mol)
CT1	+2.76
CT2	+7.76
CT3	+7.75

Figure S14. Calculated CT complex **CT1**–**CT3** and their binding energies (B3LYP-D3/6-311+G(d,p)-CPCM(CH_2Cl_2) level of theory)

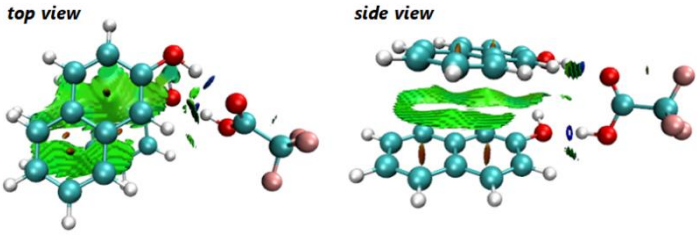

Figure S15. NCI plot of **CT1** (left: top view; right: side view)

Table S24. Major theoretical electronic transitions of **CT1**

Excited states	Energy [eV]	Wavelength [nm]	Oscillator strength (*f*)	description
1	3.7300	332.40	0.0000	H → L (0.35904) H → L+1 (0.59666)
2	3.7492	330.70	0.0002	H → L (0.60521) H → L+1 (–0.35649)
3	3.9859	311.06	0.0107	H–1 → L+1 (–0.34228) H → L+2 (0.59311)

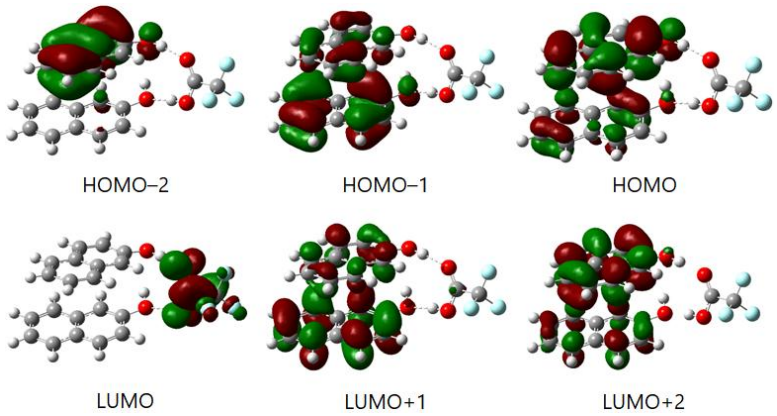

Figure S16. Frontier molecular orbitals of **CT1** (isovalue = 0.03)

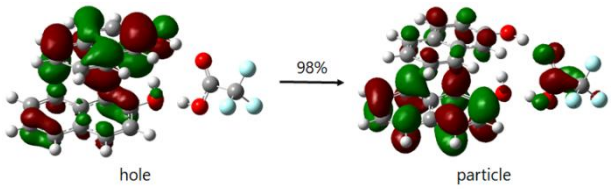

Figure S17. Hole and particle wavefunctions (for excited state 1, isovalue = 0.03)

8-2. Exploration of possible CT complex geometry of two 2-methoxynaphthalenes and TFA

Two possible CT complexes were identified, and their optimized geometries and their corresponding binding energies are summarized in Figure S16. NCI plot, TD-DFT calculation and NTO analysis of **CT4** are shown in Figures S18–S21 and Table S20, respectively.

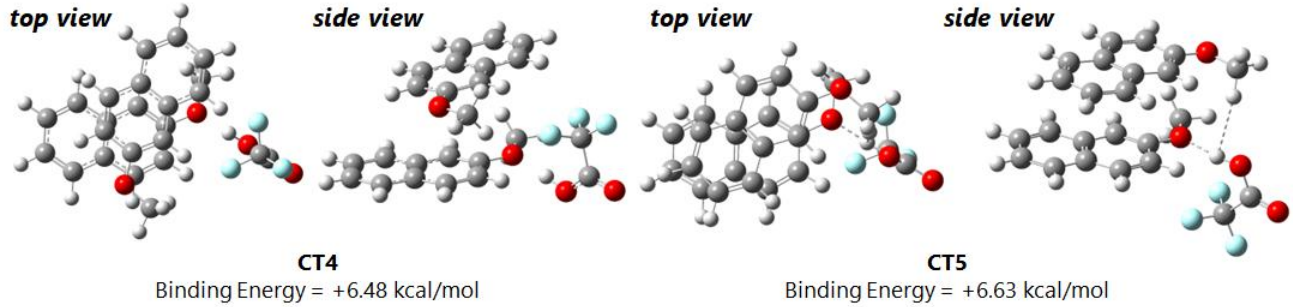

Figure S18. Calculated CT complex **CT1**–**CT3** and their binding energies

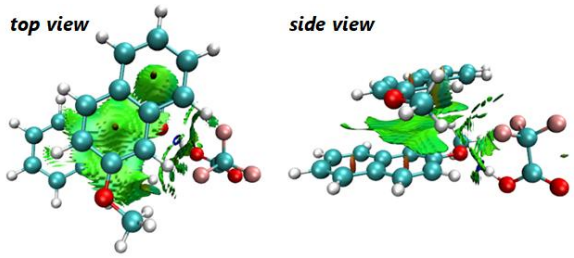

Figure S19. NCI plot of **CT4** (left: top view; right: side view)

Table S25. Major theoretical electronic transitions of **CT4**

Excited states	Energy [eV]	Wavelength [nm]	Oscillator strength (*f*)	description
1	3.8880	318.89	0.0060	H → L (0.67697) H → L+1 (0.17582)
2	4.0590	305.45	0.0428	H–2 → L+2 (0.11893) H–2 → L+4 (–0.12937) H → L (–0.10364) H → L+1 (0.33176) H → L+2 (0.55933) H → L+4 (0.13658)
3	4.1188	301.02	0.0219	H–1 → L (0.63315) H–1 → L+2 (–0.1990) H–1 → L+3 (–0.11599)

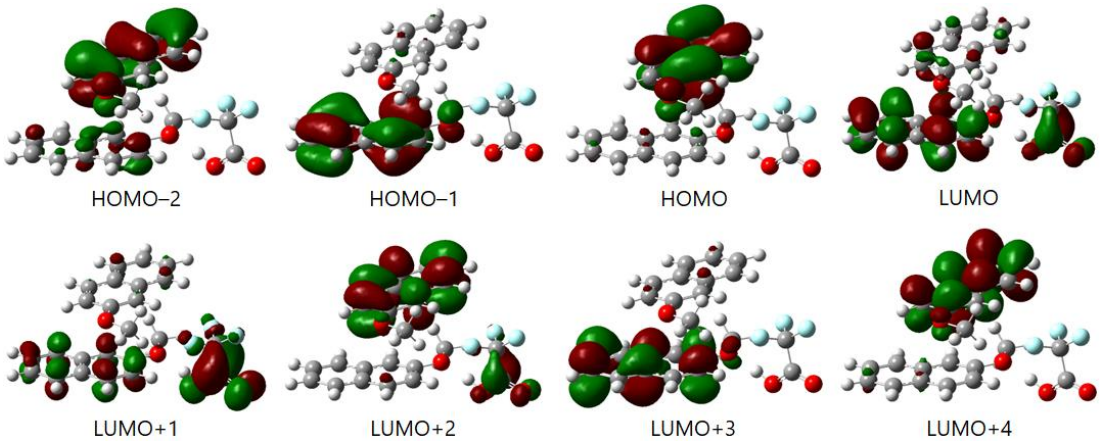

Figure S20. Frontier molecular orbitals of **CT4** (isovalue = 0.03)

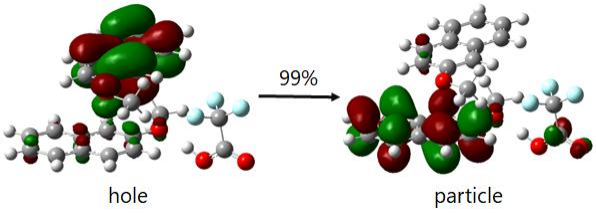

Figure S21. Hole and particle wavefunctions (for excited state 1, isovalue = 0.03)

8-3. Predicted UV-vis and ECD spectra

Electronic transitions were simulated by TD-DFT calculations at the B3LYP/6-31+G(d)-CPCM(CH_2Cl_2) or UB3LYP/6-31+G(d) level of theory using optimized geometries at the same level of theory. The ECD spectrum of (*R*)-**2a'** was computed at the B3LYP/6-31+G(d)-CPCM($CHCl_3$) level of theory.

Table S26. Major theoretical electronic transitions of **1a'**

Excited states	Energy [eV]	Wavelength [nm]	Oscillator strength (*f*)	description
1	2.6091	475.19	0.0664	H → L (0.69611)
2	2.9242	424.00	0.3221	H–1 → L (0.69438)
3	3.3854	366.23	0.0266	H–2 → L (0.64187) H → L+1 (0.26217)

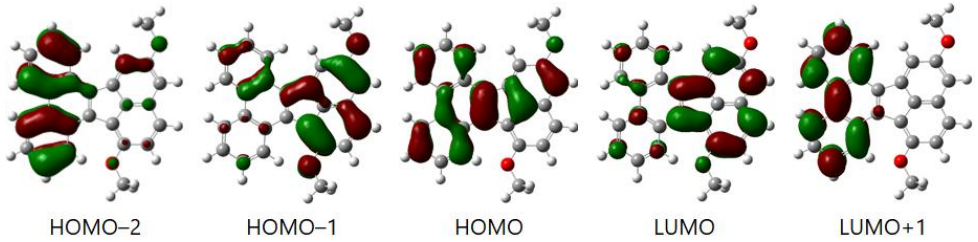

Figure S22. Frontier molecular orbitals of **1a'** (isovalue = 0.03)

Table S27. Major theoretical electronic transitions of **2a'**

Excited states	Energy [eV]	Wavelength [nm]	Oscillator strength (*f*)	description
1	2.5853	479.58	0.1220	H–1 → L+1 (–0.16786) H → L (0.59458) H → L+1 (0.31071)
2	2.6604	466.04	0.0824	H–1 → L (0.52447) H–1 → L+1 (–0.36132) H → L+1 (–0.25145)
3	2.7822	445.63	0.0238	H–2 → L (0.32351) H–2 → L+1 (–0.22095) H–1 → L (0.15857) H–1 → L+1 (–0.17857) H → L (–0.25347) H → L+1 (0.46557)

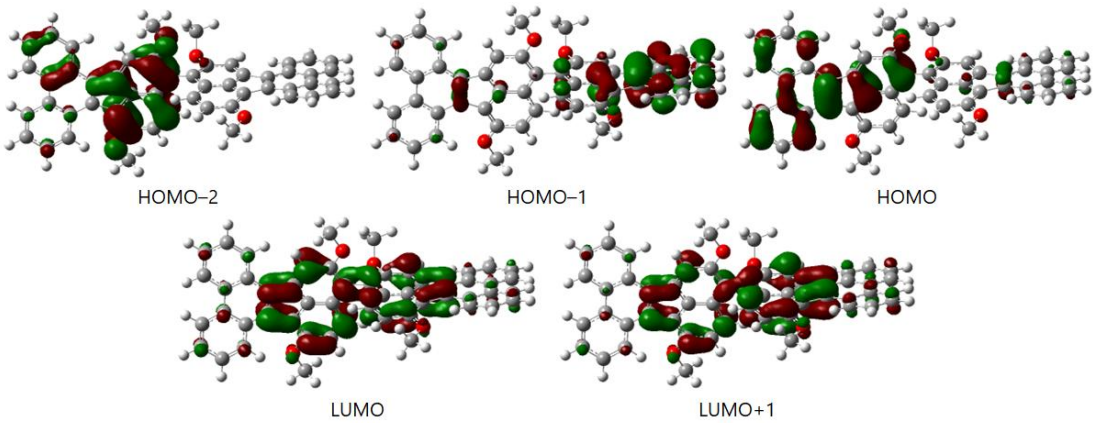

Figure S23. Frontier molecular orbitals of **2a'** (isovalue = 0.03)

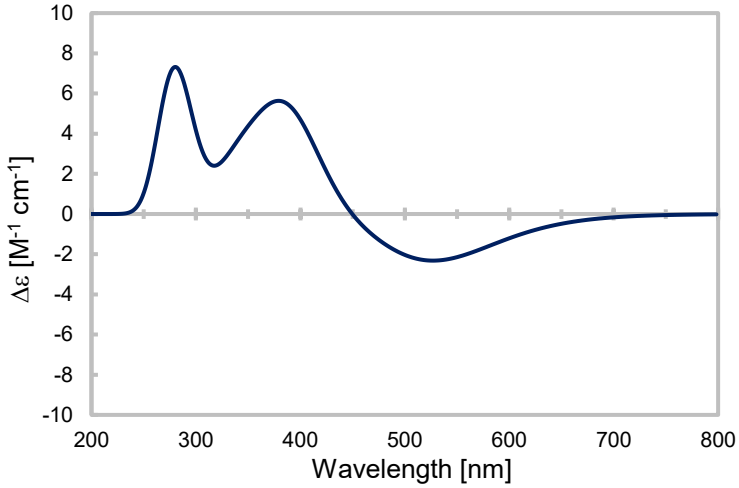

Figure S24. Predicted ECD spectra of (*R*)-**2a'**

A negative Cotton effect near 520 nm was predicted, consistent with the negative band at ca. 490 nm observed for (–)-**2a**. Taken together, these data suggest that compound **2a** exhibiting negative specific rotation corresponds to the (*R*)-enantiomer.

Table S28. Major theoretical electronic transitions of radical cation **1a**$^{\bullet+}$

Excited states	Energy [eV]	Wavelength [nm]	Oscillator strength (*f*)	description
1	0.4382	2829.39	0.0045	110B → 111B (0.99120)
2	1.0988	1128.33	0.0021	109B → 111B (0.98675)
3	1.4956	828.99	0.0091	108B → 111B (0.98516)
4	1.7806	696.31	0.0083	110A → 112A (0.15344) 111A → 112A (0.69292) 107B → 111B (0.40604) 110B → 112B (–0.53506)
5	2.0621	601.26	0.0150	110A → 112A (0.33712) 111A → 112A (–0.21156) 106B → 111B (0.64672) 107B → 111B (0.58200) 110B → 112B (0.23336)
6	2.1118	587.09	0.1088	110A → 112A (–0.14145) 106B → 111B (0.71240) 107B → 111B (–0.53666) 110B → 112B (–0.33273)

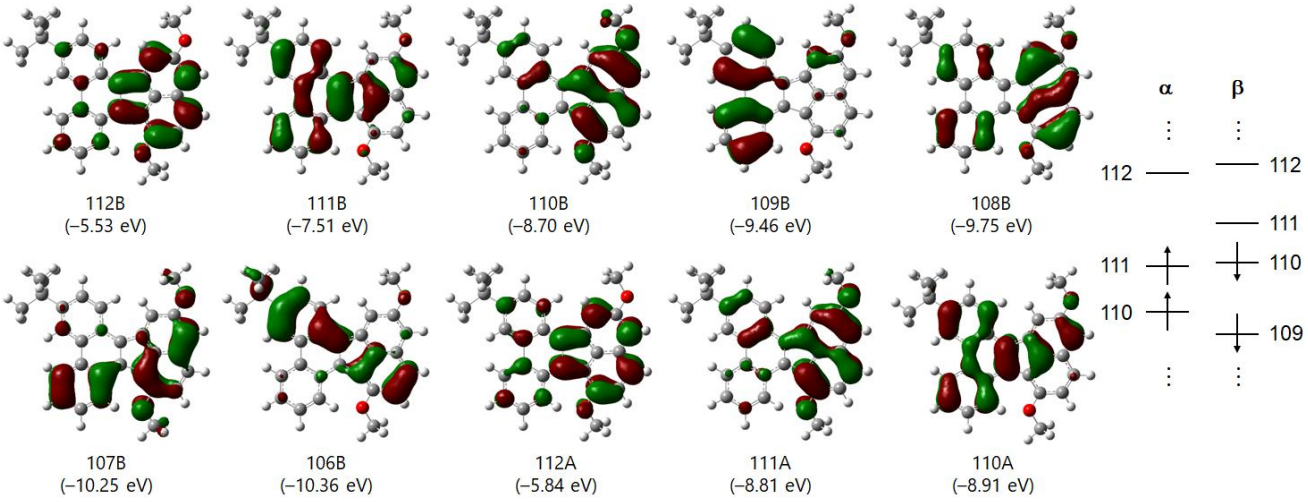

Figure S25. Frontier molecular orbitals of radical cation **1a**$^{\bullet+}$ (isovalue = 0.03)

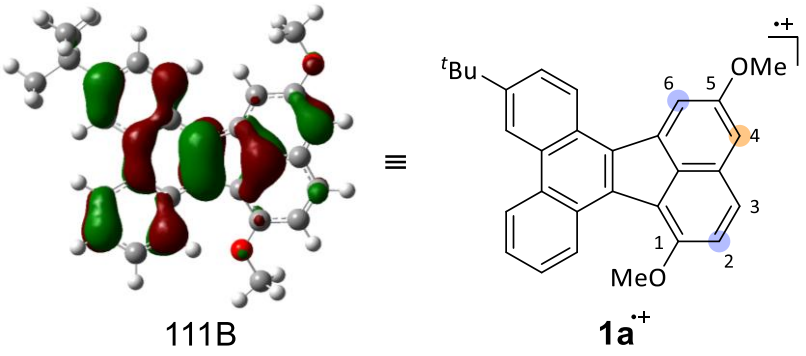

Figure S26. Selected frontier molecular orbital (111B) of radical cation **1a**$^{\bullet+}$

Despite the presence of three plausible reactive sites (C2, C4, and C6) adjacent to the two OMe groups, biaryl coupling reaction occurred exclusively at C4 position. This regioselectivity can be rationalized by the LUMO (**111B**) of the radical cation, which is predominantly localized at the experimentally observed coupling site, suggesting that C4 position is the most electrophilic site for bond formation.

8-4. Racemization process of **2a'**

Geometry optimizations were conducted at the M06-2X/6-31G(d,p) level of theory. The vibrational frequencies were computed at the same level in order to check whether each optimized structure is an energy minimum (no imaginary frequency) or a transition state (one imaginary frequency). The intrinsic reaction coordinate (IRC) method was used to track minimum energy paths from transition structures to the corresponding local minima.[25–28] Further single-point energy calculations were performed at the same function, and the relative energies were corrected for the Gibbs free energies.

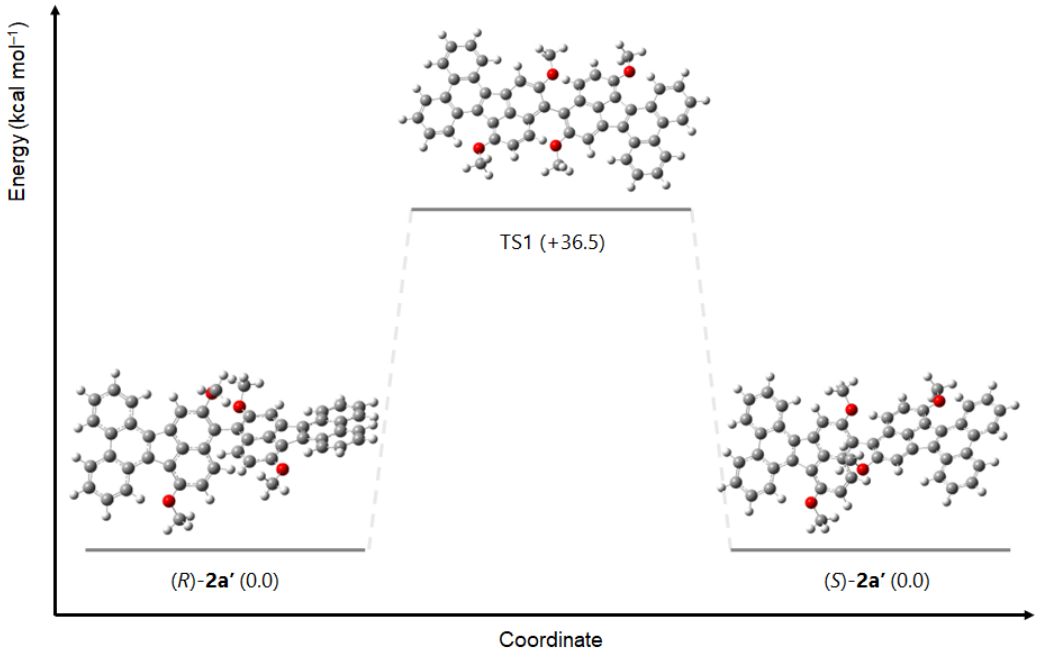

Figure S27. Computed racemization process of the **2a'** via TS1

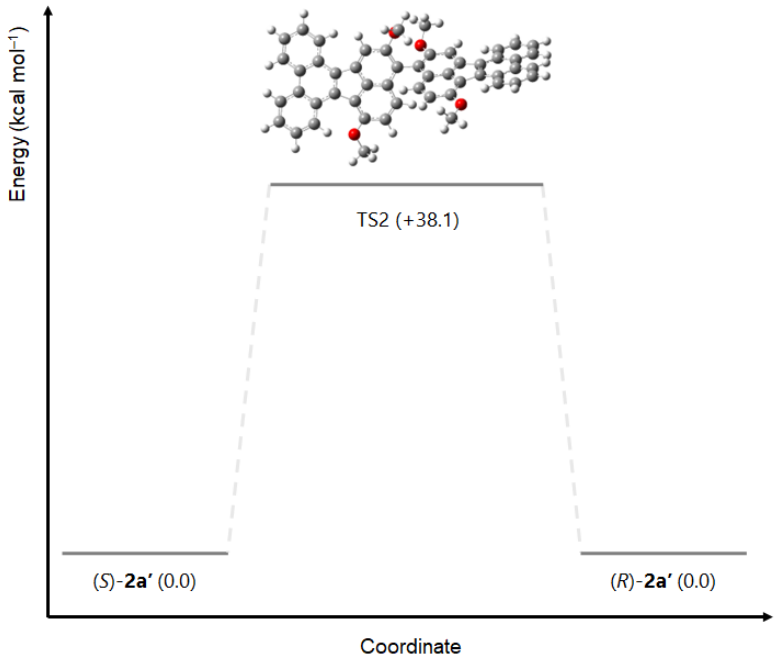

Figure S28. Computed racemization process of the **2a'** via TS2

We computed the clockwise and counterclockwise rotation of one fluoranthene unit in **2a′** and located two transition states (TS1, TS2); TS1 is slightly lower in energy than TS2 ($\Delta\Delta G$ = 1.6 kcal mol^{-1}), suggesting that racemization proceeds via TS1.

Optimized geometry of **CT1** (B3LYP-D3/6-311+G(d,p)-CPCM(CH_2Cl_2) level of theory)

Gibbs free energy: -1449.242125 Hartree

C	0.98164500	1.64584200	-0.89458200
C	2.20016800	2.04686700	-0.26150800
C	2.15341500	2.46719400	1.09408700
C	0.97615200	2.46314300	1.79767200
C	-0.22102700	2.03463100	1.17281700
C	-0.22613000	1.65931200	-0.15120300
C	1.02655200	1.21220400	-2.24648700
C	2.21887300	1.16789700	-2.93157100
C	3.42507000	1.55934200	-2.30198100
C	3.41203100	1.99169600	-0.99605900
O	-1.33040700	1.96419100	1.97575500
H	3.07267600	2.77747700	1.57910300
H	0.93968800	2.76056700	2.83909400
H	-1.14491600	1.32981300	-0.62261900
H	0.10477300	0.90332900	-2.72820200
H	2.23935100	0.82584200	-3.96039300

H	4.35812400	1.51116000	-2.85158100
H	4.33382900	2.28463000	-0.50476800
H	-2.10656800	1.69058700	1.45366200
C	2.57967700	-1.28059900	0.99045000
C	2.51369800	-2.06235200	-0.20582500
C	1.24319000	-2.50261300	-0.66185400
C	0.09372900	-2.17690500	0.01448000
C	0.17651300	-1.39222200	1.18580300
C	1.38132800	-0.96403500	1.67924800
C	3.84723500	-0.83238600	1.44652100
C	4.99275500	-1.14361200	0.75261700
C	4.92855100	-1.91805000	-0.43125700
C	3.71510500	-2.36625900	-0.89838500
O	-1.02670400	-1.07537900	1.80287800
H	-0.92326500	-0.32859700	2.41132900
H	1.18574200	-3.09696600	-1.56710500
H	-0.87637600	-2.50008900	-0.34331400
H	1.42567600	-0.35481500	2.57444700
H	3.89631900	-0.22983600	2.34696000
H	5.95398200	-0.79004400	1.10844800
H	5.83995800	-2.15220700	-0.96931400
H	3.65957500	-2.95671900	-1.80694100
F	-6.01578700	-1.19068600	0.01238000
C	-5.17090100	-0.37161900	-0.63965500
C	-3.88393200	-0.12348200	0.19694400
O	-3.30603500	-1.25680000	0.49193200
O	-3.53261400	0.99725300	0.48250200
F	-4.85732400	-0.94718300	-1.81665100
H	-2.45405600	-1.13003000	1.00727800
F	-5.80695800	0.77540400	-0.89042500

Optimized geometry of **CT2** (B3LYP-D3/6-311+G(d,p)-CPCM(CH_2Cl_2) level of theory)

Gibbs free energy: -1449.234154 Hartree

C	3.14099900	-0.96247500	-0.75834600
C	3.31589000	-1.82830500	0.36700000
C	2.16221200	-2.35040600	1.00970900
C	0.90057100	-2.02310100	0.57954800
C	0.74535800	-1.15470900	-0.52474400

C	1.82918100	-0.64400500	-1.19161400
C	4.29194100	-0.43445400	-1.40060600
C	5.55316900	-0.74402800	-0.94792200
C	5.72693600	-1.59901700	0.16793200
C	4.63118400	-2.12981200	0.80822200
O	-0.55495700	-0.85526700	-0.89401400
H	2.28717100	-3.00967100	1.86180300
H	0.02098300	-2.40746900	1.08098300
H	1.69227600	0.02605000	-2.03245000
H	4.16003100	0.22777200	-2.24916700
H	6.42349200	-0.33001800	-1.44468400
H	6.72717000	-1.83294700	0.51417200
H	4.75821200	-2.78599000	1.66303100
H	-0.59121500	-0.04934400	-1.42819200
O	-2.43804100	-1.45901200	0.88397400
C	-3.73669900	-1.30897000	0.72891000
C	-4.23297700	-0.90677100	-0.69379700
F	-5.31063600	-0.12243600	-0.62314700
F	-3.28993100	-0.26533600	-1.41309700
F	-4.57069500	-2.02316400	-1.37421500
O	-4.54588900	-1.52452000	1.59027800
H	-1.86485700	-1.17844000	0.12197100
C	1.85160900	2.79847900	-0.86096900
C	2.98451600	2.57748300	-0.11491000
H	1.92308300	3.21485500	-1.86041100
C	-0.62082600	2.65819400	-1.10080100
C	0.56965700	2.47234700	-0.34671700
H	-0.55010700	3.06876900	-2.10235800
H	3.96041900	2.81556300	-0.52097800
C	-1.85007000	2.33408400	-0.58093100
C	2.88370100	2.01572000	1.18003600
C	0.46503600	1.92275200	0.97017900
C	1.65597600	1.69946400	1.71145000
H	-2.75899500	2.47198500	-1.15273400
C	-1.94372900	1.80490100	0.72920500
C	-0.81536400	1.59803000	1.48816700
H	3.78533500	1.82657400	1.75134600
O	-3.20857600	1.48986300	1.15808900

H	1.58240100	1.26426400	2.70226000
H	-0.89454100	1.17120600	2.48293200
H	-3.18943200	1.22432300	2.08597800

Optimized geometry of **CT3** (B3LYP-D3/6-311+G(d,p)-CPCM(CH_2Cl_2) level of theory)

Gibbs free energy: -1449.234169 Hartree

C	2.10572000	-1.52747000	-0.76479400
C	1.99169000	-2.20962300	0.48751200
C	0.73002600	-2.23104900	1.13935300
C	-0.36339700	-1.61012800	0.59103700
C	-0.23019500	-0.93228200	-0.64051100
C	0.96410200	-0.88573200	-1.31058800
C	3.36325500	-1.50789000	-1.42134600
C	4.45491100	-2.13214800	-0.86547900
C	4.34445200	-2.80343200	0.37549100
C	3.13828100	-2.84016100	1.03616300
O	-1.37461900	-0.31894800	-1.13073800
H	0.63698600	-2.74624800	2.08915800
H	-1.32473800	-1.62302200	1.08835800
H	1.05112500	-0.34800800	-2.24860200
H	3.45370000	-0.97949100	-2.36380900
H	5.41189300	-2.10316600	-1.37427500
H	5.21521300	-3.28681800	0.80369400
H	3.04784000	-3.35249300	1.98840700
H	-1.17677900	0.18694300	-1.92978300
O	-3.19789100	0.89314000	0.33426100
C	-4.41314500	0.39095400	0.46839800
C	-4.62972700	-0.98799600	-0.22865200
F	-5.84743300	-1.46780400	0.01643300
F	-4.47826000	-0.86687700	-1.56311300
F	-3.72128600	-1.88722100	0.20666400
O	-5.30061400	0.92810900	1.06756300
H	-2.55533600	0.34840300	-0.20294100
H	3.15233600	2.84555500	-2.02480200
H	0.70042200	3.26321200	-1.73660800
H	-2.30808200	2.83512100	0.00438500
C	3.18193400	2.35136100	-1.05918300
C	0.75184800	2.77553100	-0.76952600

O	-1.55922200	3.16911600	-0.50762400
H	5.26227000	1.89247100	-1.18059000
C	4.35850200	1.82008200	-0.58567000
C	1.98420700	2.25688700	-0.29968500
C	-0.38983800	2.65338300	-0.01079900
C	4.40088300	1.16616100	0.66923700
C	2.03020600	1.59837800	0.97052100
C	-0.34903700	2.01481600	1.25430100
C	3.26014300	1.05868800	1.42772500
C	0.83271000	1.49736300	1.72315500
H	5.33205000	0.73711200	1.01999600
H	-1.26018300	1.92422700	1.83409900
H	3.28162100	0.54584600	2.38342500
H	0.85604600	0.99201000	2.68236900

Optimized geometry of **CT4** (B3LYP-D3/6-311+G(d,p)-CPCM(CH_2Cl_2) level of theory)

Gibbs free energy: -1527.805205 Hartree

C	-2.65812000	-0.85395600	-1.25731400
C	-2.65577600	-1.96583700	-0.36085300
C	-1.40609300	-2.49301200	0.06218500
C	-0.22721800	-1.93958300	-0.35898500
C	-0.24209800	-0.82563200	-1.23595400
C	-1.42446200	-0.29641200	-1.68913900
C	-3.90312000	-0.31196900	-1.66885700
C	-5.08741200	-0.83947600	-1.20709500
C	-5.08436800	-1.93808800	-0.31468600
C	-3.89191000	-2.48960900	0.09567400
O	1.00109900	-0.32849000	-1.57121500
C	1.07518000	0.83686600	-2.41450400
H	-1.39341000	-3.33413600	0.74633000
H	0.72287900	-2.32764700	-0.01604600
H	-1.44699400	0.56042300	-2.34772400
H	-3.90767700	0.53667600	-2.34464600
H	-6.03135900	-0.41029000	-1.52406900
H	-6.02434300	-2.34156200	0.04409100
H	-3.88195500	-3.33031700	0.78158900
H	2.13281100	1.07494500	-2.49657500
H	0.66163700	0.61878300	-3.40181600

H	0.54918700	1.67105200	-1.94998900
F	2.64389300	-0.92572500	1.02311100
C	3.77640900	-0.67175300	0.33041900
C	4.03194300	-1.79250100	-0.72555100
O	3.08809500	-1.92962200	-1.63420200
O	5.02668300	-2.46184600	-0.67541700
F	3.62565200	0.52522600	-0.27405700
H	2.31683800	-1.29811600	-1.55586600
F	4.78370700	-0.57949700	1.19737200
H	-0.80831200	-2.13745000	3.91322000
C	-0.40588900	-1.29096300	3.36008000
H	0.15712300	-0.64354400	4.03995600
H	0.25369100	-1.65259900	2.56613300
O	-1.53462700	-0.60808300	2.81335300
H	0.83631500	0.58081200	2.16127000
C	-1.30809400	0.48317300	2.02906000
C	-0.06683200	1.01649400	1.75727500
C	-2.47806700	1.06445300	1.47130600
H	2.20594200	2.29149900	1.03603300
H	-3.43386900	0.60609400	1.69405100
C	0.05147400	2.14838200	0.90662800
C	1.31258400	2.72638300	0.60301700
C	-2.38392400	2.14906600	0.64344700
C	-1.12234100	2.72293200	0.32579500
C	1.40864000	3.80952400	-0.24096000
H	2.38030200	4.23424800	-0.46733600
H	-3.28011800	2.57125400	0.20185500
C	-0.99028800	3.83385200	-0.54579200
C	0.24802900	4.36766500	-0.82723200
H	-1.88496600	4.25858900	-0.98958400
H	0.33753300	5.21558200	-1.49665100

Optimized geometry of **CT5** (B3LYP-D3/6-311+G(d,p)-CPCM(CH_2Cl_2) level of theory)

Gibbs free energy: -1527.804962 Hartree

C	1.61830200	1.67490300	-0.90861100
C	1.70776500	2.10154400	0.45143100
C	0.70123200	1.68019300	1.36121000
C	-0.33616000	0.88670600	0.95098200

C	-0.41681200	0.47425500	-0.40177000
C	0.53136000	0.85537700	-1.31758400
C	2.62995000	2.07877400	-1.81788300
C	3.67403300	2.87320100	-1.40150100
C	3.75877300	3.29941700	-0.05561800
C	2.79619200	2.91691800	0.85015800
O	-1.49767800	-0.33224000	-0.70501100
C	-1.67864900	-0.77454400	-2.06254500
H	0.76834000	1.98659800	2.39912300
H	-1.09080400	0.55251900	1.65178500
H	0.48718400	0.53129300	-2.34779700
H	2.57026000	1.74790100	-2.84950500
H	4.44113200	3.17218100	-2.10722700
H	4.58936400	3.92026600	0.26036700
H	2.86155400	3.22974300	1.88697300
H	-2.57079600	-1.39597600	-2.05579000
H	-1.82541200	0.08196500	-2.72380800
H	-0.82201300	-1.36788100	-2.38147000
H	-1.02437700	-4.36148300	1.20250000
C	-1.46757400	-3.77234900	0.39334800
C	4.56625700	-0.16010000	1.14511900
C	4.20964400	-0.69464300	-0.07104200
C	3.74294800	-0.36384800	2.27657300
C	3.01869800	-1.45062100	-0.20960800
C	2.61569900	-2.01320800	-1.45082600
C	2.57805900	-1.08831700	2.17171800
C	2.18055600	-1.64968700	0.93007700
C	1.44955700	-2.72305300	-1.56072900
C	0.97032500	-2.38222800	0.79437900
C	0.60976400	-2.90236900	-0.42895500
O	-0.54148100	-3.59224300	-0.67977700
H	-2.31238300	-4.31271700	-0.02945200
H	5.47115500	0.42887800	1.23777000
H	4.83046700	-0.53292500	-0.94574500
H	3.24452800	-1.86706000	-2.32270000
H	4.02746600	0.06776900	3.22985800
H	1.13661300	-3.15091900	-2.50602600
H	1.94071500	-1.22970000	3.03823400

H	0.33849400	-2.49867300	1.66460700
H	-1.80865600	-2.80977900	0.78409700
F	-5.48576300	2.06013300	-0.01730700
C	-4.41069400	1.27529300	-0.07212000
C	-4.50553100	0.10640500	0.95890700
O	-3.47465700	-0.71463800	0.96586800
O	-5.46151200	-0.00044900	1.67602900
F	-4.30214400	0.79103200	-1.32865800
H	-2.75152900	-0.49977900	0.30857600
F	-3.31885200	2.03063900	0.16797500

Optimized geometry of 2-naphthol (B3LYP-D3/6-311+G(d,p)-CPCM(CH_2Cl_2) level of theory)

Gibbs free energy: -461.138428 Hartree

C	-0.28465100	-0.62131900	0.00000000
C	-0.53038200	0.78872900	-0.00000200
C	0.58392500	1.67121700	0.00000100
C	1.86935200	1.19294000	0.00000500
C	2.10492500	-0.20493100	0.00000700
C	1.05416400	-1.09401700	0.00000500
C	-1.39660100	-1.50605000	-0.00000300
C	-2.68382900	-1.01939400	-0.00000800
C	-2.92582400	0.37558200	-0.00001000
C	-1.86966900	1.25782500	-0.00000700
O	3.41884900	-0.59008700	0.00001000
H	3.48398200	-1.55264200	0.00001700
H	0.40603700	2.74126600	0.00000000
H	2.72081400	1.86298200	0.00000800
H	1.24034300	-2.16359200	0.00000600
H	-1.21548500	-2.57579200	-0.00000100
H	-3.52182400	-1.70749500	-0.00001000
H	-3.94514300	0.74425700	-0.00001400
H	-2.04797900	2.32822900	-0.00000900

Optimized geometry of 2-methoxynaphthalene (B3LYP-D3/6-311+G(d,p)-CPCM(CH_2Cl_2) level of theory)

Gibbs free energy: -500.189851 Hartree

C	-0.56381500	-0.53000700	-0.00012700
C	-1.06154500	0.81056000	0.00005700
C	-0.12358400	1.87989100	0.00007200

C	1.22461600	1.63890600	-0.00008000
C	1.71574400	0.30486100	-0.00024400
C	0.83987700	-0.76024600	-0.00028200
C	-1.49704700	-1.60066700	-0.00015600
C	-2.85258500	-1.35598500	-0.00002200
C	-3.34294300	-0.02907800	0.00016100
C	-2.46249300	1.03019400	0.00020000
O	3.07551800	0.20140500	-0.00043700
C	3.65701800	-1.10422500	0.00058800
H	-0.49092800	2.90079000	0.00019800
H	1.94358300	2.44999600	-0.00007500
H	1.19413500	-1.78269600	-0.00042700
H	-1.12501700	-2.62015100	-0.00029100
H	-3.55158900	-2.18515300	-0.00005400
H	-4.41225100	0.14967600	0.00026700
H	-2.83099100	2.05102900	0.00033500
H	4.73462300	-0.94978600	0.00090200
H	3.36706600	-1.66453300	0.89526100
H	3.36776200	-1.66562900	-0.89362800

Optimized geometry of TFA (B3LYP-D3/6-311+G(d,p)-CPCM(CH_2Cl_2) level of theory)

Gibbs free energy: -526.969667 Hartree

C	0.59463100	-0.00117000	-0.00000900
C	-0.95232300	0.15779400	-0.00002500
O	-1.52088500	-1.04166000	-0.00001400
O	-1.49482300	1.22524300	-0.00001300
F	1.18887600	1.19411100	-0.00039600
F	1.00332700	-0.67788800	1.08927400
F	1.00334900	-0.67860100	-1.08883100
H	-2.48815200	-0.94700800	-0.00000600

Optimized geometry of **1a'** (B3LYP/6-31+G(d)-CPCM(CH_2Cl_2) level of theory)

C	2.18191600	-4.45114700	0.40425100
C	2.85791400	-3.25647900	0.22444300
C	2.17454700	-2.02240000	0.08613000
C	0.74569300	-2.02810300	0.13597000
C	0.08059200	-3.26590800	0.33831800
C	0.77642800	-4.45457200	0.46641400

C	2.88439000	-0.76187600	-0.10522700
C	2.16425100	0.47922200	-0.13345800
C	0.72334800	0.45476800	0.00210900
C	0.04206600	-0.77512800	0.03008800
C	4.28983400	-0.73071700	-0.28507500
C	4.97739700	0.45183200	-0.49523700
C	4.26962700	1.66572400	-0.54213400
C	2.89727000	1.67231400	-0.36604600
C	-1.55531100	0.89411900	-0.01117900
C	-2.81165800	1.52535400	-0.02813600
C	-3.96498000	0.71058200	-0.11659600
C	-3.82929000	-0.67256100	-0.17704900
C	-2.55340400	-1.29898800	-0.12913400
C	-1.40710100	-0.51524100	-0.02915200
C	-0.29149200	1.54602100	0.04161300
C	-0.32938100	2.94001700	0.17802500
C	-1.59401100	3.61397800	0.16128200
C	-2.79472600	2.94635700	0.05141000
O	0.82249500	3.63978100	0.35054200
C	0.79850700	5.06302600	0.50876100
O	-5.00026500	-1.38054200	-0.28075900
C	-4.95342100	-2.80611700	-0.34418300
H	2.73874800	-5.37825400	0.51083400
H	3.94117700	-3.28169700	0.20480500
H	-0.99592500	-3.28861100	0.42935900
H	0.23613100	-5.38360200	0.62829900
H	4.85548000	-1.65500300	-0.27695500
H	6.05520900	0.43526900	-0.63439200
H	4.79500500	2.60010300	-0.72327200
H	2.36346600	2.60914500	-0.40891100
H	-4.95855700	1.14945000	-0.14331900
H	-2.50498200	-2.37598000	-0.19005100
H	-1.61091600	4.69399500	0.24069300
H	-3.72523200	3.50832100	0.03955900
H	1.84251100	5.35341200	0.63201300
H	0.38405000	5.55350400	-0.37845200
H	0.23048400	5.35055600	1.39984400
H	-5.99246900	-3.12934900	-0.42161200

H	-4.39933300	-3.14826300	-1.22666100
H	-4.50671000	-3.23137500	0.56271400

Optimized geometry of **2a'** (B3LYP/6-31+G(d)-CPCM(CH_2Cl_2) level of theory)

C	8.21250600	-3.03404800	-1.75479500
C	8.45468600	-1.97147400	-0.90104900
C	7.40990600	-1.14174900	-0.42245200
C	6.07271000	-1.42419800	-0.84197100
C	5.85686500	-2.50944400	-1.73135000
C	6.89811900	-3.30275800	-2.17857000
C	7.66144200	-0.02168400	0.47858300
C	6.59307200	0.85817800	0.85879400
C	5.26146000	0.59984100	0.35335400
C	5.00737400	-0.56777400	-0.38679000
C	8.95253500	0.21450800	1.01322600
C	9.20478300	1.25323200	1.89228500
C	8.15388000	2.10233900	2.28119600
C	6.88187600	1.90370300	1.77439900
C	2.97512400	0.48016800	-0.03807800
C	1.59336600	0.73677700	-0.07460100
C	0.73071700	-0.23895800	-0.65424600
C	1.30293700	-1.40690800	-1.16973400
C	2.70582100	-1.63493700	-1.15188000
C	3.55494500	-0.68418300	-0.59940800
C	3.97043500	1.32411900	0.53118500
C	3.52247800	2.56061300	1.01354400
C	2.12101700	2.85123700	0.99553900
C	1.18313900	1.97873500	0.48671600
C	-0.74687600	-0.03164400	-0.69843300
C	-1.59691700	-0.54895800	0.33062300
C	-2.98249800	-0.33474500	0.22961700
C	-3.57811400	0.42578200	-0.81321700
C	-2.74084900	0.92489600	-1.79853700
C	-1.34233600	0.68026300	-1.73513300
C	-1.16435900	-1.27212600	1.47495800
C	-2.08113700	-1.69362500	2.41527200
C	-3.48474100	-1.45244700	2.28794400
C	-3.96755600	-0.80033100	1.14452300

C	-6.97218000	-1.59719500	1.97527200
C	-8.28476500	-1.89550100	2.29536300
C	-9.33560400	-1.24529000	1.62483300
C	-9.04571100	-0.32258900	0.63494600
C	-5.02411800	0.44769400	-0.53618700
C	-5.27681500	-0.34406800	0.59653600
C	-6.64089200	-0.64140700	0.97965200
C	-7.71358900	0.00145100	0.27573000
C	-6.85378300	2.75557100	-2.89970500
C	-5.82886000	2.06739600	-2.27569300
C	-6.07894700	1.14748300	-1.22400000
C	-7.42930300	0.94477500	-0.80088900
C	-8.45579500	1.66943700	-1.45677900
C	-8.18351800	2.55329100	-2.48693600
O	0.42520400	-2.31447800	-1.70470700
C	0.91791700	-3.54701200	-2.23035500
O	4.41362000	3.48008100	1.46748900
C	3.96936500	4.75357500	1.94957800
O	-0.53818900	1.23735200	-2.71401500
C	-0.63653800	0.62772300	-4.01042200
O	-4.34309000	-1.82193900	3.27302600
C	-3.86166000	-2.46677700	4.45805100
H	9.03866600	-3.64696900	-2.10512400
H	9.48001400	-1.77438700	-0.61064800
H	4.86174700	-2.71038700	-2.10188100
H	6.69915400	-4.12114000	-2.86551200
H	9.77446900	-0.43993600	0.74783700
H	10.20739900	1.39969400	2.28550600
H	8.33435300	2.91149200	2.98445800
H	6.08182000	2.55868700	2.08306200
H	3.07814500	-2.56288300	-1.55947500
H	1.77780100	3.79773300	1.39475500
H	0.13280000	2.25410500	0.50339200
H	-3.09338400	1.50803700	-2.64007400
H	-0.10963400	-1.48465400	1.62276300
H	-1.71718100	-2.22307400	3.28719200
H	-6.17359700	-2.10510200	2.49359500
H	-8.49853100	-2.63743700	3.06064800

H	-10.37021000	-1.47214900	1.86865100
H	-9.87362300	0.14494900	0.11511900
H	-6.62726400	3.45841700	-3.69713500
H	-4.81293900	2.26420800	-2.58672300
H	-9.48755200	1.54854300	-1.14795300
H	-8.99529200	3.09497600	-2.96498700
H	0.03606300	-4.08937400	-2.57437600
H	1.59420100	-3.37867700	-3.07707600
H	1.42825300	-4.13484600	-1.45796500
H	4.87883300	5.28165900	2.23840700
H	3.45398100	5.31430900	1.16266700
H	3.31772100	4.64121200	2.82261500
H	0.03812900	1.18696100	-4.66166800
H	-0.32478700	-0.42242800	-3.96418800
H	-1.65813500	0.69022900	-4.40451700
H	-4.74851600	-2.63850800	5.06906100
H	-3.38743800	-3.42541000	4.22237700
H	-3.16190400	-1.82171400	4.99979100

Optimized geometry of **1a**$^{\bullet+}$ (UB3LYP/6-31+G(d) level of theory)

C	3.93997300	0.47793400	0.20625300
C	3.25725300	-0.72828700	-0.00076300
C	1.86057500	-0.81252700	-0.11590800
C	1.09372600	0.38897800	-0.01302100
C	1.78585100	1.60949400	0.21782000
C	3.15935800	1.65305800	0.31928200
C	1.17546900	-2.09308200	-0.34100400
C	-0.25945700	-2.17401200	-0.27823100
C	-1.01107800	-0.97540200	-0.05986400
C	-0.32452400	0.31288000	-0.08411400
C	1.89166500	-3.26303100	-0.63486200
C	1.25184700	-4.48120900	-0.86239300
C	-0.14438900	-4.56259400	-0.80905100
C	-0.88364400	-3.42759900	-0.52108700
C	-2.57802800	0.70900500	0.02431300
C	-3.79299000	1.41566800	0.08669600
C	-3.74247900	2.81541700	-0.05736600
C	-2.51543000	3.46738200	-0.25241800

C	-1.29755700	2.74863100	-0.27607200
C	-1.32286200	1.36029500	-0.11663200
C	-2.43798300	-0.71259100	0.10252400
C	-3.61348200	-1.44183600	0.36001400
C	-4.85847300	-0.74174200	0.43896000
C	-4.95953500	0.62516900	0.29539800
C	5.46631100	0.55800900	0.33202200
C	6.15034100	-0.81379300	0.17518300
C	5.82968100	1.12732000	1.72816600
C	6.01308300	1.50413400	-0.76820500
O	-2.60045500	4.81071300	-0.40862900
C	-1.41538400	5.57984900	-0.61770400
O	-3.54657800	-2.77358300	0.54798800
C	-4.71418200	-3.52848000	0.91320900
H	3.84044600	-1.63601200	-0.05762100
H	1.22576200	2.52275800	0.36600200
H	3.63910300	2.60750500	0.50939600
H	2.97177900	-3.23631100	-0.71152400
H	1.84482100	-5.36192200	-1.09207200
H	-0.64788300	-5.50530200	-1.00076400
H	-1.96044300	-3.48744900	-0.48801000
H	-4.64684600	3.41639900	-0.03210100
H	-0.37394100	3.28321900	-0.44573400
H	-5.76444600	-1.30826400	0.61517000
H	-5.93532700	1.09971800	0.35503100
H	5.83876700	-1.52273200	0.95156700
H	5.95708700	-1.26166900	-0.80701700
H	7.23451300	-0.69070500	0.26691600
H	5.45470300	0.48078700	2.52988300
H	6.91910600	1.19272100	1.82756400
H	5.42288900	2.13187500	1.88472000
H	5.77313200	1.12847200	-1.76957800
H	5.60915600	2.51826100	-0.68098500
H	7.10355000	1.57481100	-0.68548000
H	-1.75341400	6.61140200	-0.71629800
H	-0.73647100	5.49849500	0.24019600
H	-0.90299700	5.27333300	-1.53782300
H	-4.35874800	-4.54962200	1.05082800

H	-5.13752800	-3.15657500	1.85143300
H	-5.46244300	-3.50244900	0.11456000

Optimized geometry of (*R*)-**2a'** (B3LYP/6-31+G(d)-CPCM($CHCl_3$) level of theory)

C	-8.20261900	-2.92133300	1.95570600
C	-8.44825400	-1.91920800	1.03282300
C	-7.40633600	-1.12063300	0.49861600
C	-6.06820100	-1.37022300	0.93526100
C	-5.84878200	-2.39262700	1.89528600
C	-6.88728300	-3.15720200	2.39547000
C	-7.66153300	-0.06480400	-0.47572600
C	-6.59622100	0.79116900	-0.91416800
C	-5.26406900	0.57187100	-0.39259300
C	-5.00590400	-0.54293500	0.42324500
C	-8.95302100	0.13001900	-1.02551000
C	-9.20852100	1.10606400	-1.97262800
C	-8.16047900	1.93063600	-2.41768600
C	-6.88816900	1.77138400	-1.89827000
C	-2.97703100	0.48596600	0.00426300
C	-1.59629600	0.74923000	0.02320300
C	-0.72980500	-0.18338700	0.66514200
C	-1.29841400	-1.31579900	1.25775700
C	-2.70051300	-1.54910900	1.25594300
C	-3.55302800	-0.64037000	0.64191200
C	-3.97555900	1.28714300	-0.61847300
C	-3.53217300	2.49104200	-1.17997100
C	-2.13186800	2.78688600	-1.18253800
C	-1.19052600	1.95269900	-0.61886000
C	0.74745400	0.02917100	0.69207700
C	1.59923800	-0.57386300	-0.28805400
C	2.98454200	-0.35115800	-0.20388700
C	3.57867300	0.49713100	0.76980100
C	2.73984200	1.07868300	1.70710500
C	1.34161700	0.82829100	1.66366400
C	1.16842500	-1.39082700	-1.36779900
C	2.08684600	-1.89053300	-2.26740700
C	3.49017900	-1.64036200	-2.15790400
C	3.97120300	-0.89336500	-1.07374400

C	6.97712400	-1.76151500	-1.82420100
C	8.29013300	-2.08771600	-2.11328100
C	9.33979700	-1.38171300	-1.49997600
C	9.04820500	-0.37533600	-0.59602800
C	5.02496900	0.49563200	0.49391900
C	5.27967200	-0.39150900	-0.56494100
C	6.64422800	-0.72176300	-0.91741400
C	7.71560500	-0.02019600	-0.27003100
C	6.84957800	3.00241200	2.64887400
C	5.82602700	2.26204900	2.08558100
C	6.07830800	1.25311200	1.11967000
C	7.42938700	1.01396600	0.71891000
C	8.45441200	1.79344500	1.31085400
C	8.18010400	2.76446500	2.25857100
O	-0.41769700	-2.18211800	1.85385000
C	-0.90464900	-3.38325600	2.45020900
O	-4.42720200	3.37629800	-1.69235100
C	-3.98916300	4.62451300	-2.23880200
O	0.53878500	1.46638400	2.59295600
C	0.60986400	0.93969100	3.92613800
O	4.35088000	-2.09376500	-3.10624800
C	3.87097500	-2.83070300	-4.23557000
H	-9.02682400	-3.51156400	2.34725600
H	-9.47430400	-1.74448700	0.73083000
H	-4.85282700	-2.56451100	2.27808300
H	-6.68565900	-3.92690300	3.13589700
H	-9.77253000	-0.50837300	-0.71696600
H	-10.21141900	1.22193500	-2.37530400
H	-8.34347800	2.68967400	-3.17419800
H	-6.09022000	2.40671000	-2.25028200
H	-3.06995100	-2.44881900	1.72495200
H	-1.79211700	3.70637000	-1.64321000
H	-0.14109600	2.22960000	-0.65420400
H	3.09012200	1.73228000	2.49629200
H	0.11375200	-1.61424200	-1.49891700
H	1.72415600	-2.49147300	-3.09230200
H	6.17928000	-2.31246200	-2.29767200
H	8.50524200	-2.89444200	-2.80957200

H	10.37484100	-1.62990700	-1.72014900
H	9.87508100	0.13565600	-0.11700900
H	6.62147400	3.77303200	3.38057500
H	4.80919100	2.48566700	2.37490000
H	9.48676800	1.64577200	1.01593400
H	8.99094800	3.34614600	2.68889600
H	-0.02074000	-3.89953500	2.82776100
H	-1.58409800	-3.16949900	3.28435700
H	-1.41006400	-4.01916800	1.71315300
H	-4.90088300	5.13269700	-2.55534900
H	-3.47729700	5.22812100	-1.48159400
H	-3.33585600	4.47153600	-3.10467700
H	-0.06136500	1.55197300	4.53177900
H	0.27904200	-0.10558700	3.94392800
H	1.62836700	1.00837000	4.32803400
H	4.75869000	-3.05305100	-4.82898200
H	3.39401600	-3.76674400	-3.92521000
H	3.17367400	-2.23051500	-4.82991400

Optimized geometry of (*S*)-**2a'** (M06-2X/6-31G(d,p) level of theory)

Gibbs free energy: -2301.425112 Hartree

C	7.94764100	3.68518100	-1.05766500
C	8.31089600	2.43096600	-0.61876300
C	7.35104700	1.42522100	-0.37251400
C	5.98408000	1.73490700	-0.58638800
C	5.63400900	3.03477700	-1.01511800
C	6.59282200	3.99286000	-1.25327600
C	7.72286900	0.09179600	0.08416800
C	6.71914900	-0.85480300	0.43430200
C	5.33100700	-0.47379500	0.30676300
C	4.99512600	0.73317700	-0.29376100
C	9.07620400	-0.30146000	0.16547900
C	9.44050600	-1.57037700	0.55640500
C	8.44941100	-2.51128800	0.86857300
C	7.12026700	-2.15879500	0.80306100
C	3.02336100	-0.41367400	0.08031000
C	1.66194200	-0.72164400	0.12458900
C	0.74341000	0.16831700	-0.51294100

C	1.26145100	1.29944900	-1.12297400
C	2.64444400	1.61508800	-1.12540400
C	3.53893000	0.77321600	-0.50259400
C	4.07076600	-1.19634100	0.63142600
C	3.67999700	-2.30292700	1.37464900
C	2.29482900	-2.64396000	1.44608800
C	1.31719200	-1.89801100	0.83723300
C	-0.71794300	-0.09387500	-0.50524600
C	-1.63031900	0.80790100	0.11154700
C	-2.99156100	0.49648000	0.08698100
C	-3.49899000	-0.70105100	-0.46722800
C	-2.61430900	-1.55498900	-1.09533300
C	-1.23184900	-1.23714300	-1.11501600
C	-1.28646200	2.01091600	0.78572500
C	-2.26535300	2.76955600	1.37235600
C	-3.65243600	2.42237500	1.32013100
C	-4.04203700	1.29050200	0.61824800
C	-7.09907000	2.23288800	0.77596600
C	-8.43034900	2.58024700	0.82344400
C	-9.41439400	1.63002600	0.51734900
C	-9.04126800	0.35535200	0.15430200
C	-4.95383200	-0.66973300	-0.25223000
C	-5.29798700	0.55102300	0.31624000
C	-6.68895800	0.92493300	0.43207300
C	-7.68577600	-0.03377900	0.09439900
C	-6.52734600	-3.97627800	-1.08872400
C	-5.57494800	-3.00564900	-0.87624700
C	-5.93440800	-1.68883000	-0.51052300
C	-7.30478800	-1.37815300	-0.32094100
C	-8.25807100	-2.39589000	-0.54188500
C	-7.88577700	-3.66472700	-0.92835100
O	0.42531000	2.19895800	-1.74336900
C	0.02328500	1.78935600	-3.04330100
O	4.60816500	-3.03084000	2.04191800
C	4.19356900	-4.09053800	2.87970300
O	-0.31850500	-2.02446700	-1.75333300
C	-0.73951200	-3.26731200	-2.26766800
O	-4.57786900	3.17386900	1.96355600

C	-4.16255900	4.27412100	2.74810000
H	8.70903800	4.43789700	-1.23372700
H	9.36092400	2.23144100	-0.44385300
H	4.59010000	3.29691600	-1.11475900
H	6.29897300	4.98706200	-1.57372600
H	9.85710400	0.39698100	-0.10857500
H	10.49001600	-1.84258700	0.60242600
H	8.72648400	-3.52245900	1.14923600
H	6.36105700	-2.89306400	1.02278300
H	2.92062200	2.52343200	-1.64643000
H	1.99980000	-3.52261700	2.00534700
H	0.27686100	-2.19574100	0.92271300
H	-2.95035300	-2.44441800	-1.60833200
H	-0.24995500	2.32459600	0.84485200
H	-1.97165900	3.67116300	1.89439400
H	-6.34479600	2.97376400	0.99058000
H	-8.71439800	3.59455800	1.08502000
H	-10.46535700	1.89871900	0.54778800
H	-9.81675100	-0.35159700	-0.11331200
H	-6.22635800	-4.98310400	-1.35950900
H	-4.52846600	-3.27140500	-0.93770000
H	-9.31072000	-2.19400100	-0.38666800
H	-8.64259100	-4.42608400	-1.08574200
H	-0.66589000	2.54923000	-3.41253200
H	0.88991600	1.72057300	-3.71203100
H	-0.48321100	0.81829200	-3.01109700
H	5.10305700	-4.47334400	3.34146200
H	3.51093900	-3.73724300	3.65980800
H	3.71278500	-4.89229700	2.30850800
H	0.15837700	-3.75318000	-2.64803200
H	-1.18863300	-3.89422500	-1.48725100
H	-1.45708900	-3.14551700	-3.08791700
H	-5.07124200	4.67490400	3.19594400
H	-3.47492500	3.96052200	3.54051600
H	-3.68792100	5.04901300	2.13652700

Optimized geometry of (*R*)-**2a'** (M06-2X/6-31G(d,p) level of theory)

Gibbs free energy: -2301.425051 Hartree

C	-8.28227200	-3.01737600	-1.69206700
C	-8.49653000	-1.75632600	-1.18075100
C	-7.43004900	-0.94877500	-0.72901400
C	-6.11328600	-1.46792300	-0.81165300
C	-5.92061200	-2.77284600	-1.31763800
C	-6.97964800	-3.53459100	-1.75598300
C	-7.64272900	0.38969300	-0.19215100
C	-6.55605000	1.12428700	0.36079300
C	-5.24065900	0.52589200	0.35663300
C	-5.02447700	-0.67167100	-0.31406400
C	-8.91611700	0.99772800	-0.22916400
C	-9.12325400	2.27620400	0.23805200
C	-8.04501600	3.01011200	0.75171300
C	-6.79089000	2.44492100	0.80573500
C	-2.96198700	0.09637900	0.38782600
C	-1.58483100	0.16712200	0.61621100
C	-0.74638600	-0.81000500	-0.00074000
C	-1.35329300	-1.79492000	-0.76276200
C	-2.75494800	-1.87379000	-0.95092300
C	-3.57822300	-0.93984100	-0.35886100
C	-3.93466300	0.99938100	0.89014700
C	-3.47290600	1.96157600	1.77957900
C	-2.07197900	2.05688300	2.04312800
C	-1.15289800	1.20707400	1.48068600
C	0.72848300	-0.79084900	0.15408200
C	1.51940100	0.29041400	-0.34339500
C	2.90785900	0.21053700	-0.21025800
C	3.56260500	-0.85737100	0.45321600
C	2.79060400	-1.90409000	0.90650500
C	1.37882900	-1.86172800	0.74902200
C	1.03051500	1.44288300	-1.01388600
C	1.90595300	2.41205300	-1.43726400
C	3.31975900	2.30535900	-1.26592400
C	3.84960800	1.15350300	-0.69695300
C	6.77728700	2.01807100	-1.67785000
C	8.05867600	2.34412000	-2.06124200
C	9.15111900	1.66181200	-1.50841900
C	8.93346300	0.65487600	-0.59503500

C	5.00013900	-0.54512600	0.40998100
C	5.18956400	0.60534400	-0.34570500
C	6.52599100	1.00743000	-0.72261200
C	7.63297300	0.29392500	-0.18161300
C	6.95902400	-2.88288600	2.60025400
C	5.89735000	-2.26327200	1.98141000
C	6.09673100	-1.22772600	1.04102200
C	7.41792400	-0.79667600	0.76125800
C	8.48619700	-1.44826300	1.41529800
C	8.26921000	-2.47570500	2.30691000
O	-0.58959800	-2.76654000	-1.37019000
C	-0.03837400	-2.34813400	-2.61086800
O	-4.35204100	2.78167600	2.40379900
C	-3.88954000	3.67400100	3.39766700
O	0.60496200	-2.86950800	1.24478500
C	0.99697500	-4.18663200	0.89962200
O	4.14062000	3.31669800	-1.63929400
C	3.58707600	4.51552800	-2.14325300
H	-9.12362700	-3.61508000	-2.02699200
H	-9.51545500	-1.39591600	-1.11136100
H	-4.92785100	-3.20034100	-1.31746600
H	-6.80792800	-4.53784600	-2.13206000
H	-9.75550900	0.46359300	-0.65673700
H	-10.11381000	2.71677900	0.18964400
H	-8.19324700	4.02879600	1.09567100
H	-5.96044000	3.02184900	1.18177600
H	-3.10472200	-2.68381100	-1.57894300
H	-1.71692300	2.82461500	2.71859700
H	-0.09886800	1.31882100	1.71463300
H	3.21331100	-2.78005600	1.38087100
H	-0.03445400	1.56743800	-1.18244900
H	1.50242600	3.28952500	-1.92619100
H	5.93971200	2.53121700	-2.12339800
H	8.21897800	3.12110100	-2.80188200
H	10.16356000	1.91051800	-1.80961400
H	9.78985000	0.11637600	-0.20869800
H	6.78095300	-3.66917700	3.32650500
H	4.88998800	-2.53939600	2.26052200

H	9.50558700	-1.12893100	1.23725200
H	9.11144600	-2.95321100	2.79668000
H	0.55502000	-3.18152000	-2.98954700
H	-0.83221200	-2.10843000	-3.32884200
H	0.60648300	-1.47122500	-2.47967000
H	-4.78012600	4.16298000	3.79084000
H	-3.38124300	3.13895900	4.20667500
H	-3.21647900	4.43035700	2.97926400
H	0.14402200	-4.82673200	1.12598100
H	1.22378300	-4.25310000	-0.16886600
H	1.85852200	-4.52485100	1.48736200
H	4.43282900	5.18056300	-2.31441500
H	3.05956100	4.35011700	-3.08898100
H	2.90514300	4.97388800	-1.41918900

Optimized geometry of TS1 (M06-2X/6-31G(d,p) level of theory)

Gibbs free energy: -2301.366912 Hartree

C	7.70586500	-4.02769100	-0.01389800
C	8.16156500	-2.72729200	-0.02150400
C	7.27304200	-1.63085300	0.02754400
C	5.88134600	-1.90036800	0.03759600
C	5.43798900	-3.24042300	0.10007800
C	6.32950000	-4.28860600	0.07268700
C	7.73696300	-0.25176300	0.13465600
C	6.80180800	0.82075100	0.19878400
C	5.39950800	0.52483700	0.03125500
C	4.96807800	-0.79377600	-0.01005700
C	9.11095500	0.05054300	0.25142200
C	9.55423000	1.33591700	0.46955500
C	8.62635100	2.37899000	0.60223200
C	7.28052200	2.12257900	0.47015200
C	3.07491400	0.54179900	-0.06815300
C	1.73348400	0.91817500	-0.18574900
C	0.71264100	-0.11951700	-0.16047500
C	1.20335200	-1.37075600	-0.60272300
C	2.57134000	-1.73492100	-0.52040200
C	3.50823800	-0.80685700	-0.12665600
C	4.20591600	1.40391000	-0.09501200

C	3.96220900	2.72961800	-0.42059500
C	2.61897000	3.13833300	-0.65762200
C	1.55141800	2.28159400	-0.54133500
C	-0.71262600	0.11909200	0.16069700
C	-1.73357300	-0.91850400	0.18582200
C	-3.07495800	-0.54197000	0.06818900
C	-3.50814500	0.80672500	0.12681700
C	-2.57117600	1.73464800	0.52072200
C	-1.20322900	1.37033600	0.60306700
C	-1.55168700	-2.28197700	0.54130100
C	-2.61934200	-3.13861200	0.65742400
C	-3.96251900	-2.72972800	0.42034200
C	-4.20605700	-1.40395900	0.09488600
C	-7.28070600	-2.12223500	-0.47056400
C	-8.62655500	-2.37848600	-0.60275100
C	-9.55432900	-1.33532900	-0.47000700
C	-9.11093000	-0.05002700	-0.25170000
C	-4.96797900	0.79381400	0.01012800
C	-5.39954800	-0.52474600	-0.03136100
C	-6.80186900	-0.82049000	-0.19901300
C	-7.73691200	0.25211700	-0.13481600
C	-6.32902100	4.28880200	-0.07228600
C	-5.43762100	3.24052600	-0.09975000
C	-5.88112400	1.90051200	-0.03745200
C	-7.27284900	1.63114400	-0.02751400
C	-8.16125800	2.72767200	0.02161000
C	-7.70541900	4.02802400	0.01418600
O	0.32115100	-2.21219200	-1.20254100
C	0.65793400	-3.56770000	-1.39304000
O	4.99818000	3.58931000	-0.58495800
C	4.74537700	4.89445200	-1.06134600
O	-0.32095500	2.21163200	1.20297200
C	-0.65772400	3.56708200	1.39389300
O	-4.99859800	-3.58931600	0.58455700
C	-4.74596400	-4.89459400	1.06066000
H	8.41463100	-4.84834300	-0.05196900
H	9.23062500	-2.55795200	-0.06025500
H	4.37970800	-3.44044600	0.21049800

H	5.97009300	-5.31121400	0.12475000
H	9.84493400	-0.74362500	0.19344500
H	10.61740800	1.53299100	0.56183200
H	8.96646000	3.38740100	0.81511500
H	6.56683800	2.92468100	0.58132500
H	2.86176800	-2.72809300	-0.83352100
H	2.42506100	4.15103500	-0.98803500
H	0.57125700	2.64482300	-0.82133400
H	-2.86152000	2.72781800	0.83392800
H	-0.57159600	-2.64534100	0.82135800
H	-2.42556600	-4.15136600	0.98776000
H	-6.56710100	-2.92440000	-0.58179200
H	-8.96676000	-3.38683500	-0.81576900
H	-10.61752300	-1.53227900	-0.56236800
H	-9.84482800	0.74421300	-0.19367400
H	-5.96950100	5.31137700	-0.12420400
H	-4.37931300	3.44045100	-0.21008300
H	-9.23033800	2.55844000	0.06027700
H	-8.41410000	4.84874700	0.05231200
H	-0.26166600	-4.05836300	-1.71345400
H	1.42242900	-3.68823000	-2.16864400
H	1.01175700	-4.03158600	-0.46301500
H	5.72062900	5.37361900	-1.14125000
H	4.26968100	4.87411700	-2.04784100
H	4.11845800	5.46313000	-0.36548900
H	0.26189300	4.05765200	1.71439600
H	-1.01160900	4.03124700	0.46402800
H	-1.42216000	3.68737800	2.16958700
H	-5.72127400	-5.37367000	1.14039900
H	-4.11906900	-5.46317800	0.36470500
H	-4.27032100	-4.87454400	2.04718700

Optimized geometry of TS2 (M06-2X/6-31G(d,p) level of theory)

Gibbs free energy: -2301.364441 Hartree

C	7.81766000	-3.87918900	-0.56673600
C	8.23657700	-2.58049500	-0.37633900
C	7.31712100	-1.52640000	-0.18296400
C	5.93300100	-1.82867100	-0.23907600

C	5.52739600	-3.17481800	-0.37928900
C	6.44814200	-4.18473200	-0.54255500
C	7.74306600	-0.16834700	0.13789300
C	6.77934000	0.86096400	0.33562100
C	5.39001000	0.56027000	0.08564400
C	4.99161000	-0.74740100	-0.14862300
C	9.10560600	0.14298200	0.33694100
C	9.50962400	1.38974500	0.75948400
C	8.55157000	2.37862800	1.02511600
C	7.21654900	2.11534700	0.81797800
C	3.06514200	0.54718400	-0.06672200
C	1.71389900	0.91831800	-0.17411000
C	0.72449900	-0.14573300	-0.26498000
C	1.24219700	-1.34961400	-0.78151500
C	2.62145700	-1.67682000	-0.77892500
C	3.53330400	-0.77518600	-0.28833800
C	4.17992600	1.42261500	0.04603200
C	3.92890200	2.77896200	-0.10906600
C	2.59274800	3.19324400	-0.34302900
C	1.53618200	2.31173600	-0.37582800
C	-0.71702500	-0.16083200	0.13751300
C	-1.70737600	0.89954600	0.08248500
C	-3.06356800	0.53929600	0.00800900
C	-3.52790600	-0.78291900	0.21080100
C	-2.60476700	-1.70215400	0.65012100
C	-1.22514000	-1.38108700	0.63771600
C	-1.51587600	2.29156000	0.29024300
C	-2.56720900	3.17810600	0.29470500
C	-3.91341400	2.77430900	0.09306200
C	-4.17701500	1.42184900	-0.06689000
C	-7.23297800	2.13813800	-0.73702800
C	-8.57285800	2.40992500	-0.89655600
C	-9.52601300	1.41926300	-0.62042600
C	-9.11354800	0.16301400	-0.23590900
C	-4.98925800	-0.75025000	0.10530600
C	-5.39015300	0.56345700	-0.09130200
C	-6.78541100	0.87305000	-0.29379700
C	-7.74662200	-0.15667300	-0.08648300

C	-6.44825100	-4.19126500	0.46467900
C	-5.52883500	-3.18112900	0.29518900
C	-5.93204200	-1.83031600	0.19933600
C	-7.31613100	-1.52242700	0.19267000
C	-8.23357900	-2.57718600	0.39184700
C	-7.81485000	-3.88138100	0.54012000
O	0.35787500	-2.22521500	-1.32779800
C	0.66915700	-3.60077800	-1.31800800
O	4.95763200	3.66132800	-0.12697100
C	4.69814400	5.01650000	-0.42844900
O	-0.32399100	-2.28559500	1.11770900
C	-0.79063300	-3.44703800	1.76337600
O	-4.93356500	3.66508400	0.14422600
C	-4.65460700	5.01816900	0.43782900
H	8.54942800	-4.66691900	-0.71253200
H	9.30075600	-2.37929800	-0.37222500
H	4.47440400	-3.41745900	-0.31968400
H	6.11621600	-5.21260500	-0.64684900
H	9.86119700	-0.61711800	0.18190900
H	10.56468700	1.59406900	0.91037700
H	8.85943700	3.34914200	1.40085200
H	6.47993200	2.87405000	1.03377000
H	2.92530400	-2.62659300	-1.19693300
H	2.39119200	4.23325200	-0.56645700
H	0.58577300	2.69736400	-0.70520300
H	-2.91121700	-2.66728800	1.02492500
H	-0.55499300	2.66846400	0.59675700
H	-2.35338100	4.21501900	0.52116700
H	-6.50072600	2.89850600	-0.96119900
H	-8.88846400	3.38880300	-1.24306500
H	-10.58452100	1.63000000	-0.73365700
H	-9.86680300	-0.59758800	-0.07228000
H	-6.11770900	-5.22258800	0.53331600
H	-4.48004700	-3.42736300	0.19318000
H	-9.29645600	-2.37199400	0.42555800
H	-8.54514500	-4.66945600	0.69129600
H	-0.27284200	-4.12734300	-1.48294600
H	1.36309000	-3.86554700	-2.12464700

H	1.09524400	-3.90359600	-0.35475100
H	5.66603800	5.51586800	-0.39976300
H	4.26311000	5.12661700	-1.42776000
H	4.03196100	5.47294500	0.31211300
H	0.09745400	-3.94550400	2.15295200
H	-1.46188700	-3.20667000	2.59590100
H	-1.30544700	-4.12342800	1.06862100
H	-5.61874200	5.52556700	0.43473600
H	-4.19231900	5.12525900	1.42514800
H	-4.00472300	5.46861400	-0.32060500

9. References

1. N. Ogawa, Y. Yamaoka, K. Yamada and K. Takasu, *Org. Lett.*, 2017, **19**, 3327–3330.
2. N. Ogawa, Y. Yamaoka, H. Takikawa, K. Yamada, and K. Takasu, *J. Am. Chem. Soc.*, 2020, **142**, 13322–13327.
3. K. Kurokawa, N. Ogawa, Y. Kuroda, Y. Yamaoka, H. Takikawa, K. Tsubaki and K. Takasu, *Org. Biomol. Chem.*, 2024, **22**, 5306–5313.
4. J. J. G. S. van Es, H. A. M. Biemans and E. W. Meijer, *Tetrahedron: Asymmetry*, 1997, **8**, 1825–1831.
5. T. Sakamoto, H. Yonehara and C. Pac, *J. Org. Chem.*, 1994, **59**, 6859–6861.
6. M. Noji, M. Nakajima and K. Koga, *Tetrahedron Lett.*, 1994, **35**, 7983–7984.
7. D. -R. Hwang, C. -P. Chen and B. -J. Uang, *Chem. Commun.*, 1999, 1207–1208.
8. K. Hassan, K. Yamashita, K. Hirabayashi, T. Shimizu, K. Nakabayashi, Y. Imai, T. Matsumoto, A. Yamano and K. Sugiura, *Chem. Lett.*, 2015, **44**, 1607–1609.
9. S. Li, R Li, Y. -K. Zhang, S. Wang, B. Ma, B. Zhanga and P. An, *Chem. Sci.*, 2023, **14**, 3286–3292.
10. T. Nishimura, T. Onoue, K. Ohe and S. Uemura, *J. Org. Chem.*, 1999, **64**, 6750–6755.
11. Z. He, A. P. Pulis and D. J. Procter, *Angew. Chem. Int. Ed.*, 2019, **58**, 7813–7817.
12. S. Zhang, Y. Wang, Z. Song, K. Nakajima and T. Takahashi, *Chem. Lett.*, 2013, **42**, 697–699.
13. L. Ochmann, M. Fuhrmann, F. J. Gössl, A. Makaveev and P. R. Schreiner, *Org. Lett.*, 2022, **24**, 6968–6972.
14. L. Yang, Y. Yan, N. Cao, J. Hao, G. Li, W. Zhang, R. Cao, C. Wang, J. Xiao and D. Xue, *Org. Lett.*, 2022, **24**, 9431–9435.
15. J. Fang, Z. Peng, Y. Yang, J. Wang, J. Guo and H. Gong, *Asian J. Org. Chem.*, 2018, **7**, 355–358.
16. C. A. Parker and W. Rees, *Analyst*, 1960, **85**, 587–600.
17. S. Maeda, K. Ohno and K. Morokuma, *Phys. Chem. Chem. Phys.*, 2013, **15**, 3683–3701.
18. S. Maeda, Y. Harabuchi, M. Takagi, K. Saita, K. Suzuki, T. Ichino, Y. Sumiya, K. Sugiyama and Y. Ono, *J. Comput. Chem.*, 2018, **39**, 233–251.
19. Gaussian 16, Revision C.01, M. J. Frisch, G. W. Trucks, H. B. Schlegel, G. E. Scuseria, M. A. Robb, J. R. Cheeseman, G. Scalmani, V. Barone, G. A. Petersson, H. Nakatsuji, X. Li, M. Caricato, A. V. Marenich, J. Bloino, B. G. Janesko, R. Gomperts, B. Mennucci, H. P. Hratchian, J. V. Ortiz, A. F. Izmaylov, J. L. Sonnenberg, D. Williams-Young, F. Ding, F. Lipparini, F. Egidi, J. Goings, B. Peng, A. Petrone, T. Henderson, D. Ranasinghe, V. G. Zakrzewski, J. Gao, N. Rega, G. Zheng, W. Liang, M. Hada, M. Ehara, K. Toyota, R. Fukuda, J. Hasegawa, M. Ishida, T. Nakajima, Y. Honda, O. Kitao, H. Nakai, T. Vreven, K. Throssell, J. A. Jr. Montgomery, J. E. Peralta, F. Ogliaro, M. J. Bearpark, J. J. Heyd, E. N. Brothers, K. N. Kudin, V. N. Staroverov, T. A. Keith, R. Kobayashi, J. Normand, K. Raghavachari, A. P. Rendell, J. C. Burant, S. S. Iyengar, J. Tomasi, M. Cossi, J. M. Millam, M. Klene, C. Adamo, R. Cammi, J. W. Ochterski, R. L. Martin, K. Morokuma, O. Farkas, J. B. Foresman and D. Fox, J. Gaussian, Inc., Wallingford CT, 2016.
20. T. A. Halgren, *J. Comput. Chem.*, 1996, **17**, 490–519.
21. T. A. Halgren, *J. Comput. Chem.*, 1999, **20**, 720–729.
22. CONFLEX 9, H. Goto, S. Obata, N. Nakayama and K. Ohta, CONFLEX Corporation, Tokyo, Japan, 2021.
23. H. Goto and E. Osawa, *J. Am. Chem. Soc.*, 1989, **111**, 8950–8951.
24. H. Goto and E. Osawa, *J. Chem. Soc., Perkin Trans. 2*, 1993, 187–198.
25. K. Fukui, *Acc. Chem. Res.*, 1981, **14**, 363–368.
26. K. Ishida, K. Morokuma and A. Komornicki, *J. Chem. Phys.*, 1977, **66**, 2153–2156.
27. C. Gonzalez and H. B. Schlegel, *J. Chem. Phys.*, 1989, **90**, 2154–2161.
28. C. Gonzalez and H. B. Schlegel, *J. Phys. Chem.*, 1990, **94**, 5523–5527.

10. ^{1}H and ^{13}C NMR spectra

S1: ^{1}H NMR, $CDCl_3$, 600 MHz

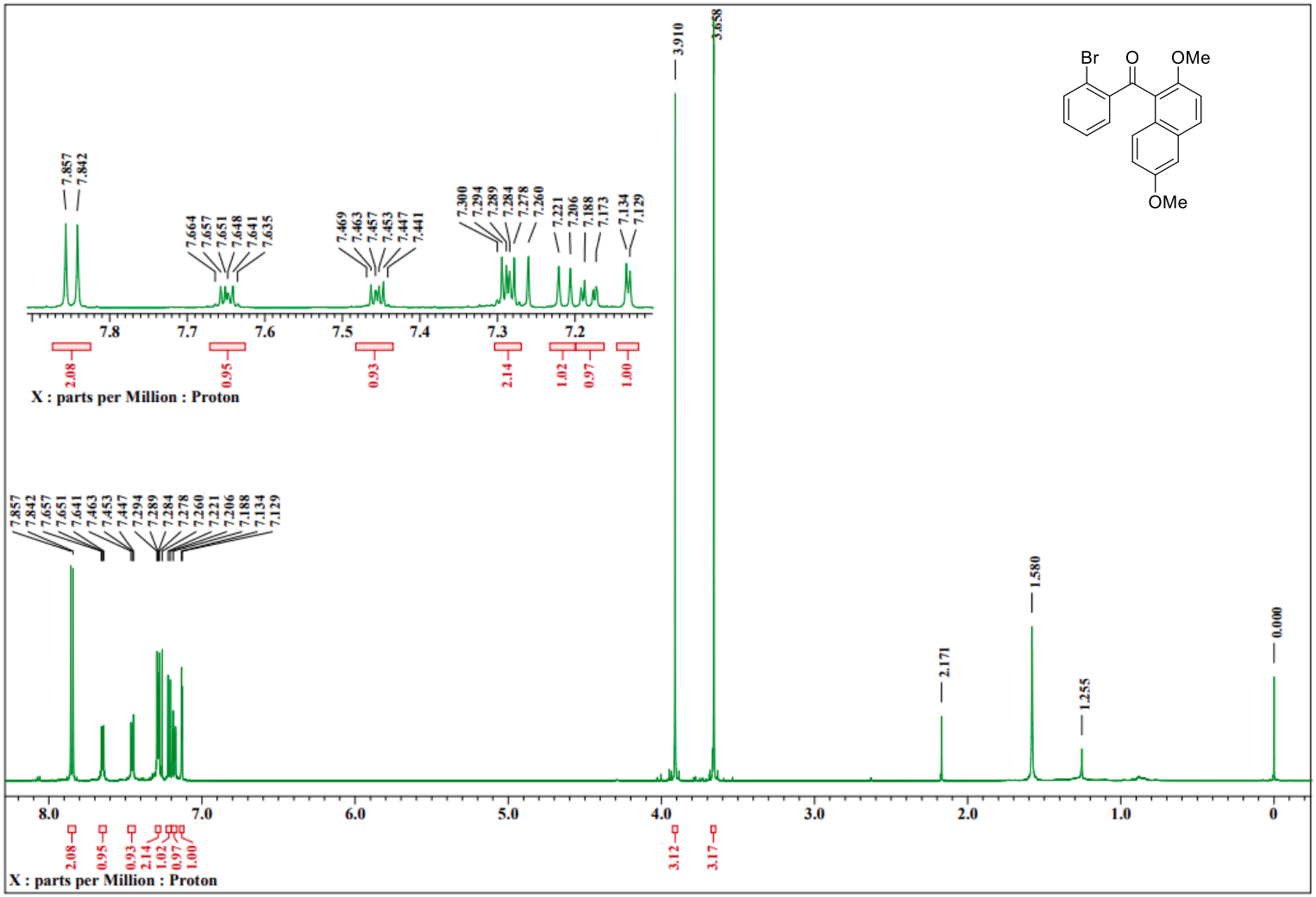

S1: ^{13}C NMR, $CDCl_3$, 151 MHz

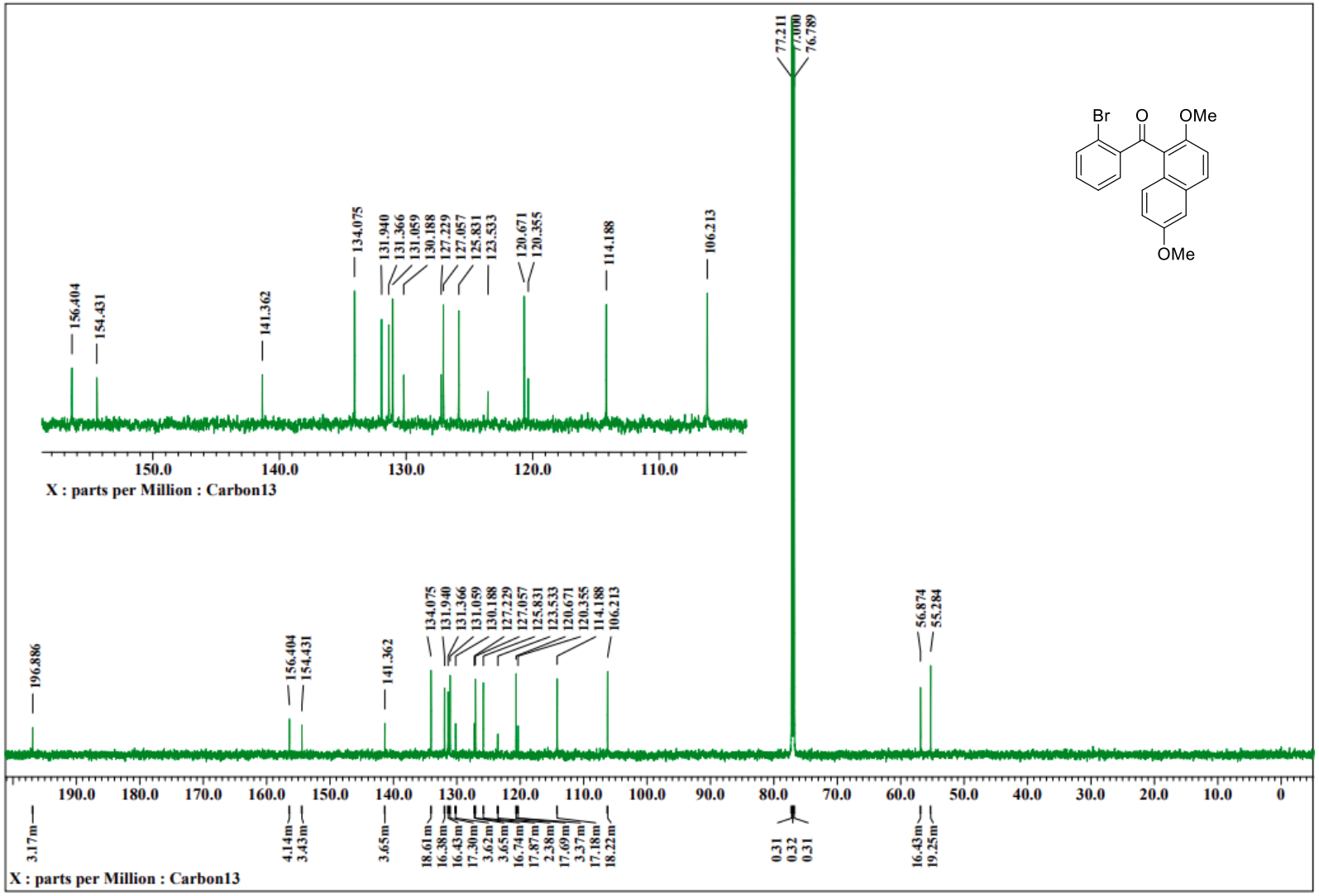

S2: ^{1}H NMR, $CDCl_3$, 600 MHz

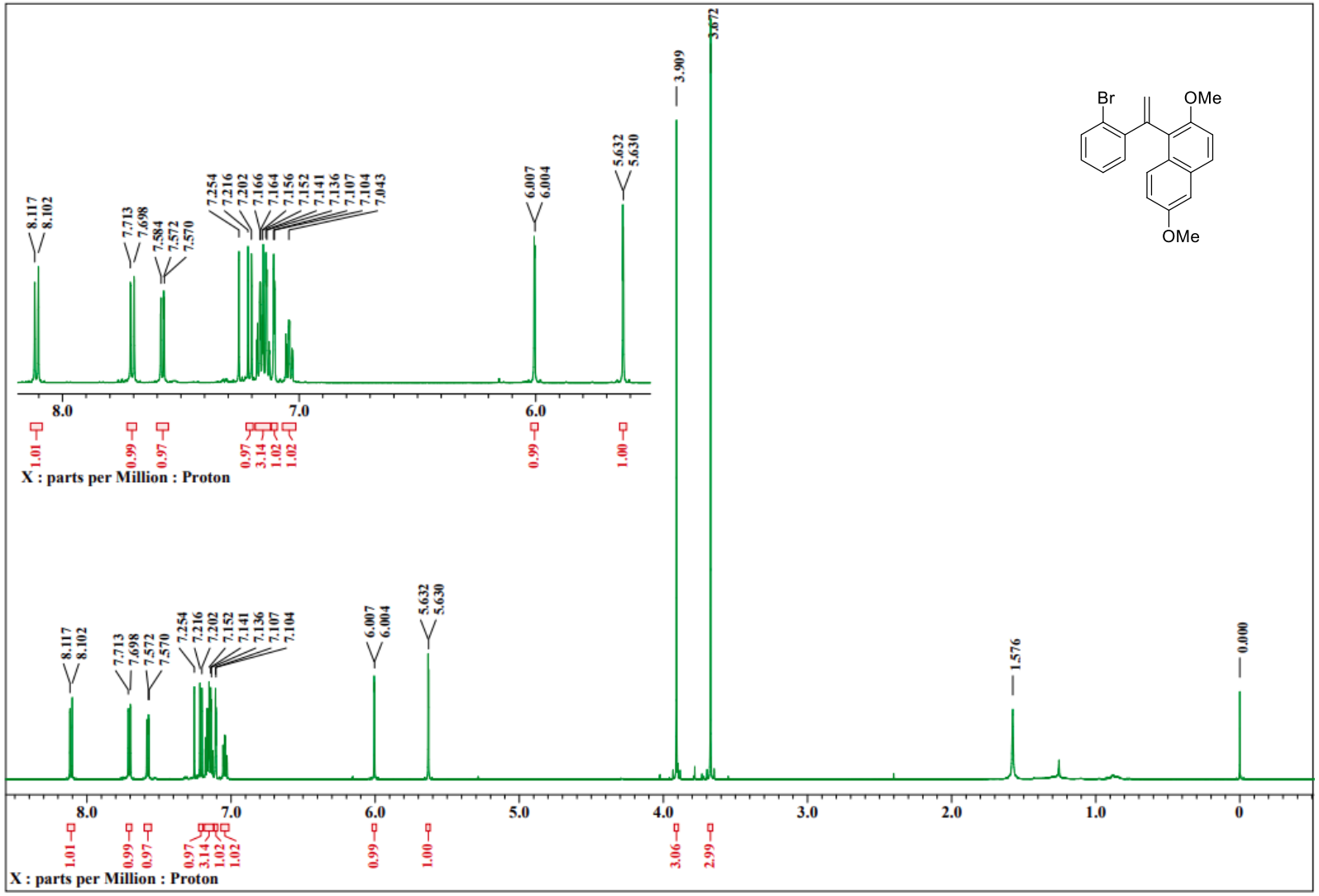

S2: ^{13}C NMR, $CDCl_3$, 151 MHz

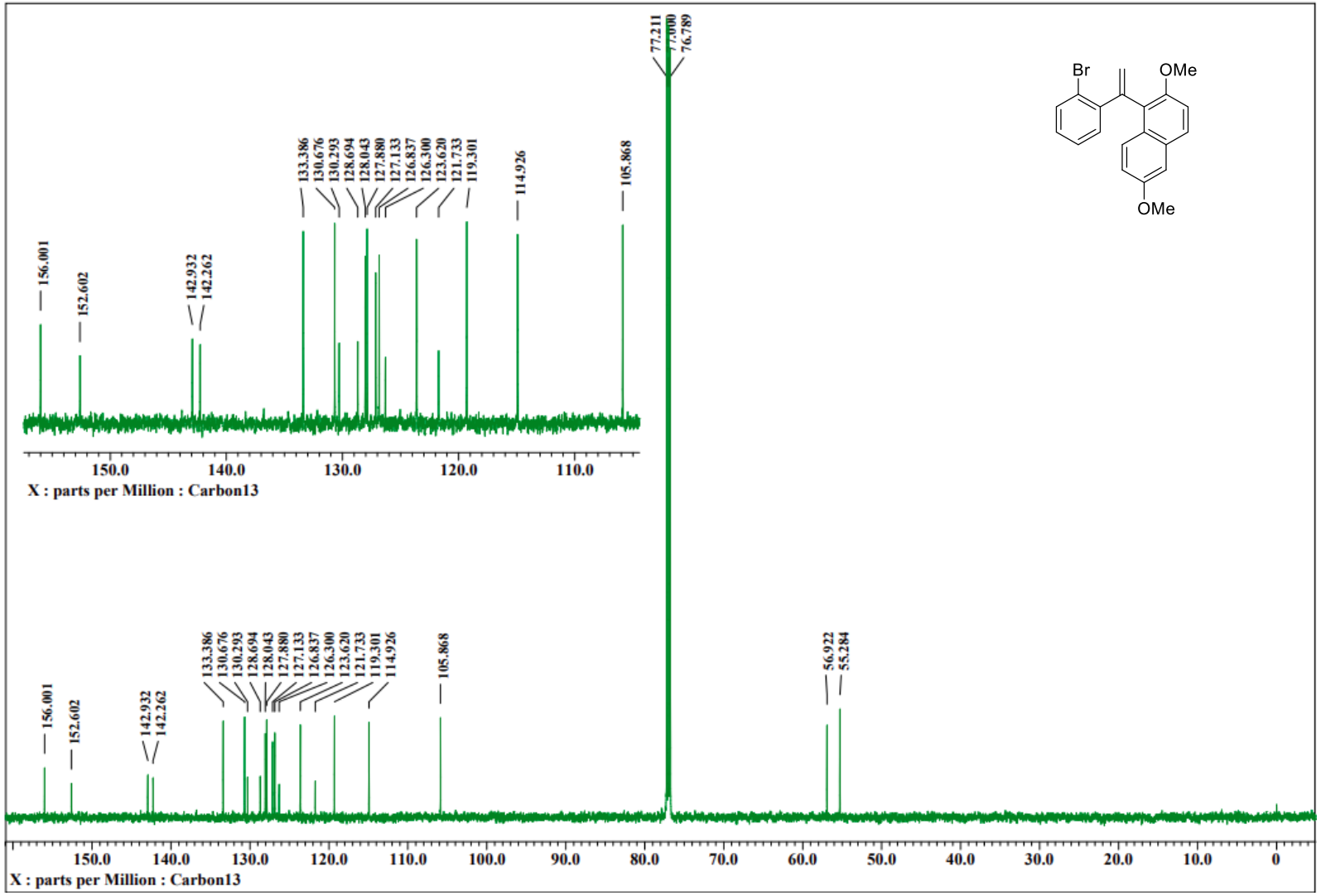

S3: ^{1}H NMR, acetone-d_6, 600 MHz

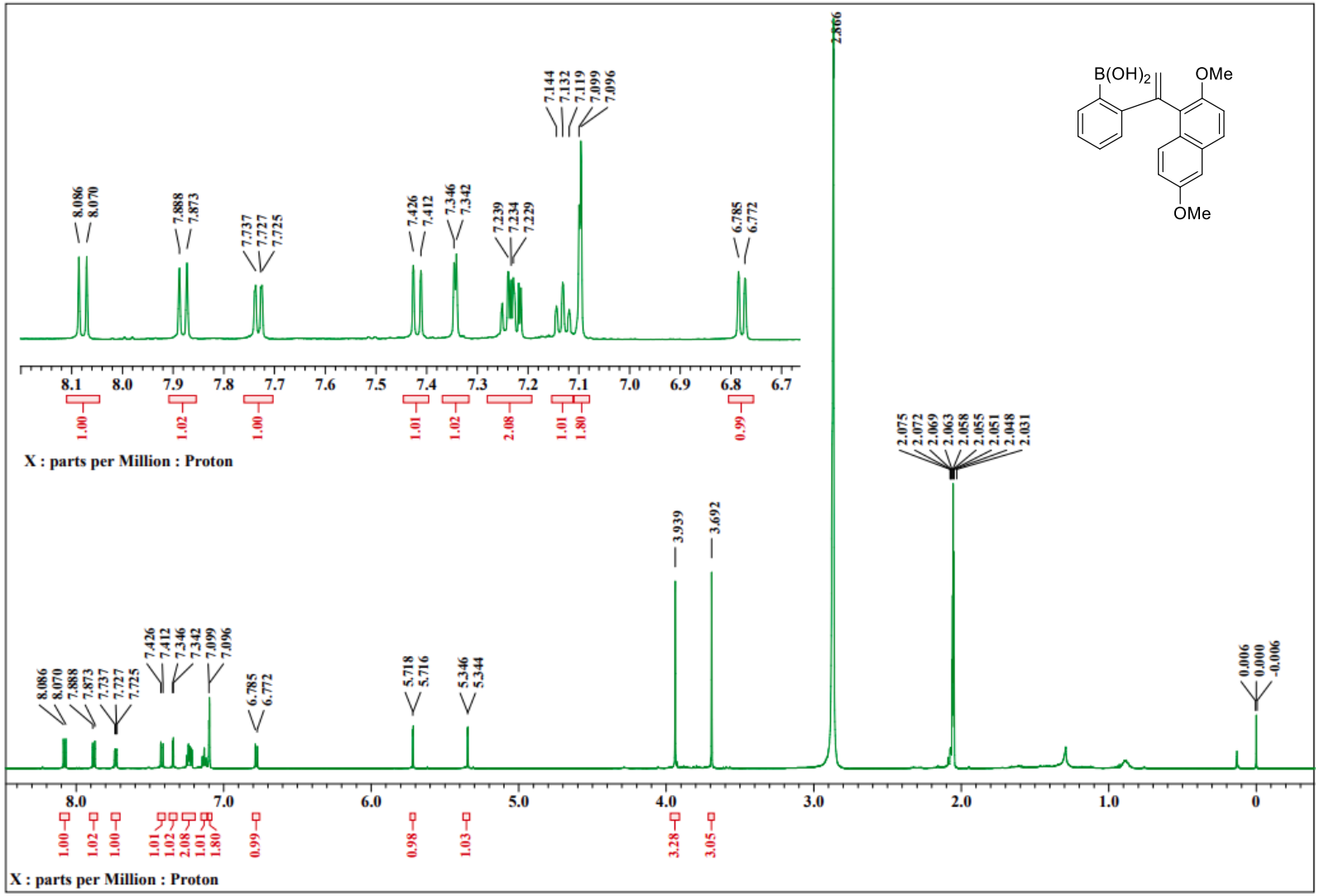

S3: ^{13}C NMR, acetone-d_6, 151 MHz

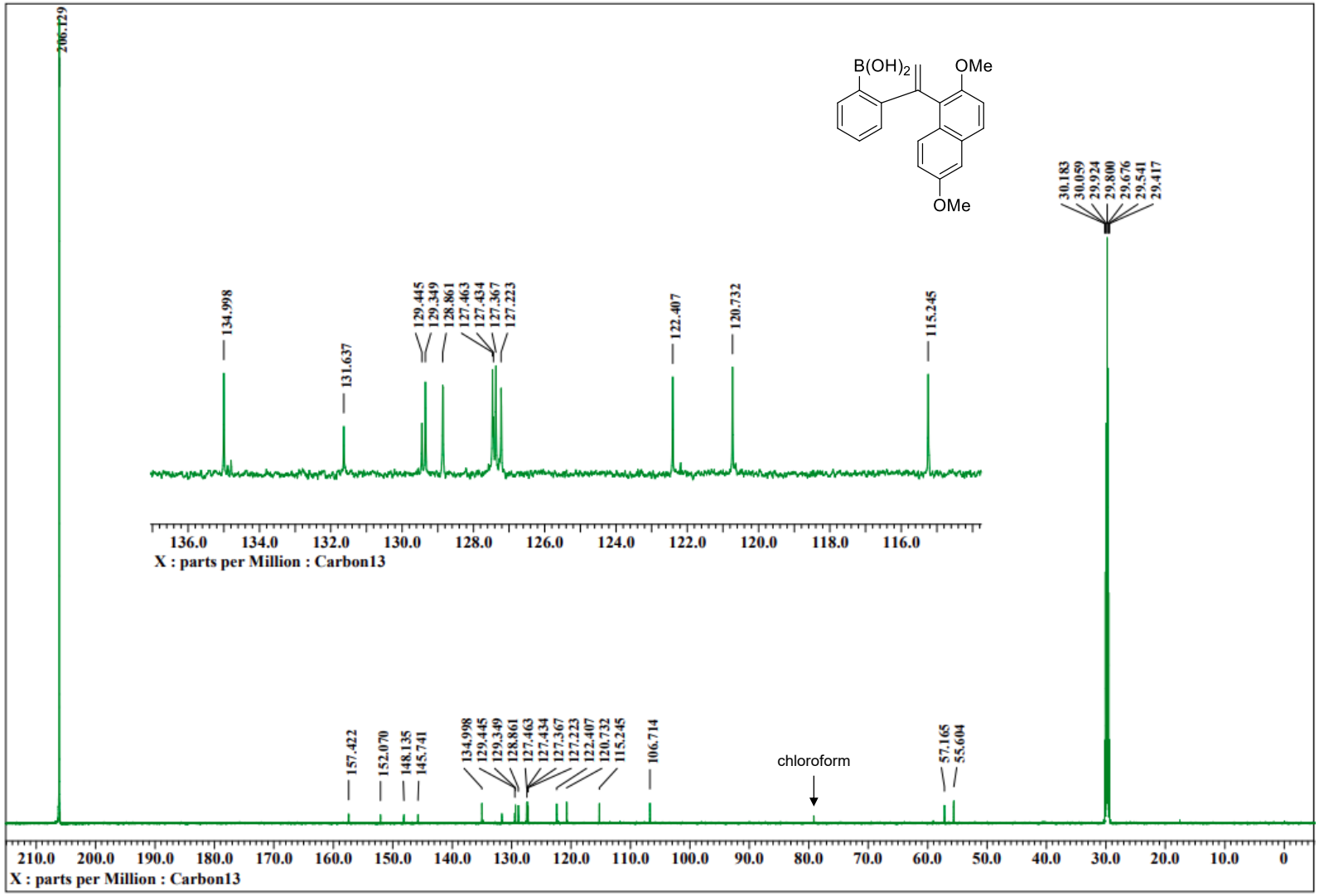

S4: ^{1}H NMR, $CDCl_3$, 600 MHz, 50 °C

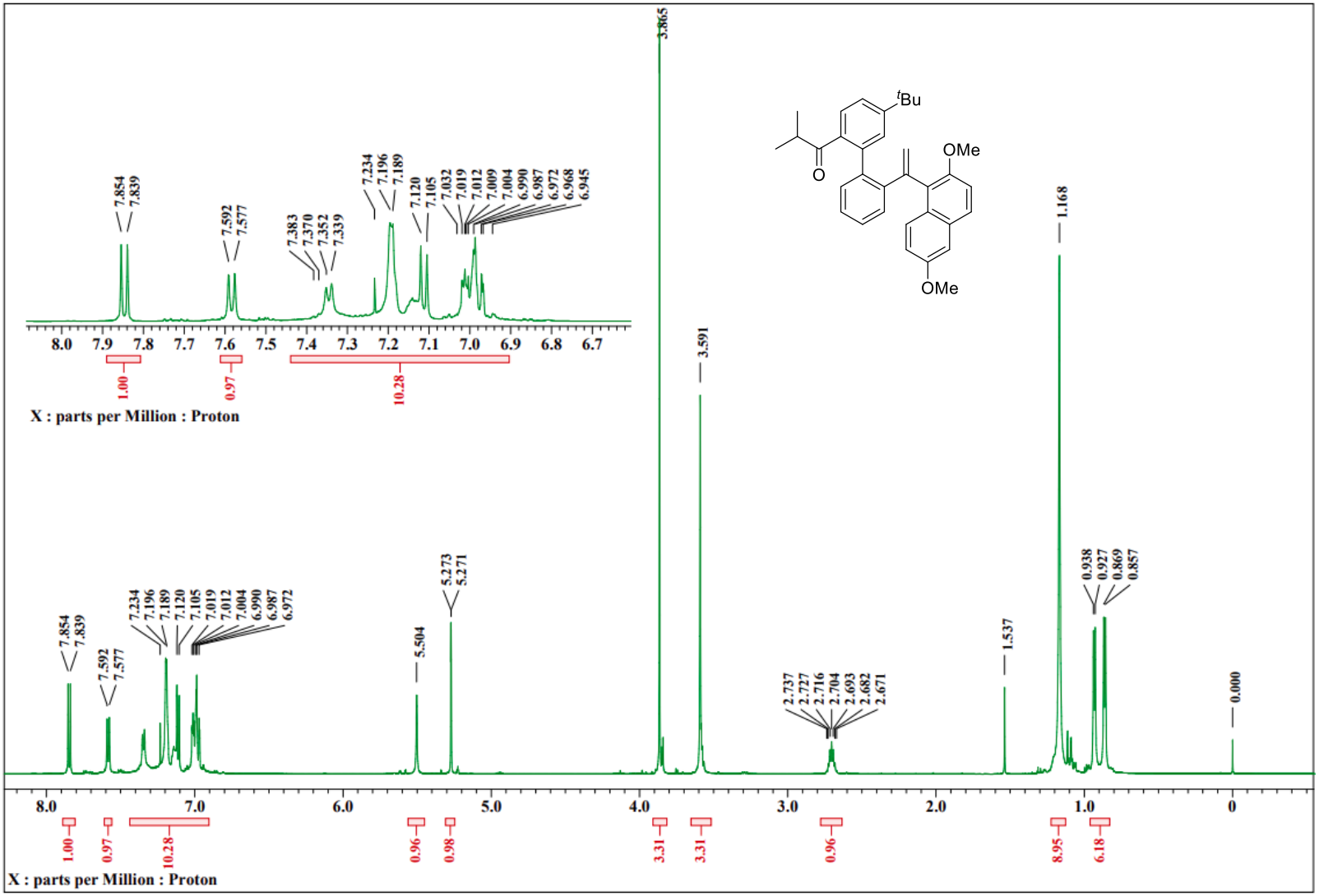

S4: ^{13}C NMR, $CDCl_3$, 151 MHz, 50 °C

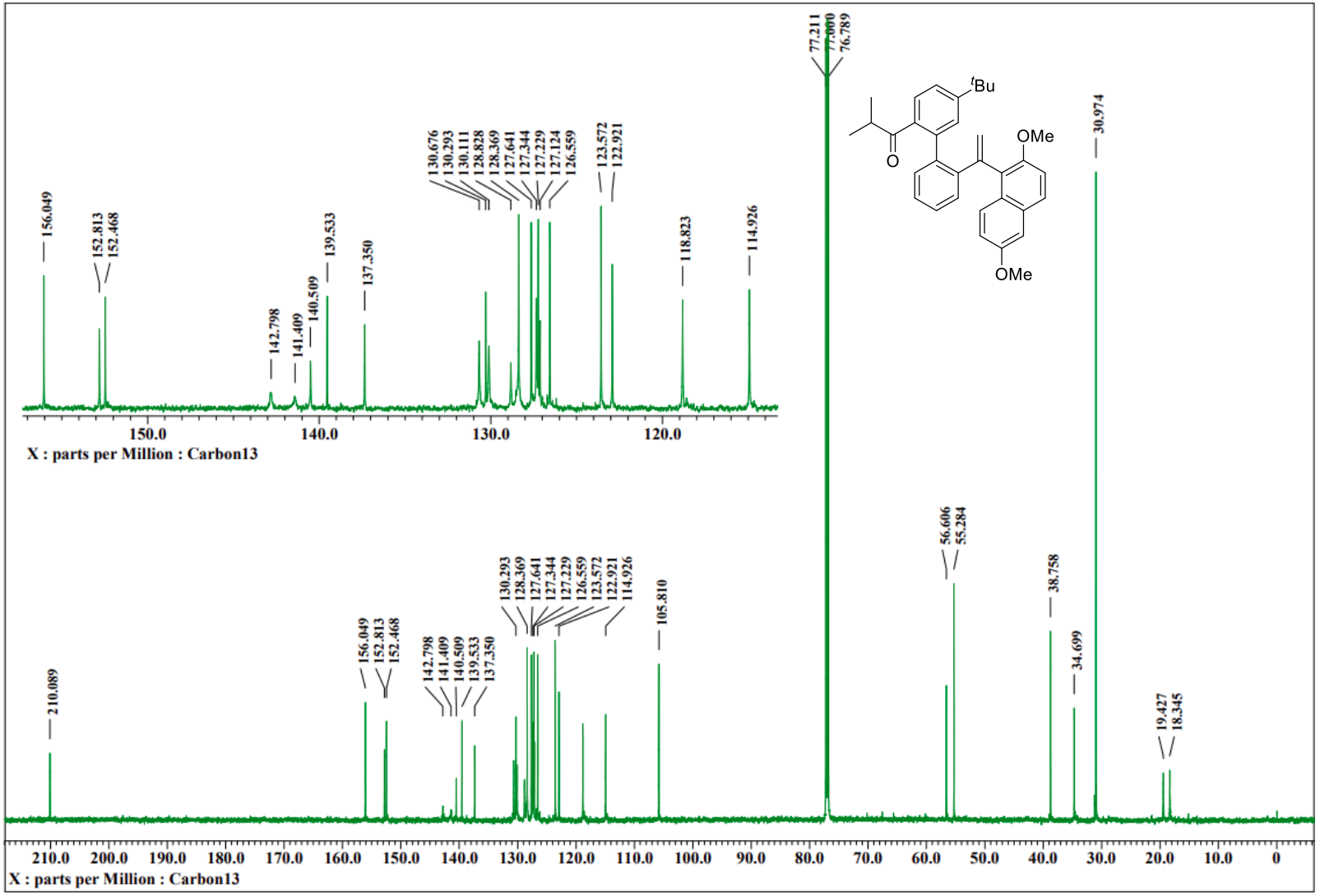

1a: ^{1}H NMR, $CDCl_3$, 600 MHz

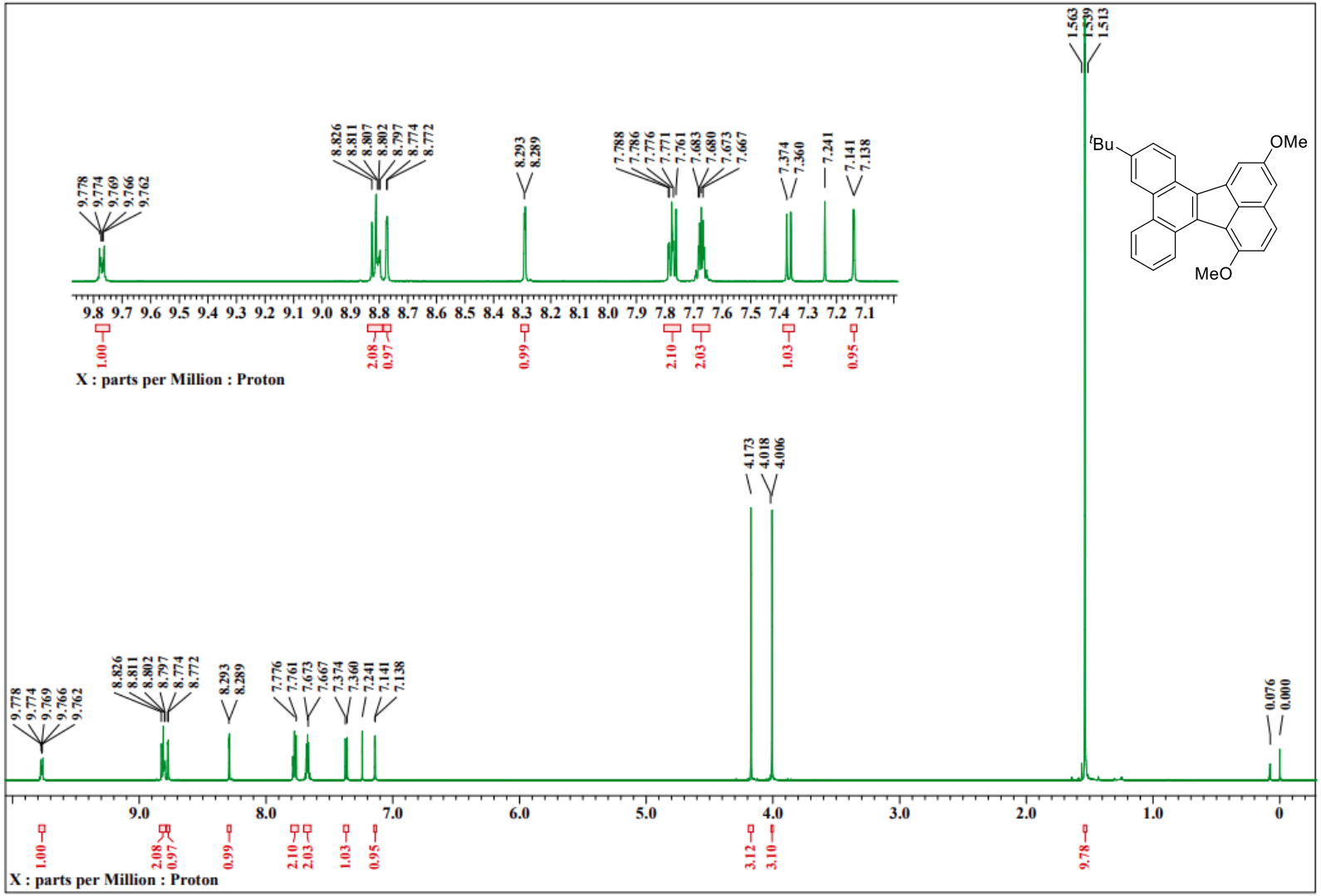

1a: ^{13}C NMR, $CDCl_3$, 151 MHz

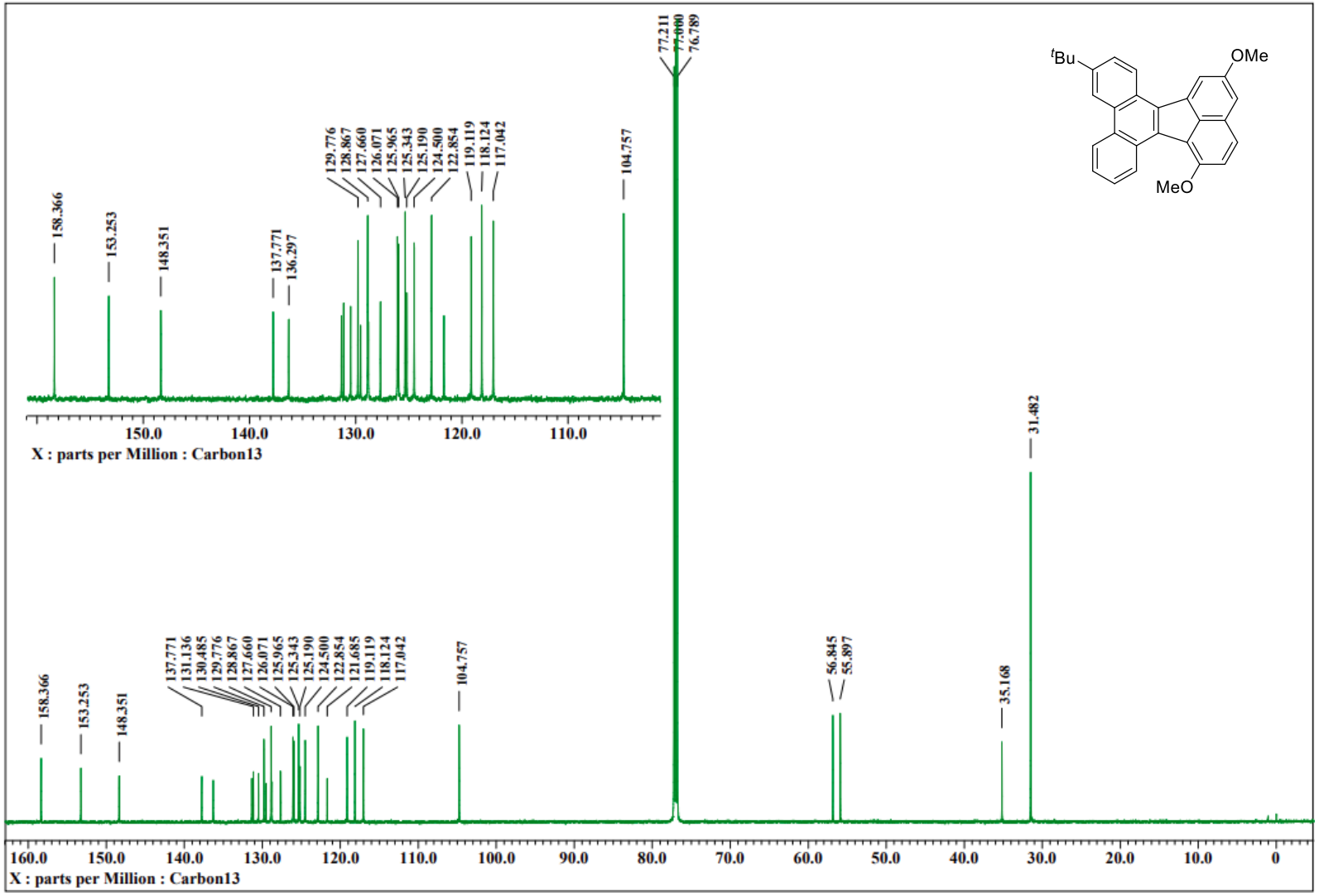

1b: ^{1}H NMR, acetone-d_6, 600 MHz

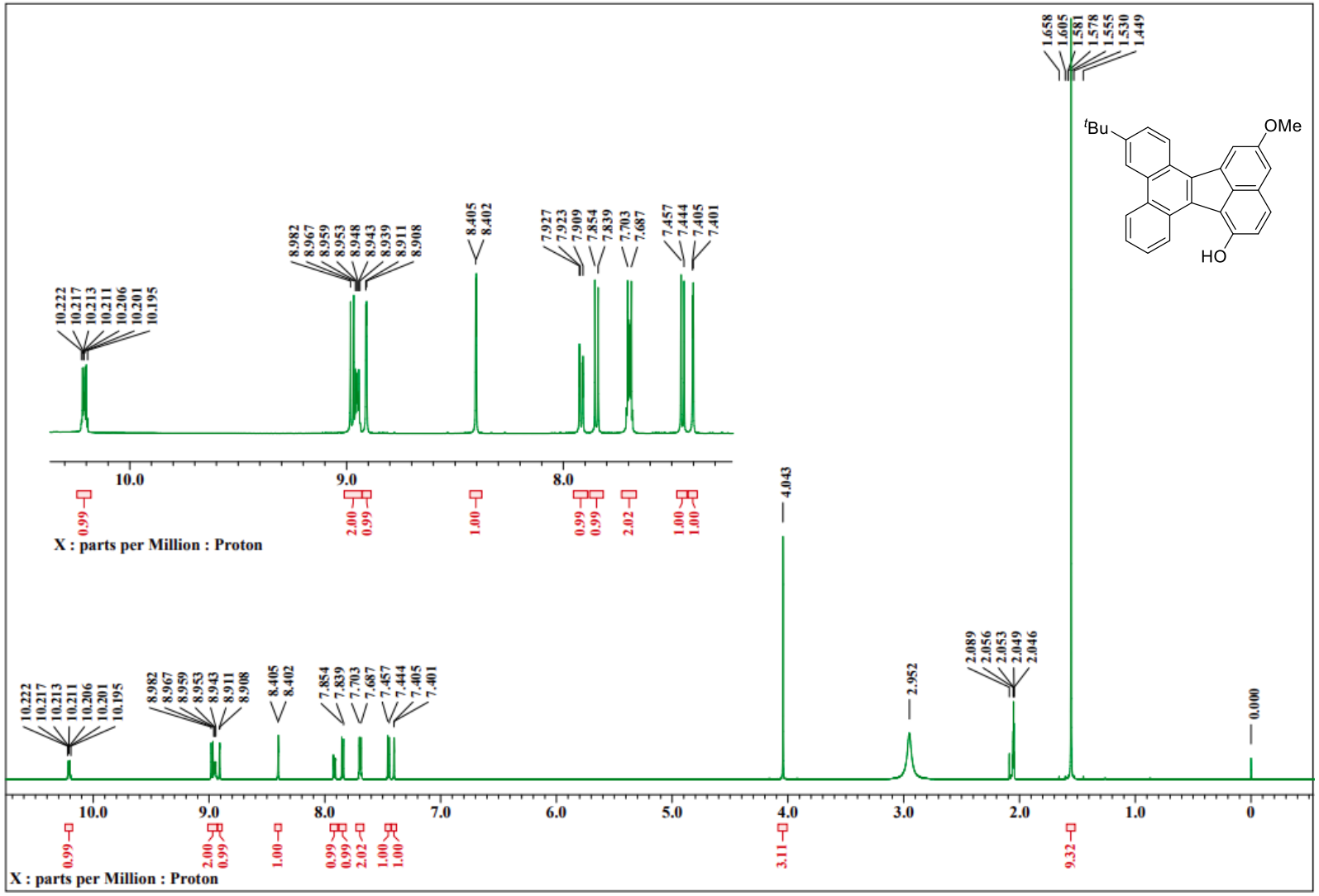

1b: ^{13}C NMR, acetone-d_6, 151 MHz

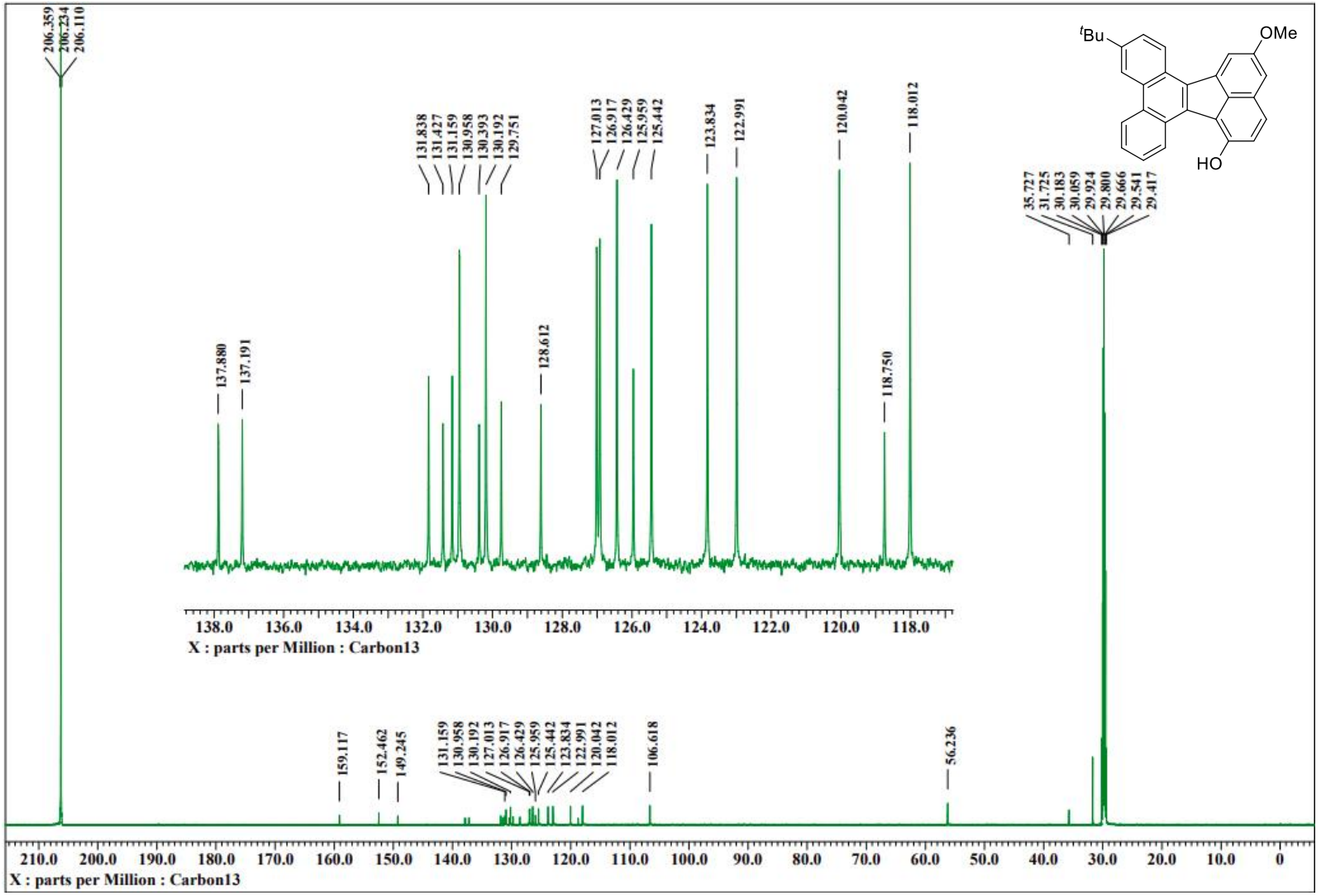

1c: ^{1}H NMR, $CDCl_3$, 600 MHz

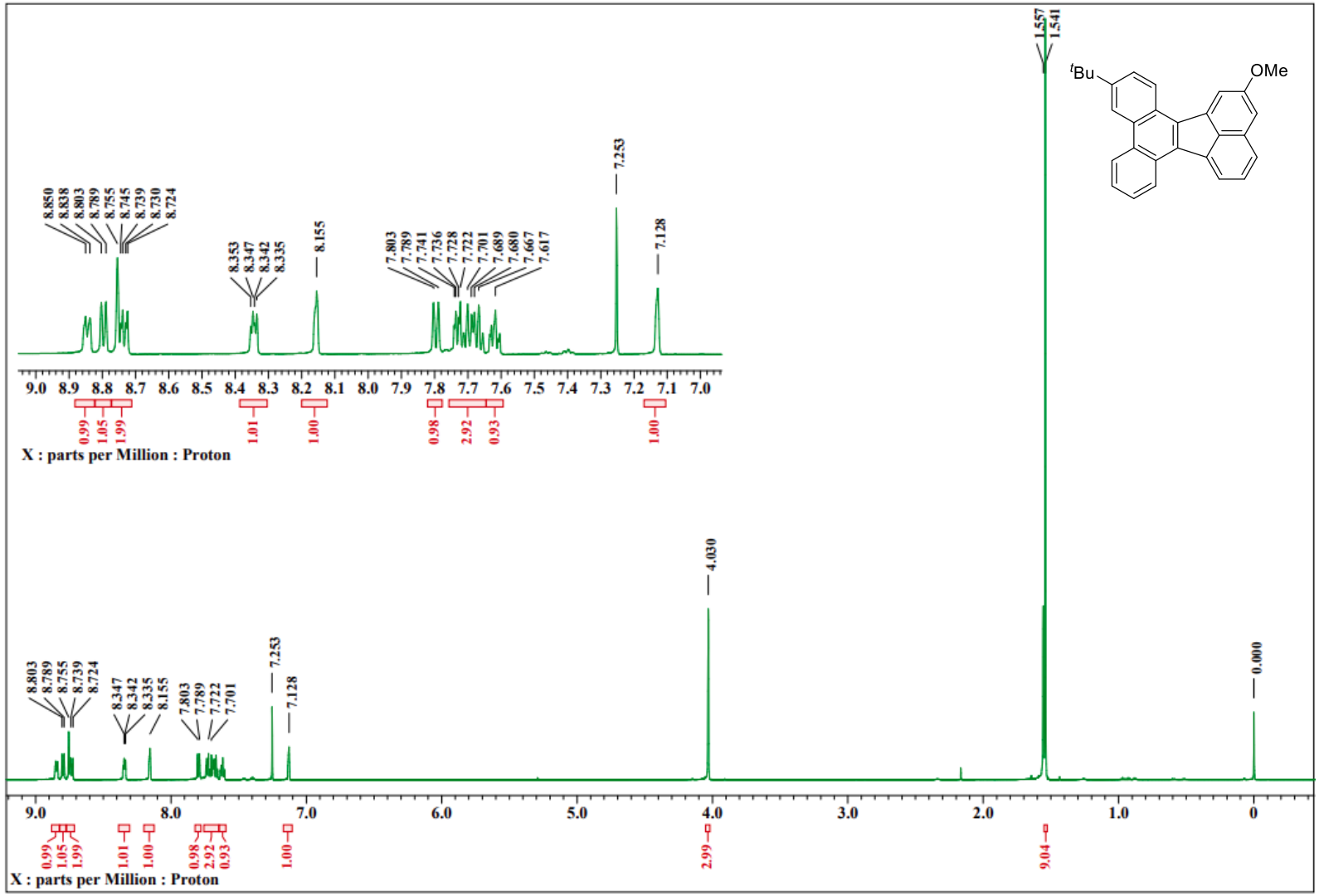

1c: ^{13}C NMR, $CDCl_3$, 151 MHz

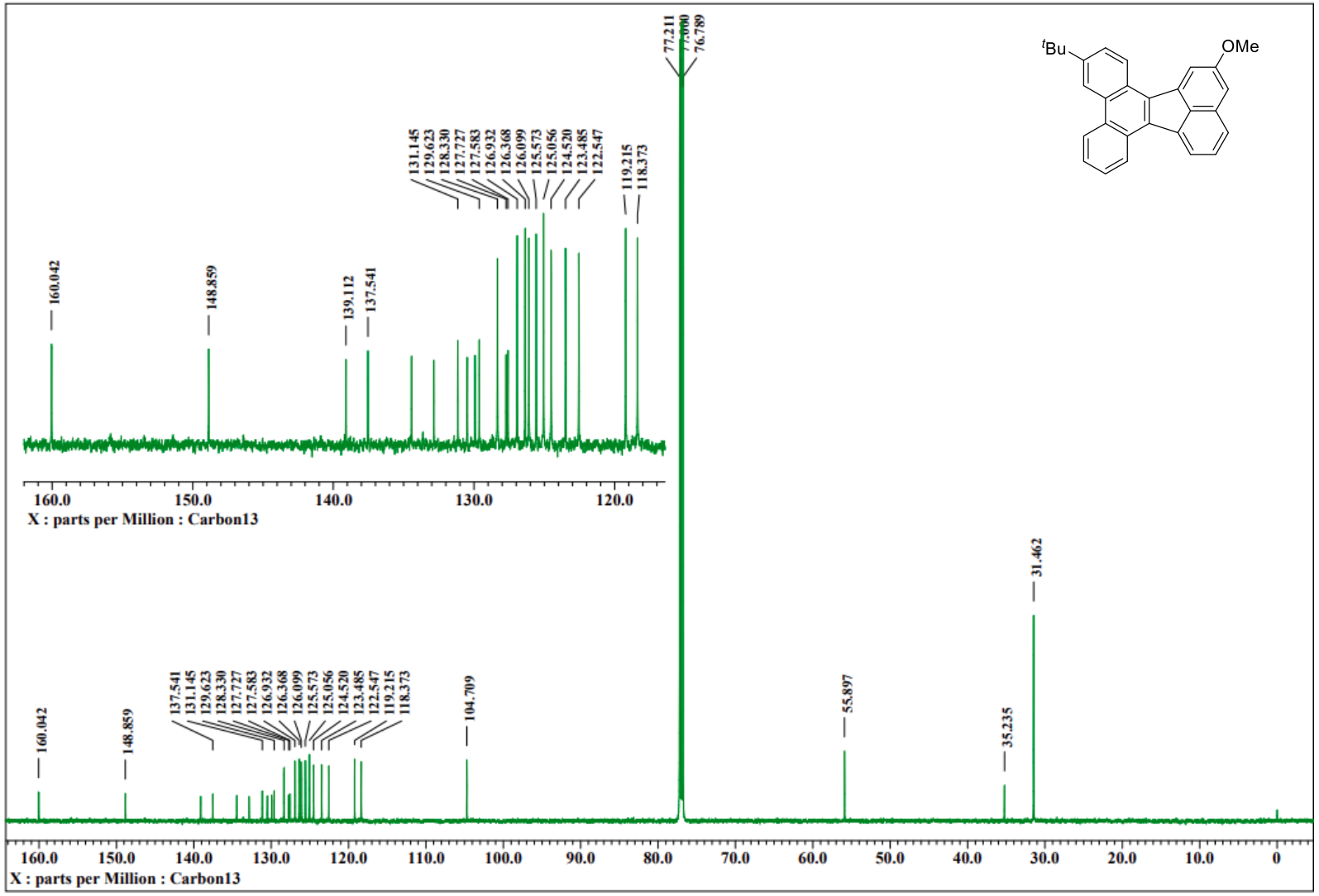

1d: ^{1}H NMR, $CDCl_3$, 600 MHz

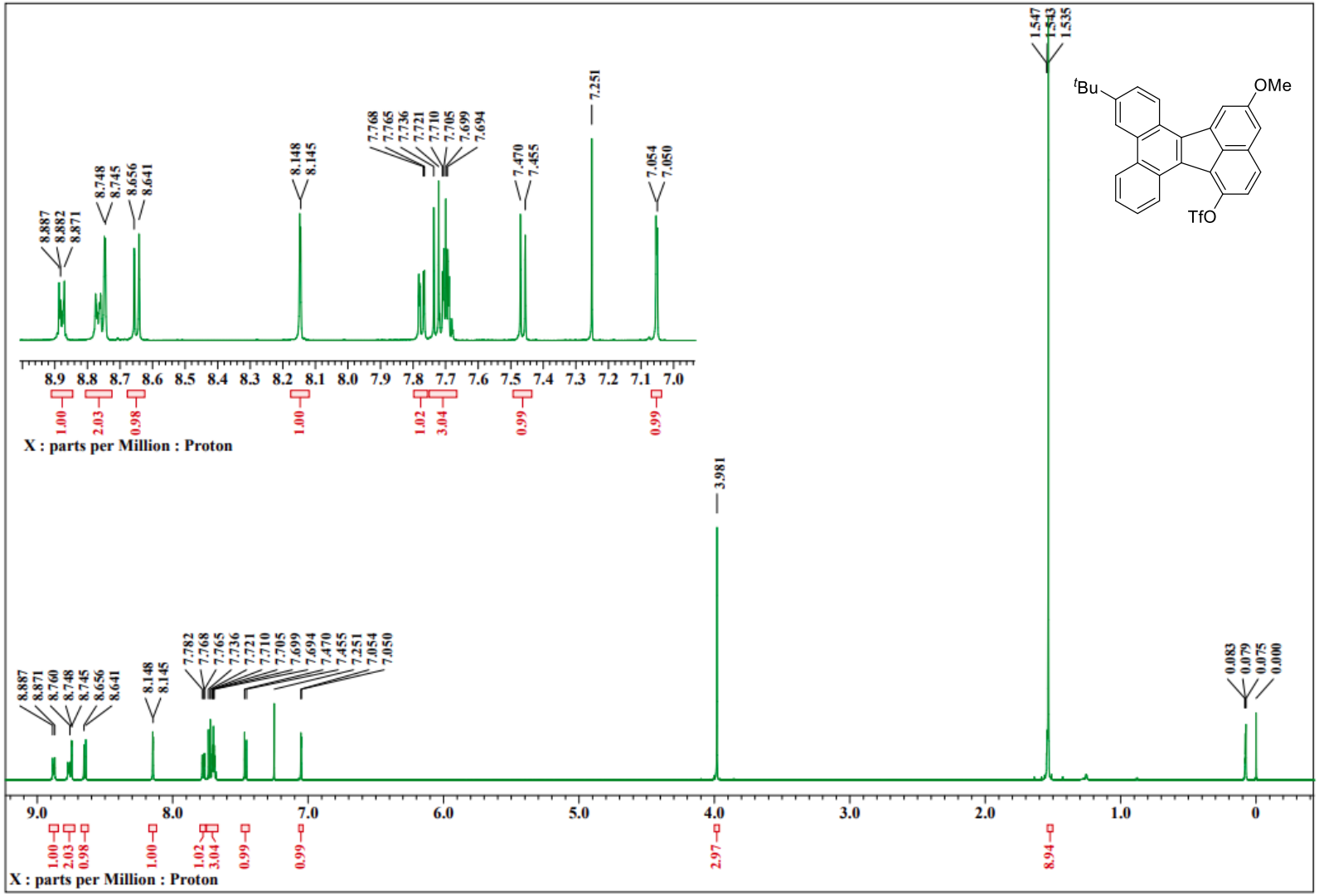

1d: ^{13}C NMR, $CDCl_3$, 151 MHz

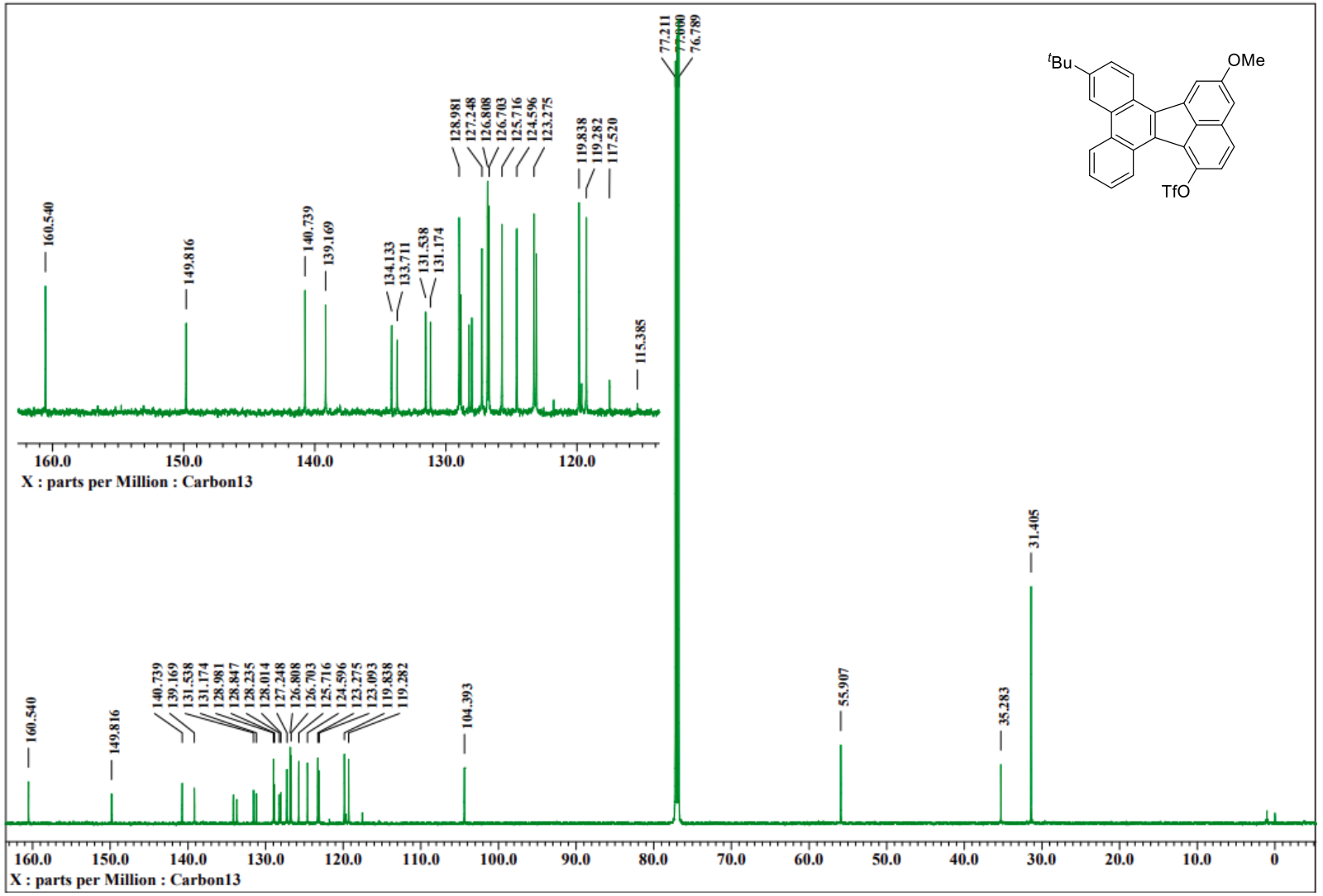

1e: ^{1}H NMR, $CDCl_3$, 600 MHz

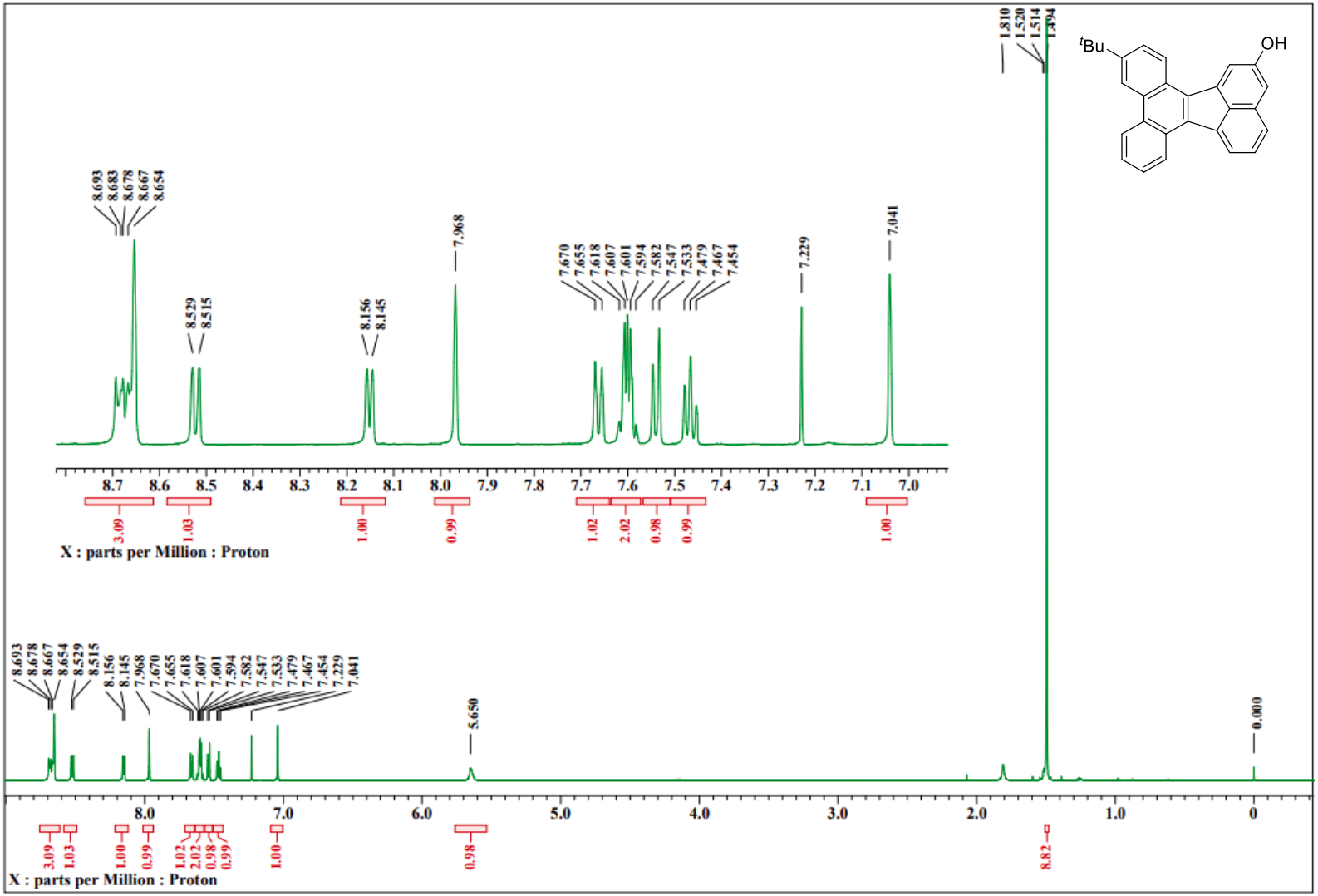

1e: ^{13}C NMR, $CDCl_3$, 151 MHz

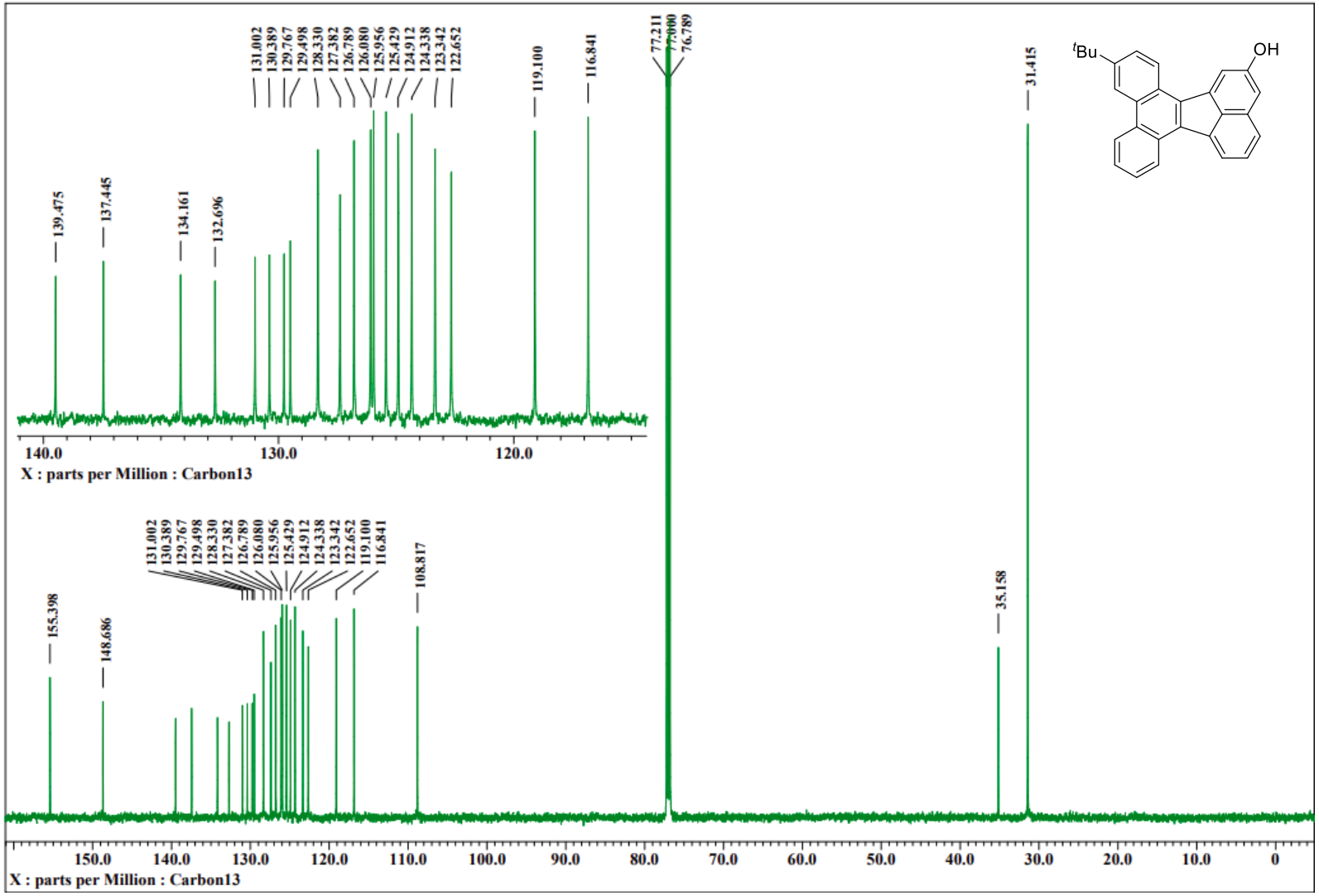

3f: ^{1}H NMR, $CDCl_3$, 600 MHz

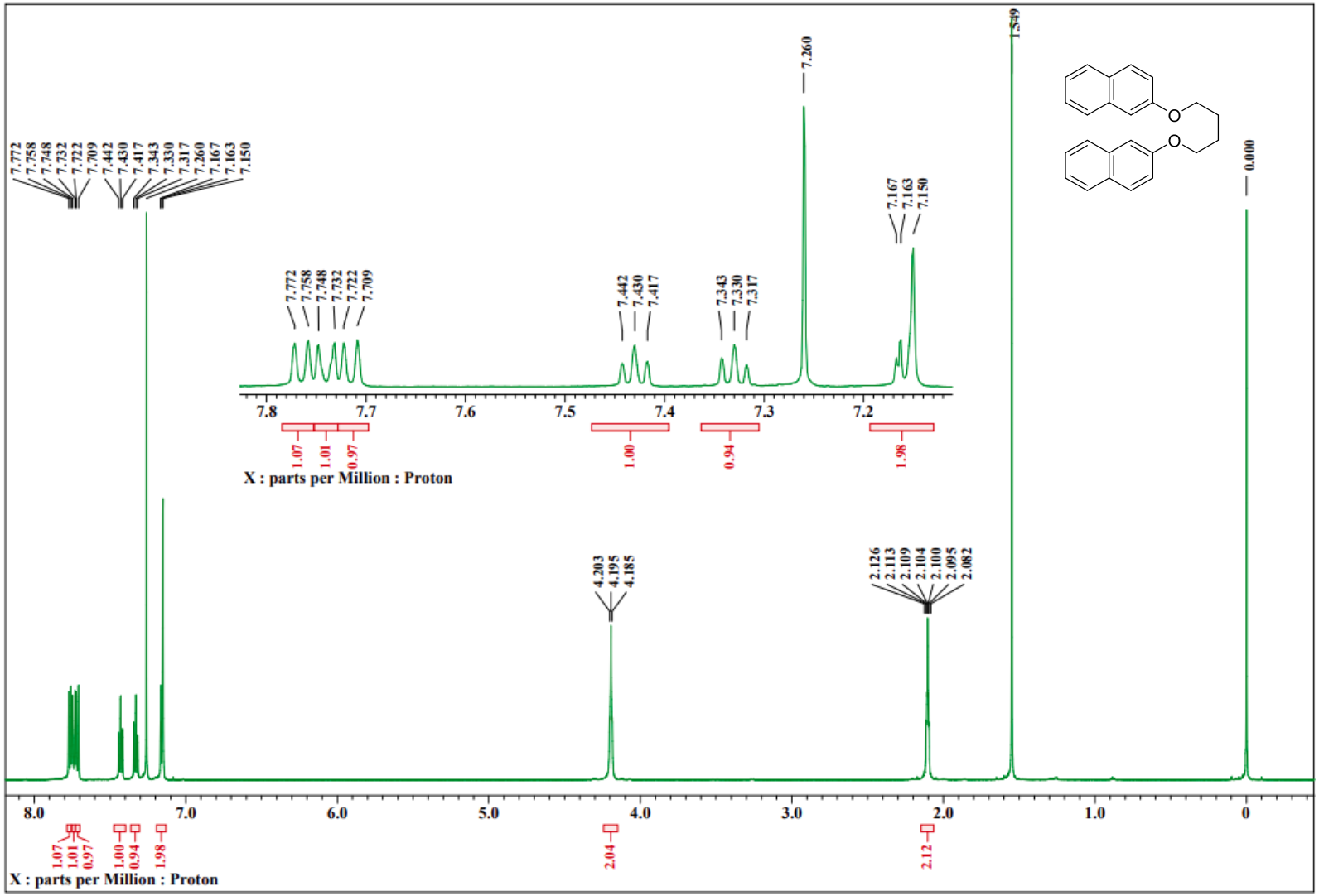

3f: ^{13}C NMR, $CDCl_3$, 151 MHz

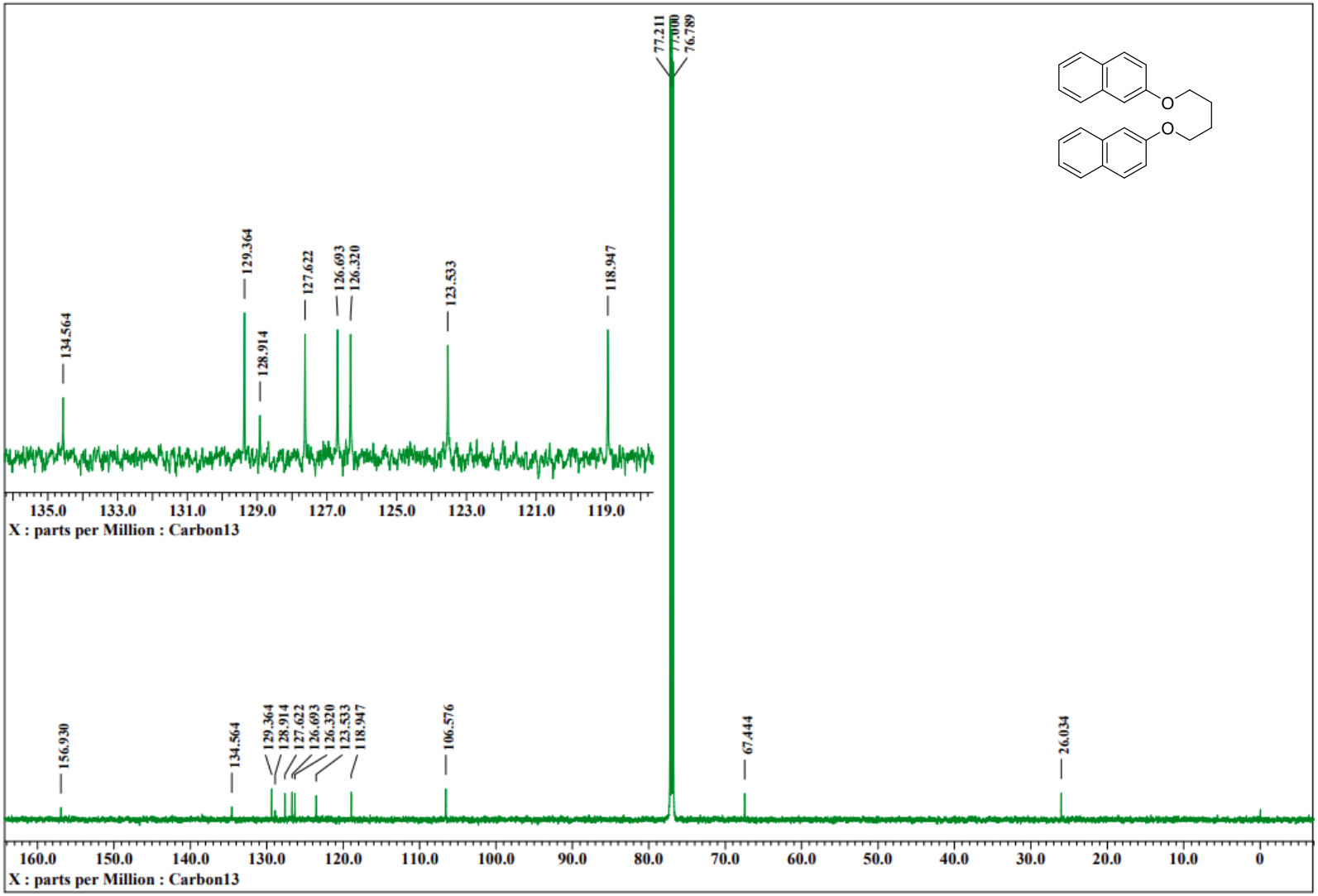

2a: ^{1}H NMR, $CDCl_3$, 600 MHz

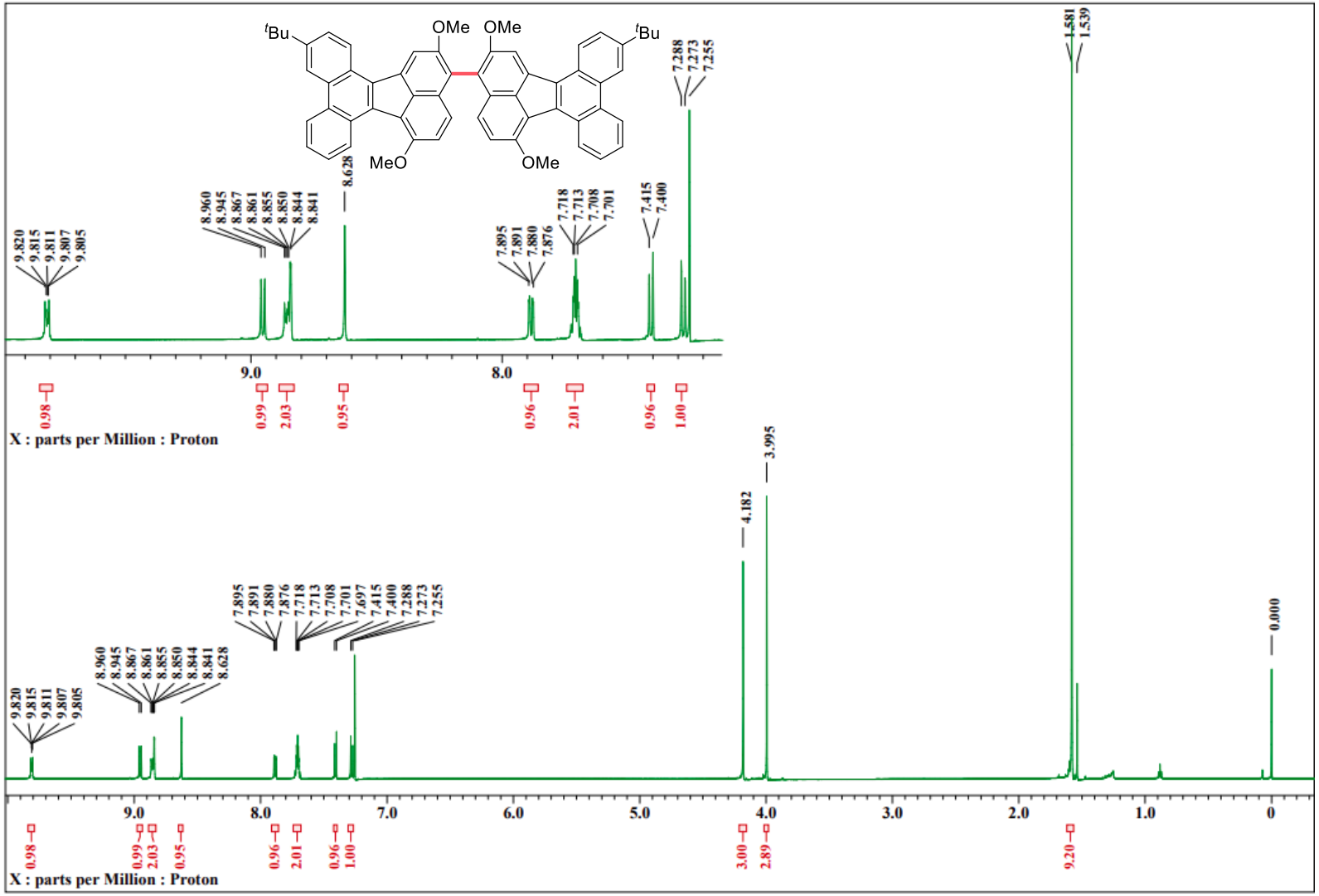

2a: ^{13}C NMR, $CDCl_3$, 151 MHz

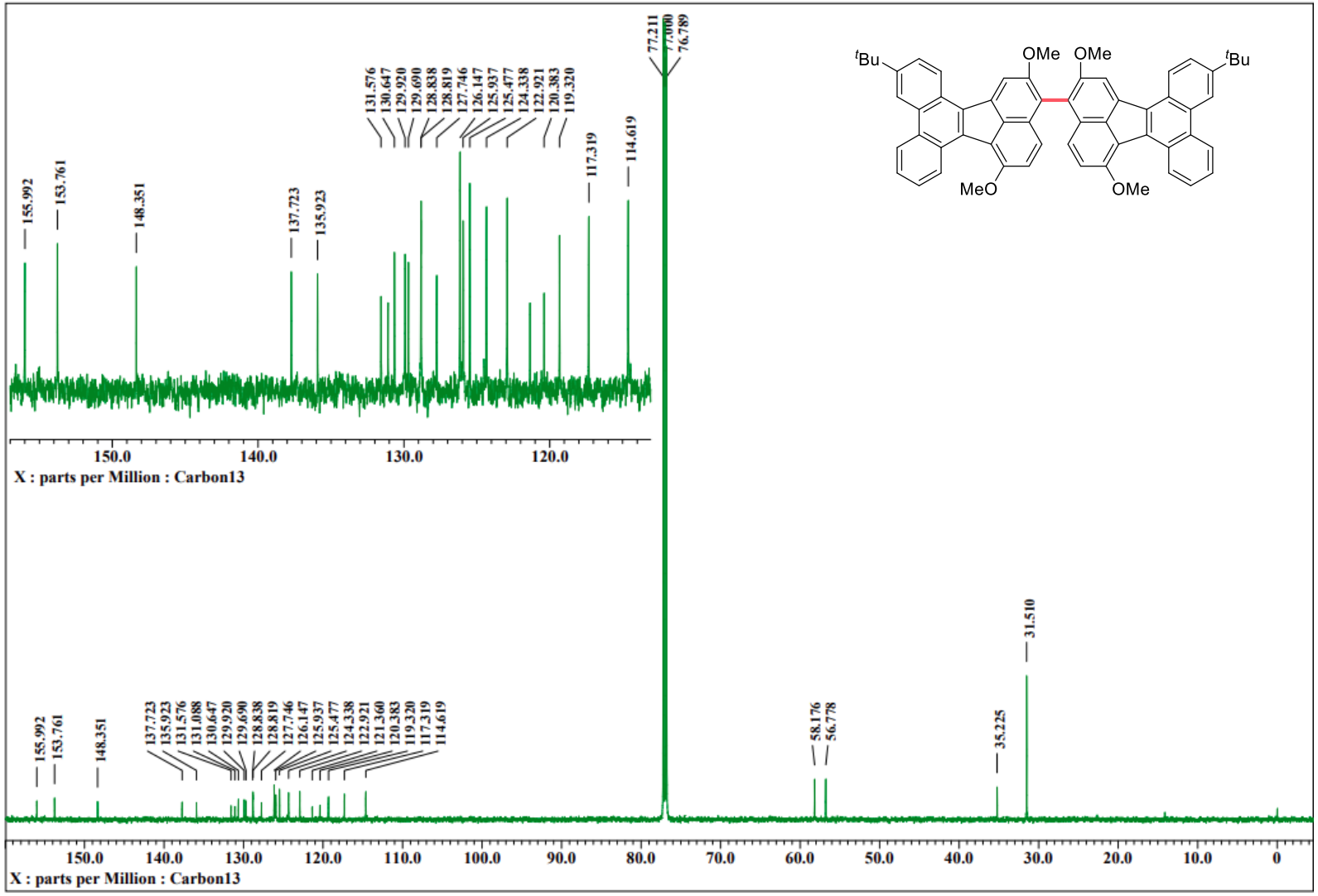

2b: ^{1}H NMR, acetone-d_6, 600 MHz

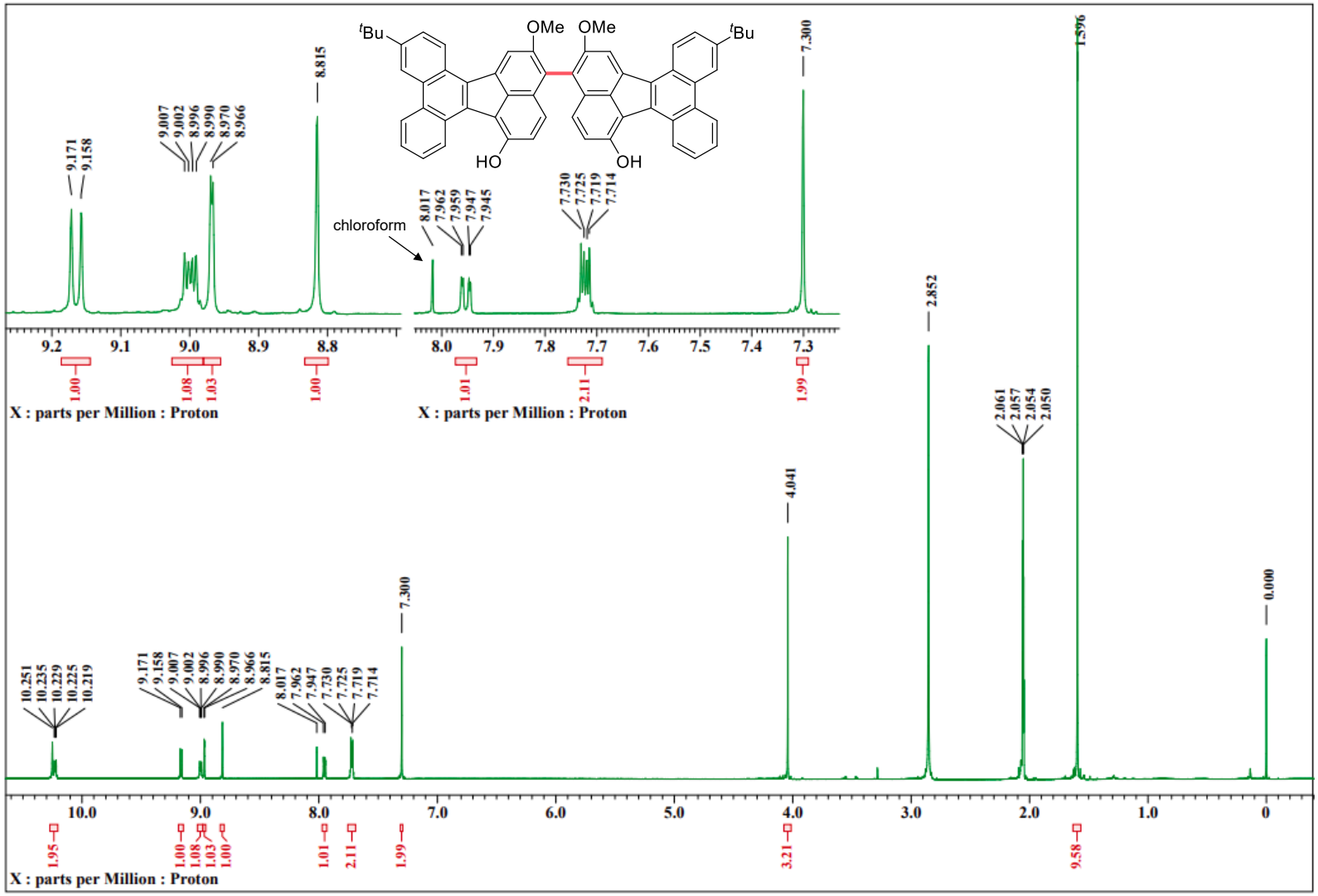

2b: ^{13}C NMR, acetone-d_6, 151 MHz

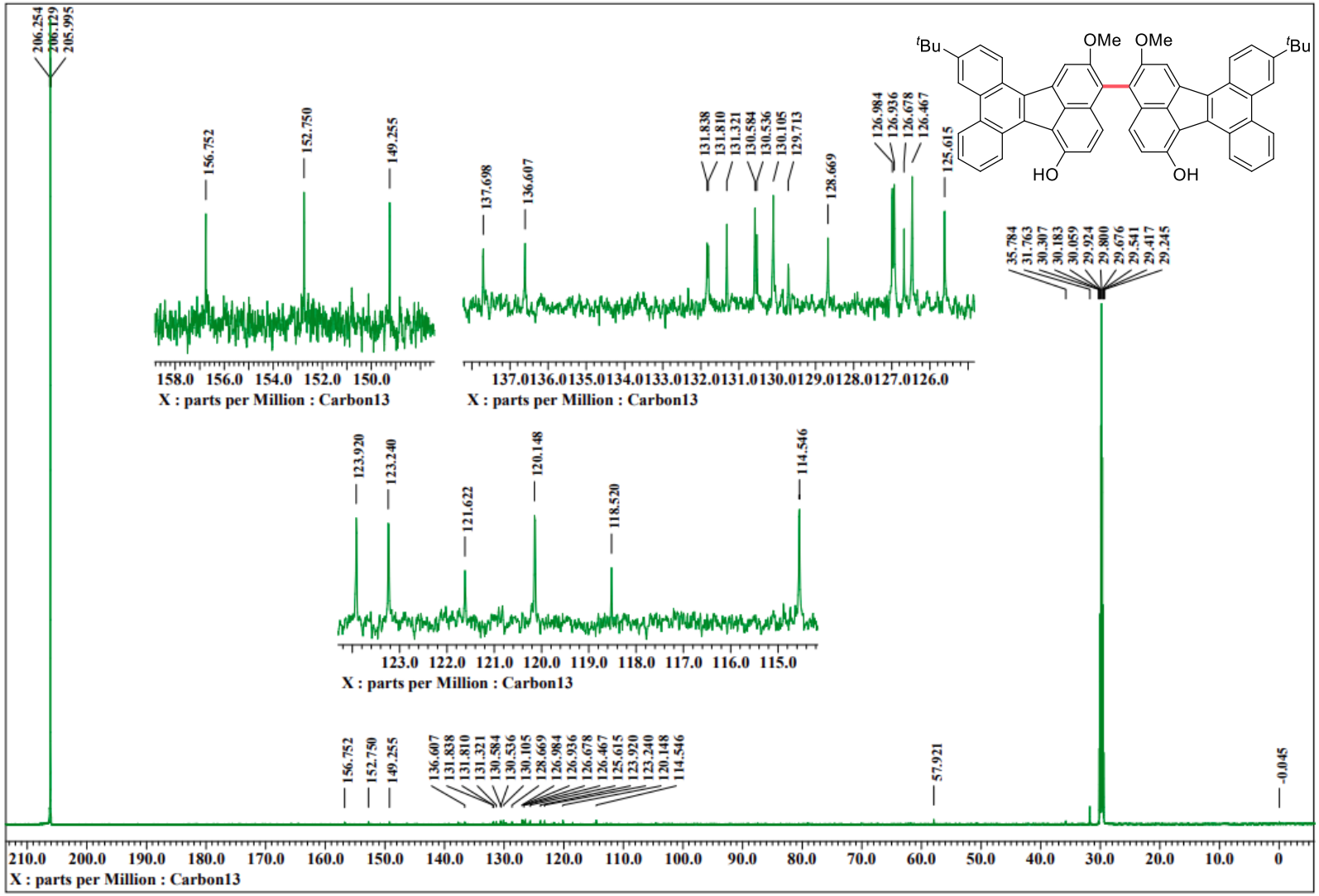

2c: ^{1}H NMR, $CDCl_3$, 600 MHz

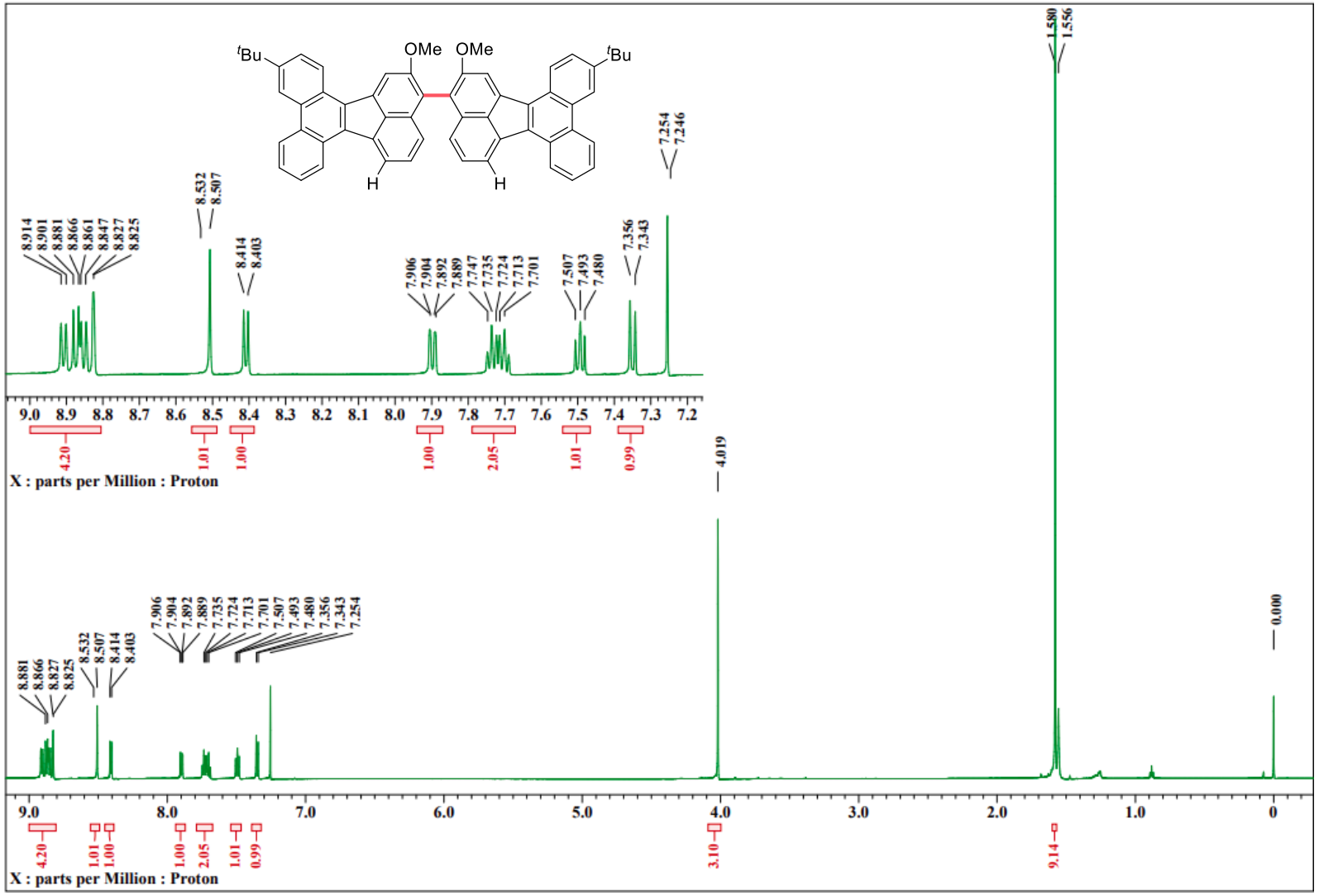

2c: ^{13}C NMR, $CDCl_3$, 151 MHz

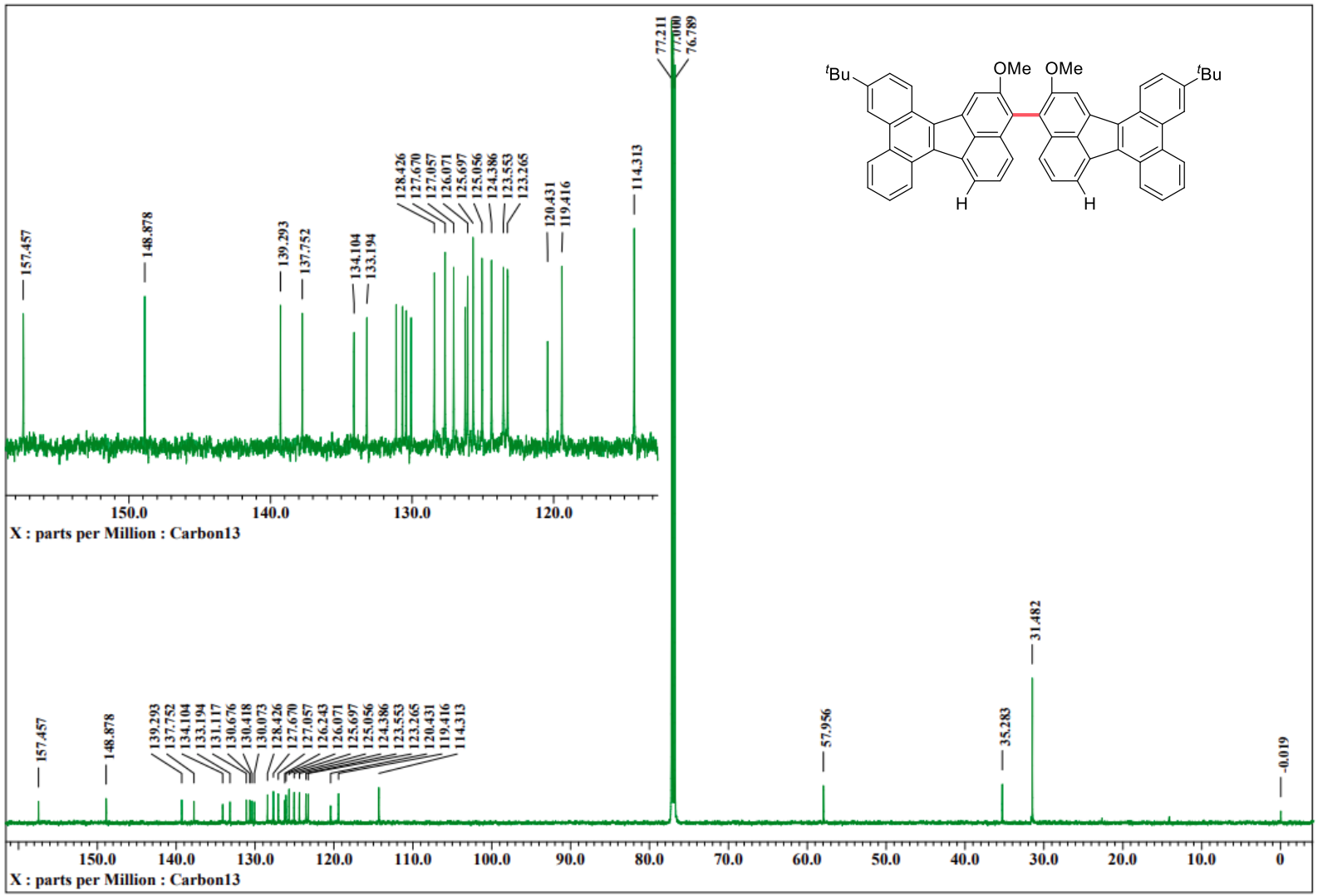

2d: ^{1}H NMR, acetone-d_6, 600 MHz

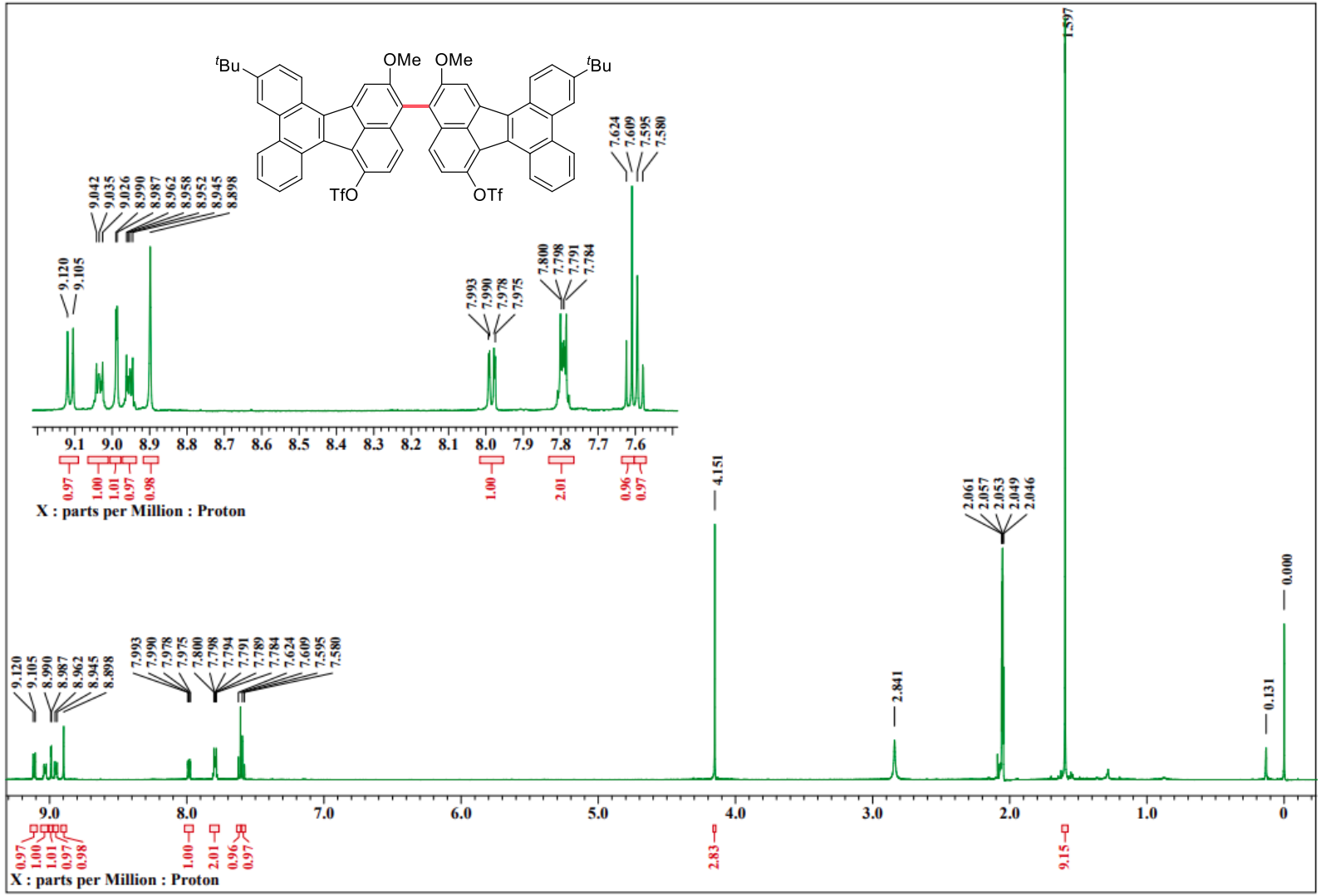

2d: ^{13}C NMR, acetone-d_6, 151 MHz

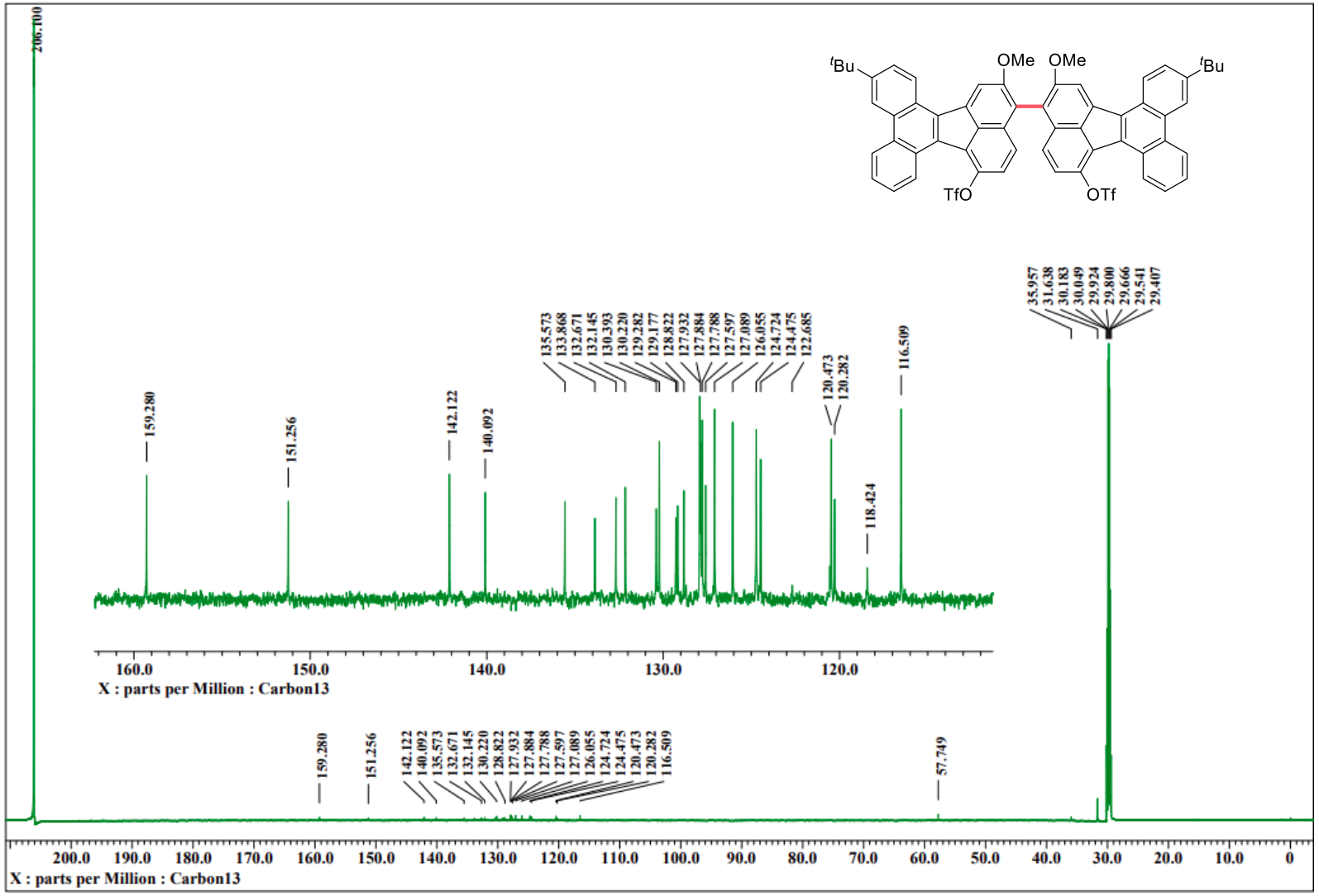

2e: ^{1}H NMR, $CDCl_3$, 600 MHz

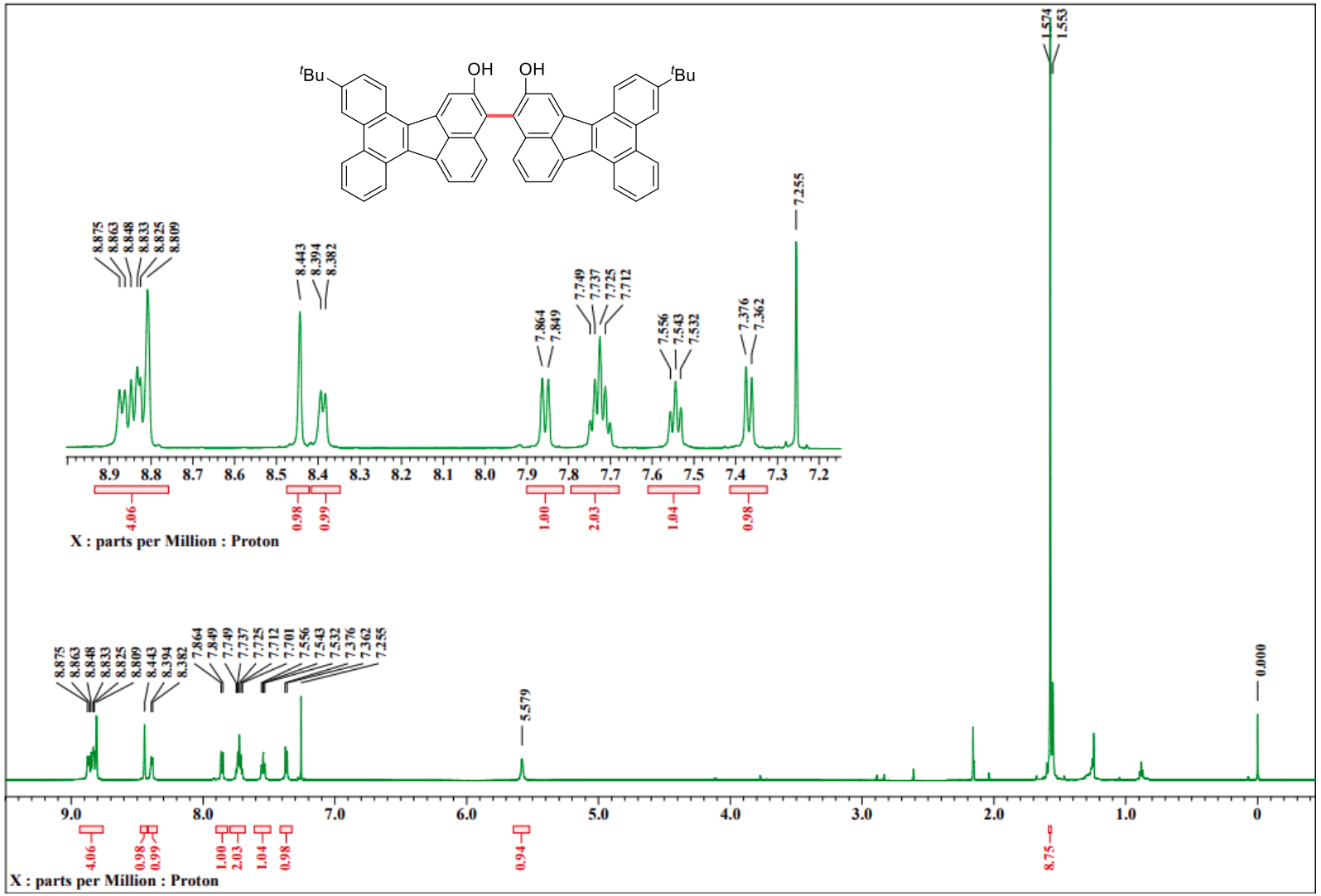

2e: ^{13}C NMR, $CDCl_3$, 151 MHz

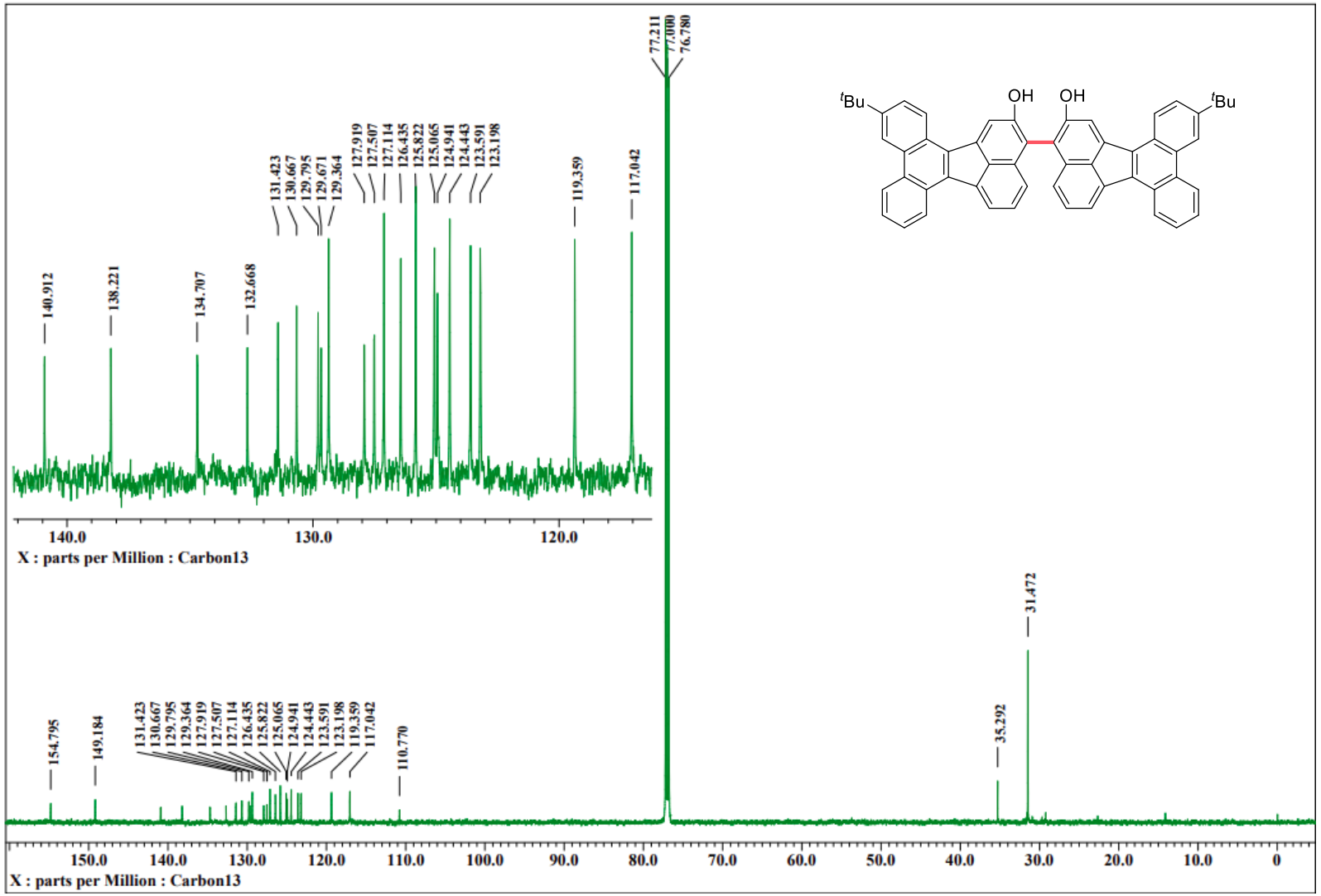

2f: ^{1}H NMR, $CDCl_3$, 600 MHz

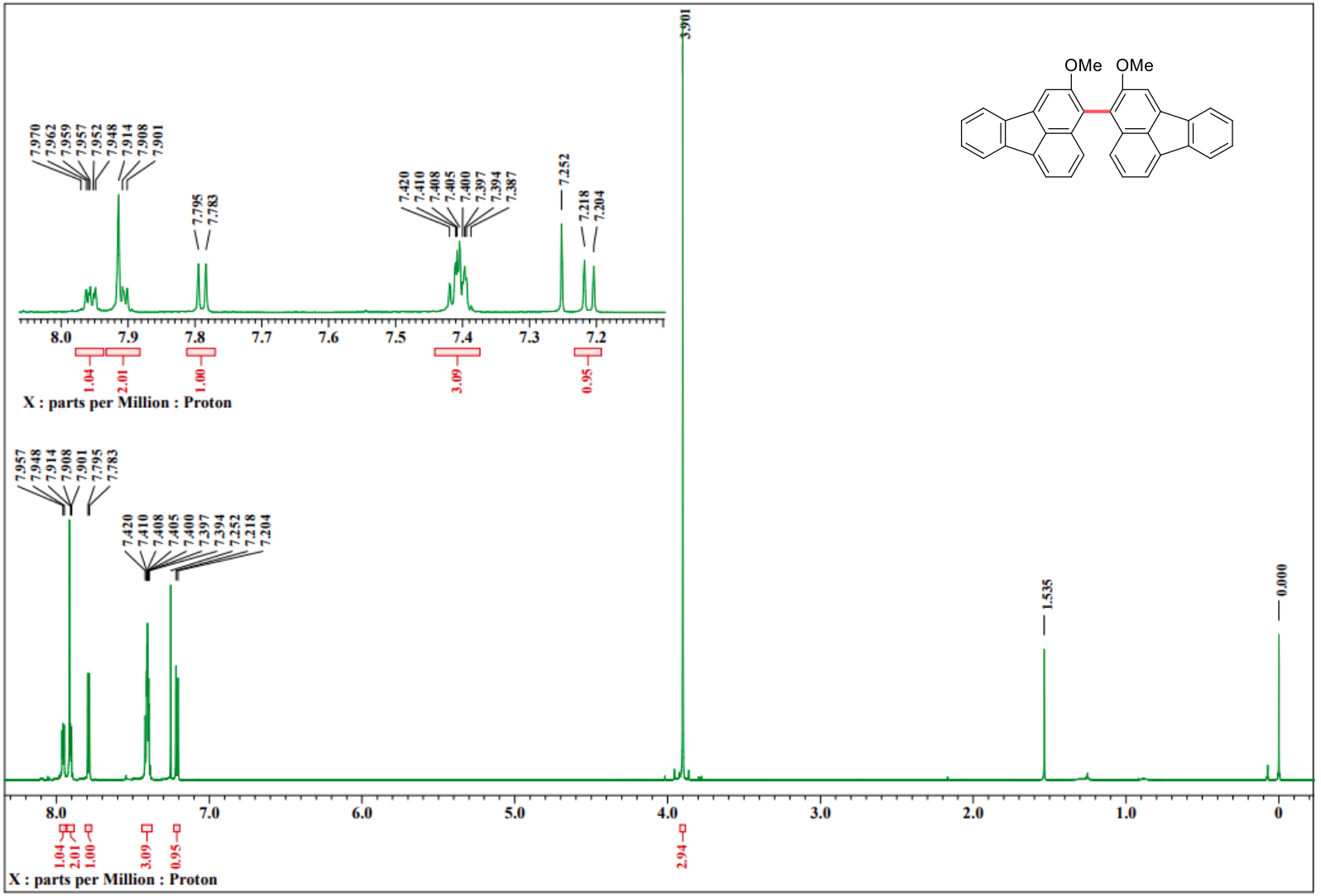

2f: ^{13}C NMR, $CDCl_3$, 151 MHz

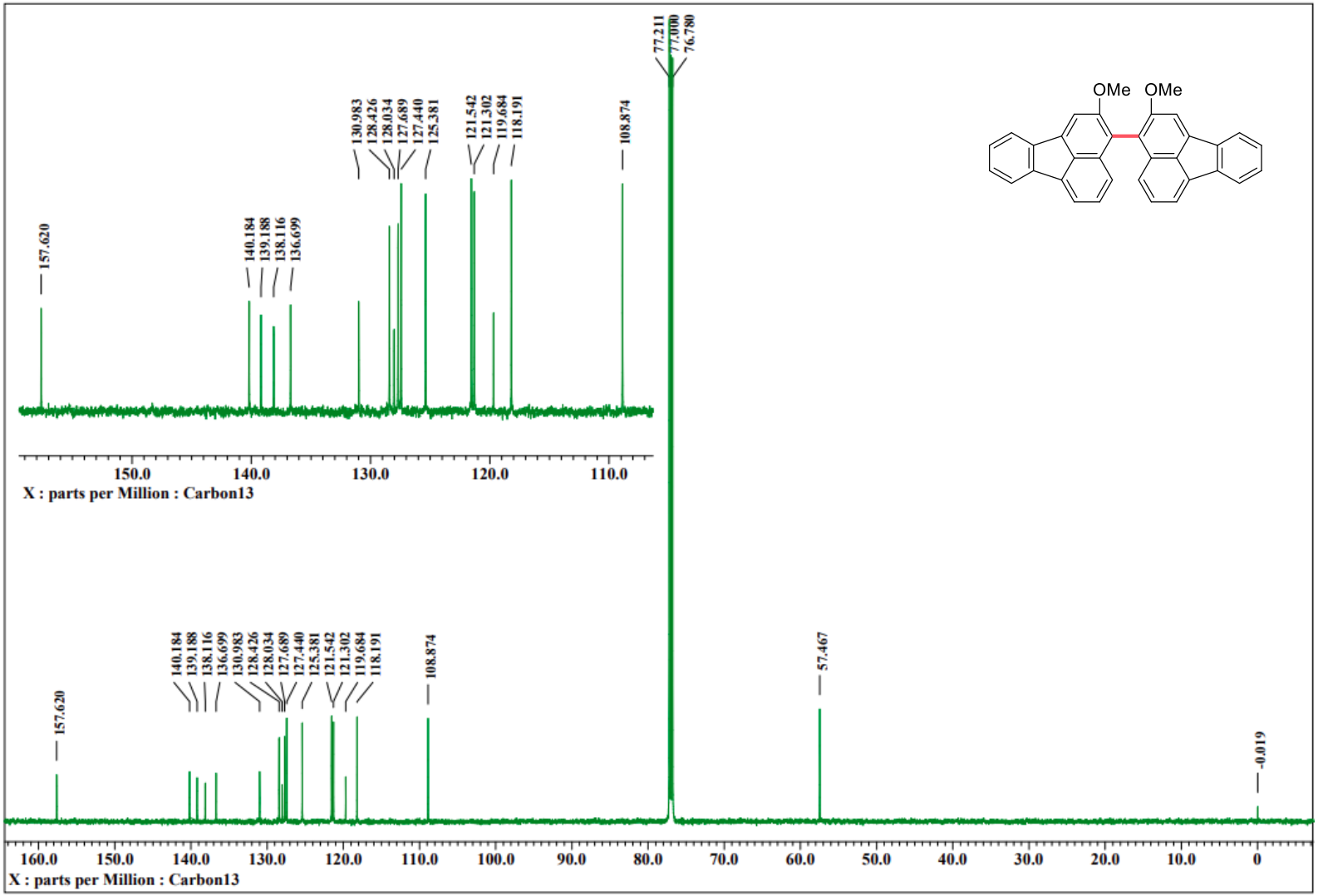

4a: ^{1}H NMR, $CDCl_3$, 600 MHz

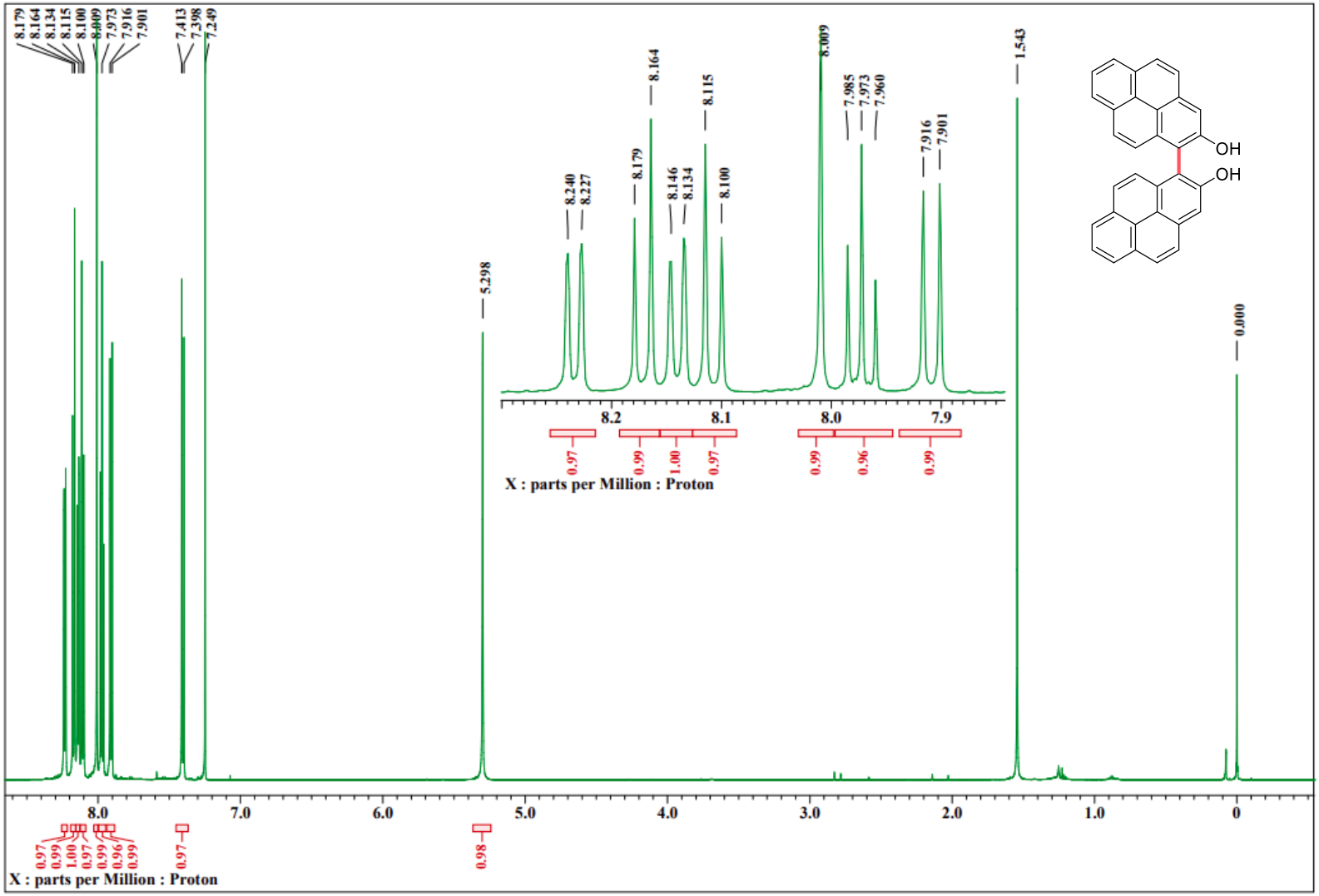

4a: ^{13}C NMR, $CDCl_3$, 151 MHz

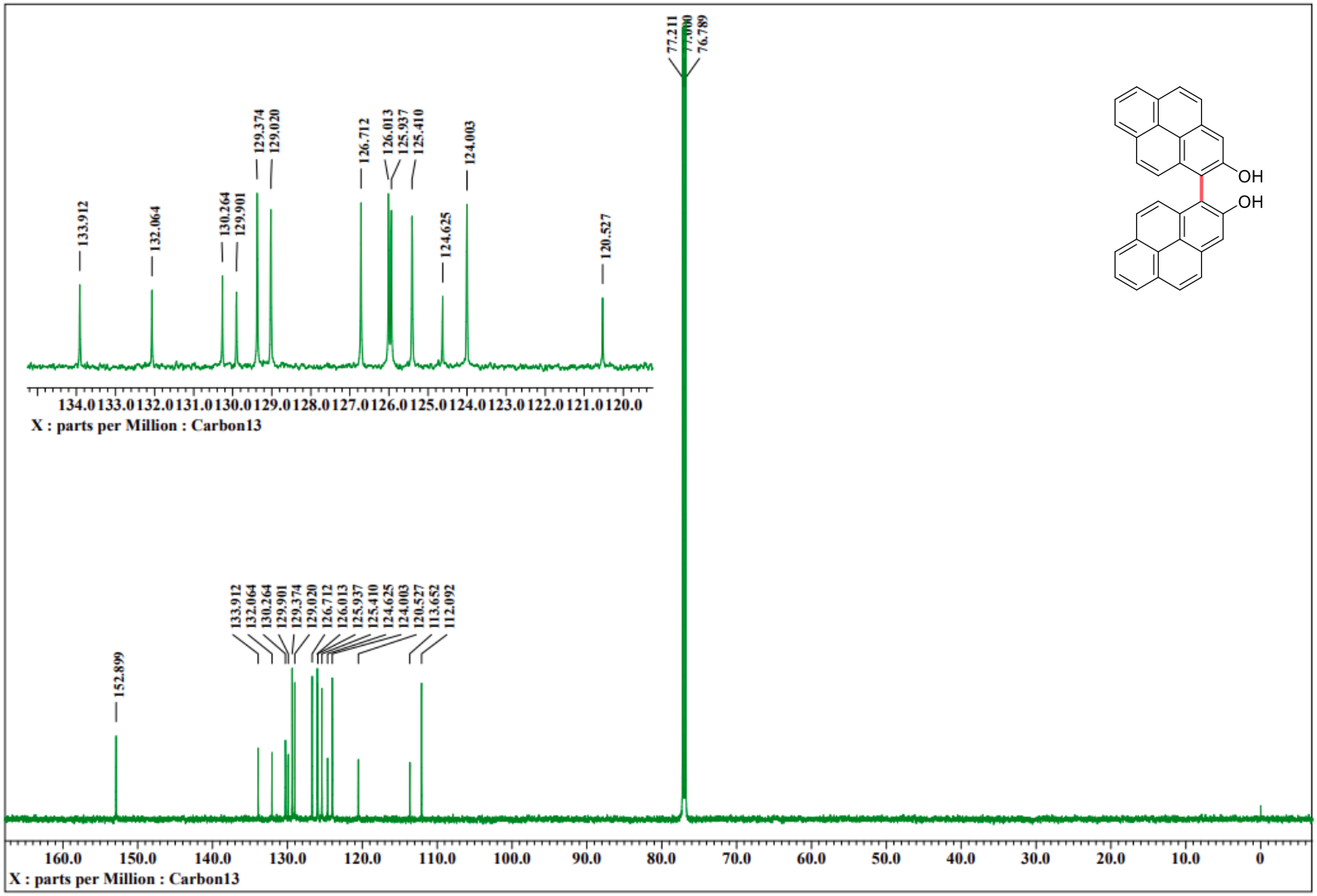

4j': ^{1}H NMR, $CDCl_3$, 600 MHz

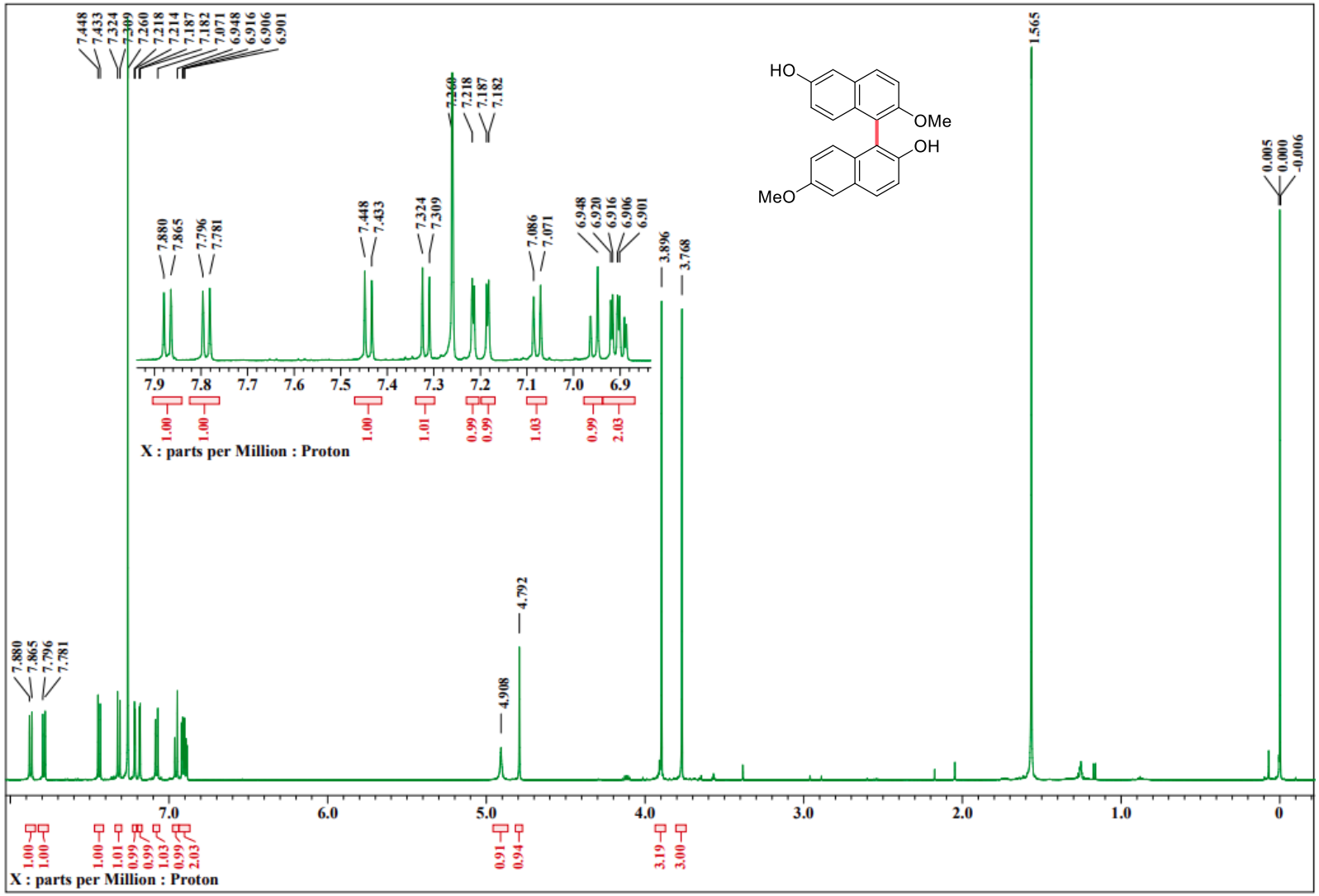

4j': ^{13}C NMR, $CDCl_3$, 151 MHz